Concrete Cracks in Composite Bridges

A Case Study of the Bothnia Line Railway Bridge over Ångermanälven

VIKTOR ANSNAES
HESHAM ELGAZZAR

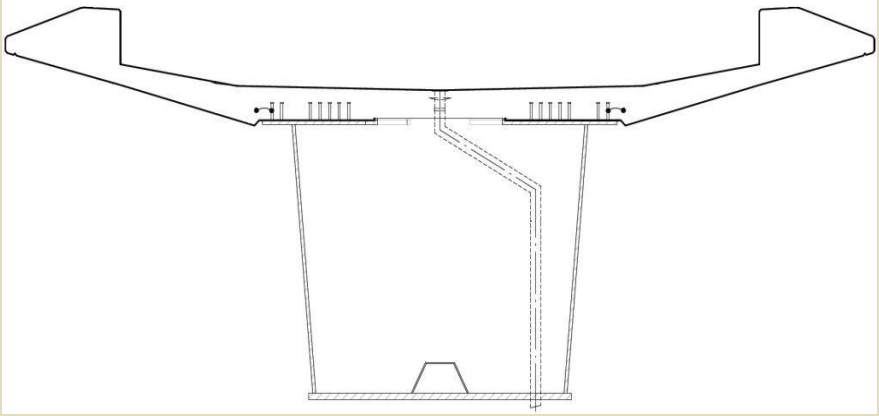

KTH Architecture and the Built Environment

Master of Science Thesis
Stockholm, Sweden 2012

KTH Architecture and
the Built Environment

Concrete Cracks in Composite Bridges

A Case Study of the Bothnia Line Railway Bridge over Ångermanälven

Viktor Ansnaes and Hesham Elgazzar

June 2012
TRITA-BKN. Master Thesis 352, 2012
ISSN 1103-4297
ISRN KTH/BKN/EX-352-SE

Royal Institute of Technology (KTH)
Department of Civil and Architectural Engineering
Division of Structural Design and Bridges
Stockholm, Sweden, 2012

Preface

We would like to thank our supervisor Henrik Gabrielsson at Reinertsen Sverige for gathering background information for this thesis and organizing the site visit. We would also thank Prof. Lars Pettersson for the guidance preparing the report and our examiner Prof. Raid Karoumi who has been very helpful during the work with this thesis.

We give our thanks to the Bridge Division at KTH Royal Institute of Technology and Reinertsen for providing working spaces for us during the thesis.

Finally, we would like to thank Anders Carolin at Trafikverket for gathering the drawings and calculations, Karl-Åke Nilsson who helped us with the crack measurement at the bridge and Lars-Göran Svensson at Botniabanan for arranging bridge inspection.

Stockholm, June 2012

Viktor Ansnaes and Hesham Elgazzar

Abstract

Cracks in the concrete slab of continuous composite bridges are common due to the tensile stresses at the supports. These bridges are allowed to crack as long as the cracking is controlled and not exceeding the design crack width (according to Bro 94 the crack should be injected if they are bigger than 0.2 mm). The Ångermanälven Bridge (railway bridge part of the Bothnia line project) was designed with big edge beams of width 1.2 m, 40 % of the total area of the concrete deck cross-section. During the final inspection cracks larger than the design crack width (0.3 mm according to Bro 94) were observed over the supports.

In this thesis the design and the construction procedure of the bridge is studied to clarify the causes of the cracking in the edge beam. The objectives of this thesis were addressed through a literature study of the different types of cracks and the Swedish bridge codes. The expected crack width was calculate according to the same code, using a 2-D FEM model for the moment calculation, and compared with the crack width measured at the bridge.

The result of the calculations shows that tensile stress due to ballast and only restraining moment due to shrinkage is not big enough to cause the measured crack width. Shrinkage force and temperature variation effects may have contributed to the concrete cracking in the edge beams. The large cross-section area of the edge beams indicates that it should be designed as part of the slab, taking that into consideration, 1.1 % reinforcement ratio in the edge beams is believed to limit the crack width to the code limits (0.3 mm).

Keywords: Composite Bridge, Cracks, Edge Beam, Bothnia Line, Reinforcement for Crack Control.

Sammanfattning

Sprickor i betongplattan, på grund av dragspänningar vid stöden, är vanligt förekommande i kontinuerliga samverkansbroar. Dessa brotyper tillåts att spricka, så länge som sprickorna kan begränsas och inte överstiga den tillåtna sprickbredden (enligt Bro 94 ska sprickbredder över 0,2 mm injekteras). Bron över Ångermanälven (järnvägsbro som en är del av Botniabanan) konstruerades med stora kantbalkar med en bredd på 1,2 m, 40 % av betongplattans tvärsnittsarea. Under slutbesiktningen påträffades sprickor vid stöden som var större än den tillåtna sprickbredden (0,3 mm enligt Bro 94).

I detta examensarbete studeras konstruktionen och byggprocessen av bron för att klargöra orsakerna till sprickorna i kantbalken. Arbetet behandlades genom en litteraturstudie av olika spricktyper och den svenska bronormen. Den förväntade sprickbredden beräknades enligt samma norm, med hjälp av en FEM-modell i 2-D för momentberäkningarna, och jämfördes sedan med de uppmätta sprickorna från bron.

Resultatet av beräkningarna visar at dragspänningarna, från ballasten och endast tvångsmoment av betongens krympning, inte är tillräckligt stora för att orsaka den uppmätta sprickbredden. Normalkraft orsakad av krympning och temperaturvariationer kan ha bidragit till sprickorna i kantbalken. Kantbalkens stora tvärsnittsarea indikerar att den bör inkluderas i tvärsnittet vid dimensionering. En armeringsmängd av 1,1 % antas begränsa sprickbredden till 0,3 mm (enligt normen).

Nyckelord: Samverkansbroar, Sprickor, Kantbalk, Bro över Ångermanälven, Botniabanan, Armering för sprickbegränsning.

Notations

Roman Letters

Notation	Description	Unit
A	Area	m^2
A_c	Concrete area	m^2
$A_{c.eff}$	Effective concrete area	m^2
A_{comp}	Composite area	m^2
A_r	Reinforcement area	m^2
A_s	Steel area	m^2
a	Correction factor	-
a_c	Distance from concrete center of gravity to composite center of gravity	m
a_r	Distance from reinforcement center of gravity to composite center of gravity	m
a_s	Distance from steel center of gravity to composite center of gravity	m
c	Concrete cover	mm
d_{ef}	Effective height	m
E	Modulus of elasticity	Pa
E_c	Modulus of elasticity for concrete	Pa
$E_{c.eff}$	Effective module of elasticity for concrete	Pa
E_r	Modulus of elasticity for reinforcement	Pa
E_s	Modulus of elasticity for steel	Pa
e_c	Distance from concrete center of gravity to bottom of steel section	m

e_{comp}	Distance from composite center of gravity to bottom of steel section	m
e_r	Distance from reinforcement center of gravity to bottom of steel section	m
e_s	Distance from steel center of gravity to bottom of steel section	m
F	Force	N
f_{cck}	Concrete compressive characteristic strength	Pa
f_{ck}	Ultimate compressive strength of concrete	Pa
f_{ct}	Tensile strength of concrete	Pa
f_{ctm}	Concrete tension average strength	Pa
f_{su}	Ultimate strength	Pa
f_{sy}	(Lower) tensile yield limit	Pa
h	Height of cross-section	m
h_{eb}	Edge beam height	m
h_s	Steel height	m
$h_{sl.eb}$	Distance from middle of slab to top of the edge beam	m
$I_{c.xx}$	Moment of inertia (around x-axis) for concrete section	m^4
I_{comp}	Moment of inertia (around x-axis) for composite section	m^4
I_r	Moment of inertia (around x-axis) for reinforcement	m^4
$I_{s.xx}$	Moment of inertia (around x-axis) for steel section	m^4
k	Dimension dependent coefficient	-
L	Length	m
M	Moment	Nm
M_l	Moment due to loading	Nm
M_{shr}	Moment due to shrinkage	Nm
N	Shrinkage force	N
Δl	Additional length	m
P	Force	N
$1/r_{cs}$	Bending	1/m

s_{rm}	Crack spacing	mm
t_{cm}	Thickness of the concrete slab (middle part)	m
w	Weight	N
w_k	Characteristic crack width	mm
w_m	Mean crack width	mm
y_c	Distance from concrete center of gravity to top slab center (origin)	m
y_r	Distance from reinforcement center of gravity to top slab center (origin)	m
y_s	Distance from concrete steel of gravity to top slab center (origin)	m

Greek Letters

Notation	**Description**	**Unit**
α	Ration of modulus of elasticity between steel and concrete	-
β	Coefficient, consider long- and short-term loading	-
ε	Strain	-
ε_{ct}	Tensile strain in concrete	-
ε_{cu}	Ultimate strain of concrete	-
ε_{cc}	Creep deformation of concrete	-
ε_{cs}	Mean value for final shrinkage	-
ε_r	Permanent strain after unloading	-
ε_s	Strain in reinforcement	-
ε_{sf}	Limiting strain	-
ε_{su}	Strain at ultimate stress	-
ε_{sy}	Stress at tensile yield limit	-
ζ	Crack safety factor	-
θ	Slope deflection	-

κ_1	Reinforcement bond coefficient	-
κ_2	Coefficient, account for strain distribution	-
ρ_r	Effective reinforcement ration	-
σ	Axial stress	Pa
σ_m	Stress caused by normal moment	Pa
σ_n	Stress caused by normal forces	Pa
σ_s	Stress in reinforcement	Pa
σ_{sr}	Stress when cracking appear	Pa
σ_c	Stress in concrete	Pa
σ_{cc}	Compressive stress in concrete	Pa
σ_{ct}	Tensile stress in concrete	Pa
υ	Coefficient, account for tension stiffness in concrete between cracks	-
ϕ	Reinforcement diameter	mm
$\psi\gamma$	Load coefficient	-

Contents

1 Introduction

1.1 Overview

Bothnia Line (Botniabanan) is a 190 km high-speed railway project between Nyland and Umeå in the middle of Sweden (*see Figure 1.1*) and was finished in August 2010. The railway line has 143 bridges and 25 km of tunnels (Botniabanan, 2010).

Figure 1.1 Map over Bothnia Line, (Botniabanan, 2012).

The studied bridge (*see Figure 1.2*) passes over Ångermanälven located to the north of Nyland. It is one of the longest bridges in the project with a total length of 1034 m divided into 17 spans. The first and the last span is 48 m and the rest are 61 m long (see Appendix A).

The superstructure consists of a composite section (steel concrete box girder). The 18 supports are built using reinforced concrete. Reinforced concrete piles are used for the foundation of the supports 2-14 and the rest are supported on shallow foundation.

Figure 1.2 Photo of the Ångermanälven Bridge from north side (left) and south side (right).

1.2 Summary

For the continuous composite bridges, the negative moments at the supports develop tensile stresses at the concrete part of the bridge cross-section. This increases the risk of concrete cracking (Collin et al., 2008). The stress will be bigger the longer the distance is from the center of gravity of the cross section. This means that the risk of cracking will increase as further away from the center of gravity the slab is located (when subjected to tensile stresses).

If the large transversal cracks (with larger width than stipulated in the Swedish code) are not injected or otherwise taken care of, corrosion of the steel reinforcement and spalling of the concrete will eventually occur. This results in a shorter life time and higher maintenance cost for the bridge (Cusson and Repette, 2000).

The Ångermanälven Bridge was completed in 2006 but has so far only been used for test traffic load. On the final inspection (inspection that takes place after all construction work is finished), large cracks were found in the edge beams. In the next inspection (performed by the contractor three years after the final inspection), it was recorded that the number of cracks had increased, but on the other hand the width of the cracks decreased (still being larger than the code limits).

1.3 Aim and scope

The aim of the project is to study the design and the construction procedures of the bridge trying to clarify the causes of the cracking and how it could have been avoided or limited to acceptable values.

The main questions are:

- What are the reasons for the cracks?
- What is the theoretical required steel rebar area to limit cracks?

- What are the Swedish codes limitations for the edge beam and how should it be designed?

1.4 Limitations

- The data about the weather conditions during the curing process was not available.
- The time of appearance of the first cracks, if it was before or after placing the ballast on the bridge, was not available.
- Measured concrete temperatures during pouring of different parts of the concrete slab and edge beams were not available.
- No variable loads (temperature variation, live loads, etcetera) were considered in the thesis calculation.

2 Background

2.1 Steel Concrete Composite Bridges

A composite structure is a structure consisting of two main materials (for girder bridges normally concrete and steel) which work together as one unit. The interaction between the materials is usually solved by using studs, which transfer the shear forces. This will result in a stronger and stiffer structure than the two materials working separately.

In a composite structure, the concrete cannot shrink freely due to the steel interaction. The shrinkage is represented by a tensile force at the center of the concrete. For a continuous beam this will also lead to increased moments at the supports (Collin et al., 2008).

In the serviceability limit state; when a composite structure is subjected to positive bending moment, the concrete is in compression and the steel is mostly in tension (*see Figure 2.1*). In an economic point of view this is good, because the materials are stressed effectively according to their properties. For composite structure subjected to negative bending moment the concrete is in tension, which means that it is considered to have no resistance. All the loads will be taken by the steel and reinforcement (Sétra, 2010).

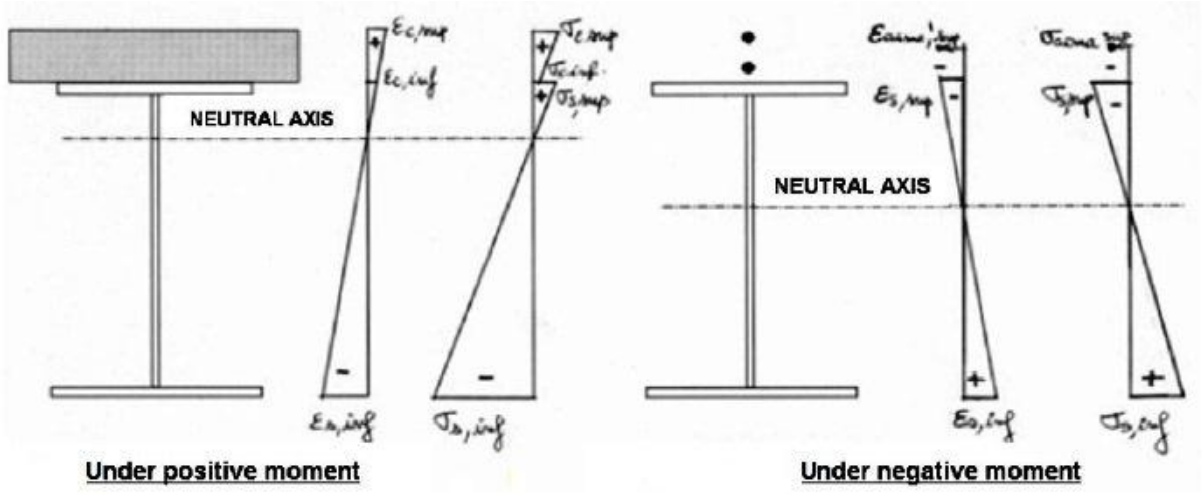

Figure 2.1 Stress distribution in a composite cross section at serviceability limit state (Sétra, 2010).

When the concrete subjected to tension, cracks will form and the stiffness of the concrete will be lost (Collin et al., 2008).

2.2 Structural Behavior

2.2.1 Concrete

When the concrete is initially subjected to small loads, it will have a linear elastic behavior. When increasing the load, defects in the form of micro cracks are formed in the material structure that makes the strain increases more rapidly than the stress resulting in a non-linear non-elastic relationship. If the section is unloaded when it has reached a large portion of the ultimate strength, some residual strain will remain due to the defects created in the microstructure.

After the ultimate strength is reached, the stress-strain curve will fall rapidly creating a very small area under the curve (*see Figure 2.2*), which represents the energy consumption during the failure process and which indicates the brittle failure of the material.

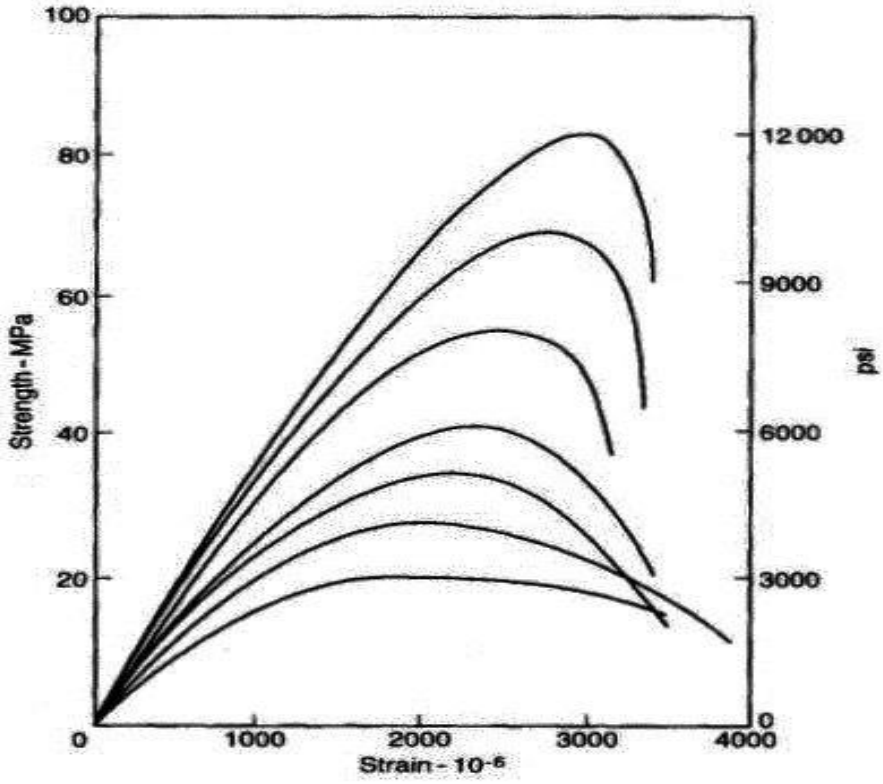

Figure 2.2 Stress- Strain curves of different concrete classes (Holmgren et al., 2010).

The behavior of the concrete is dependent on whether it is subjected to tension or compression stresses (*see Figure 2.3*). According to (Standardiseringskommissionen i Sverige, 2008), the capacity of the concrete in compression is much higher than the capacity in tension (*see Equation (2.1)*).

$$f_{ct} = 0{,}30\, f_{ck}^{2/3} \quad for\ concrete\ quality \leq C50/60 \tag{2.1}$$

Since the concrete is a porous material, the mechanical properties are largely determined by its porosity, which is represented by the water cement ratio of the concrete composition.

The properties of the concrete are also influenced by the manufacturing process which is why in some important projects, like certain bridges, the compressive strength is determined from core samples taken from the final structure.

The compressive capacity of the concrete is not a pure material property but a combination of both tensile and shear capacity of the section, which makes the results highly dependent on the test procedures adopted to determine it. To minimize the effects of test procedures, the specifications for the tests, to determine the compressive strength, must be strictly followed.

Concrete is classified according to its characteristic compressive strength e.g. C50/60 indicating characteristic cylinder strength of at least 50 MPa and characteristic cube strength of at least 60 MPa. In practice most of the used concrete are in the class range from C20/25 to C50/60 and the classes higher than that is called high strength concrete.

The tensile strength of the concrete is less important than the compressive strength because the brittleness of the concrete makes it very hard to safely utilize the tensile strength. It is also very difficult to measure tensile strength in a precise way (Holmgren et al., 2010).

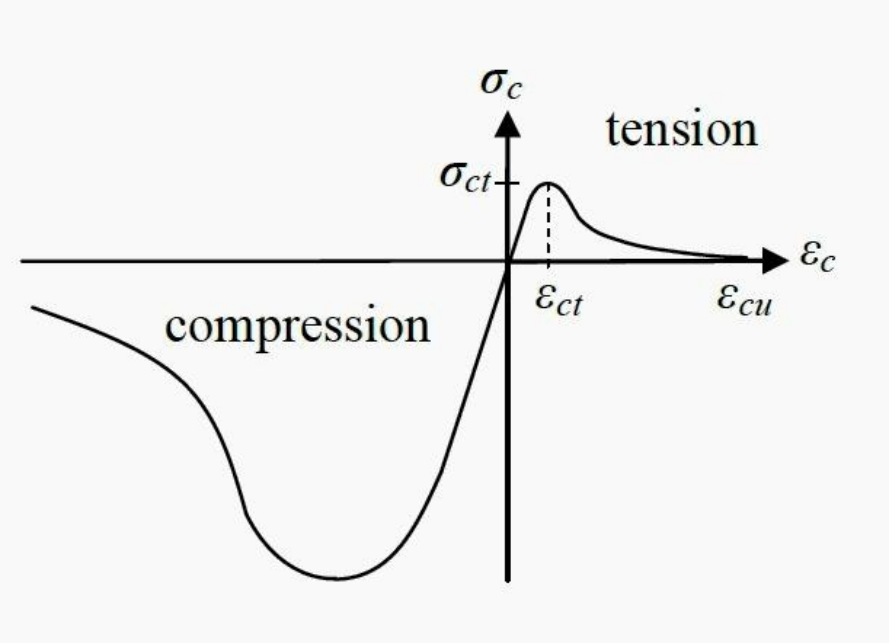

Figure 2.3 Concrete behavior in Compression and tension (Alfredsson and Spåls, 2008).

Cracking of the concrete occurs when the tension stresses in the section exceeds the tensile strength of the concrete. The initiation and development of the cracks in a concrete specimen subjected to increasing tensile deformation until failure is presented (see *Figure 2.4*).

When starting to load the specimen in tension, micro cracks starts to form at the weak points of the structure (*see Figure 2.4b*) and through increased loading, these micro cracks start to connect to one other and form a fracture zone at the weakest section until the tensile strength of the concrete is reached (*see Figure 2.4c*). When the stress exceeds the tensile strength, the stresses in the fracture zone start to decrease with the increased deformation while the strain is

decreasing in the rest of the specimen (*see Figure 2.4d*). Eventually a fully developed crack is formed in the fracture zone, which cannot transfer any stresses (*see Figure 2.4e*). The concrete around the crack, which has not reached its tensile strength during the loading process, will then be unloaded and a redistribution of the stresses and deformations within the section will occur (Johansson, 2000).

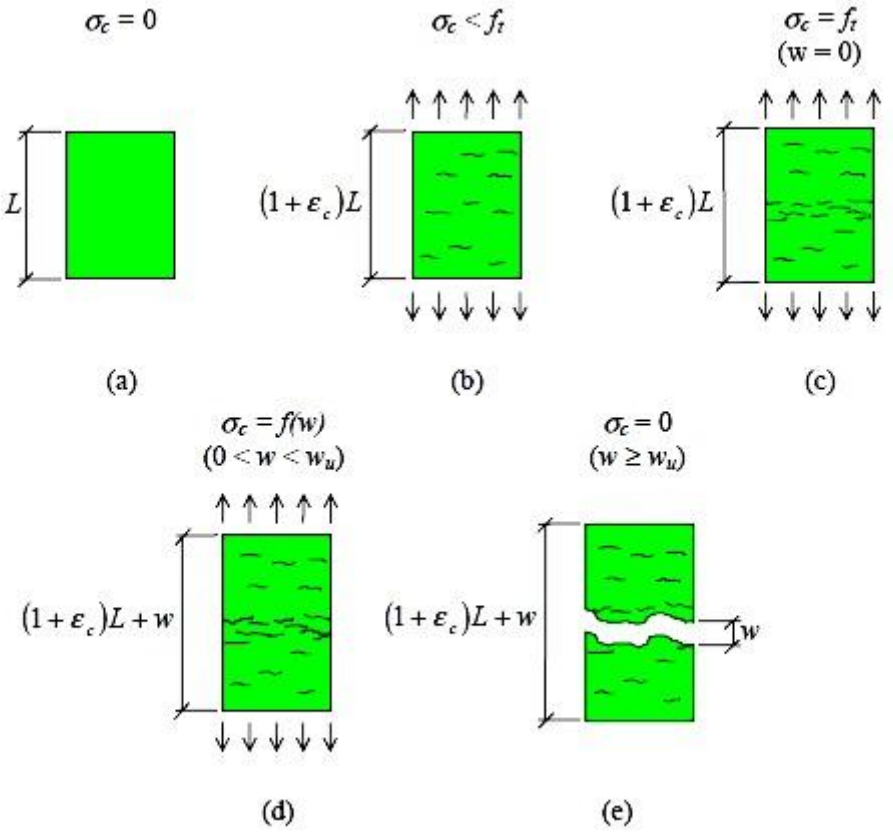

Figure 2.4 Crack initiation and development until failure in a concrete specimen (Johansson, 2000).

2.2.2 Reinforcing steel

Steel exposed to a pulling force, generates tension stresses in the material (*see Figure 2.5*). The stress depends on the force and the area of the steel reinforcement (*see Equation* (2.2)).

$$\sigma = \frac{F}{A} \tag{2.2}$$

At the same time, the material increase in length. The ratio between the additional length and the original length is called strain (*see Equation* (2.3)) (Burström, 2007).

$$\varepsilon = \frac{\Delta l}{l} \tag{2.3}$$

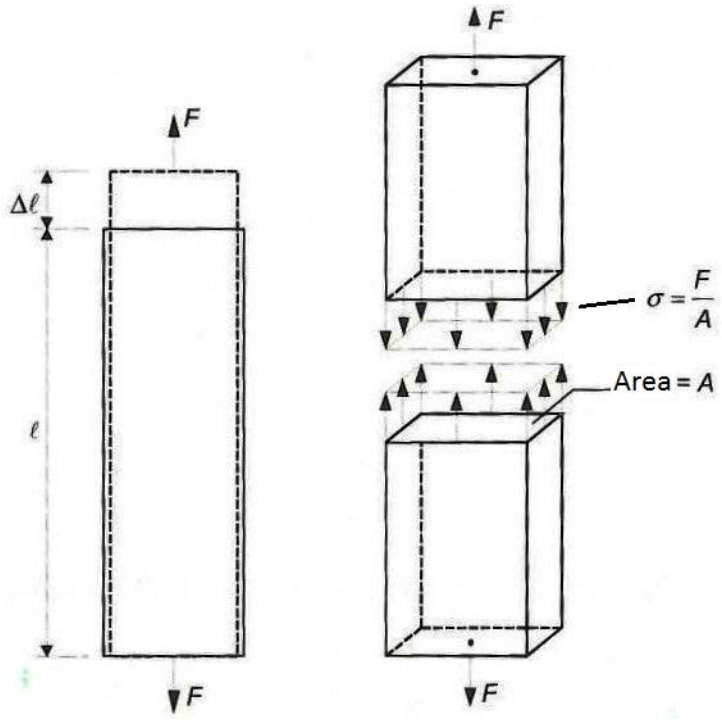

Figure 2.5 Material exposed to pulling force (Burström, 2007).

The stress-strain relation for steel (*see Figure 2.6*) is linear elastic until it reaches the tensile yield limit. During this interval, the deformation is restored if the load is removed. When the yield limit is reached the strain increase and the stress is unchanged because the steel is yielding. After the flow interval, the stress and strain increase until the ultimate strength is reached. When the ultimate strength is reached, the stress decrease and the strain increase until the failure. If the load is removed after the yield limit, the strain and stress will decrease (parallel to the linear elastic curve), but some residual deformation will remain permanently.

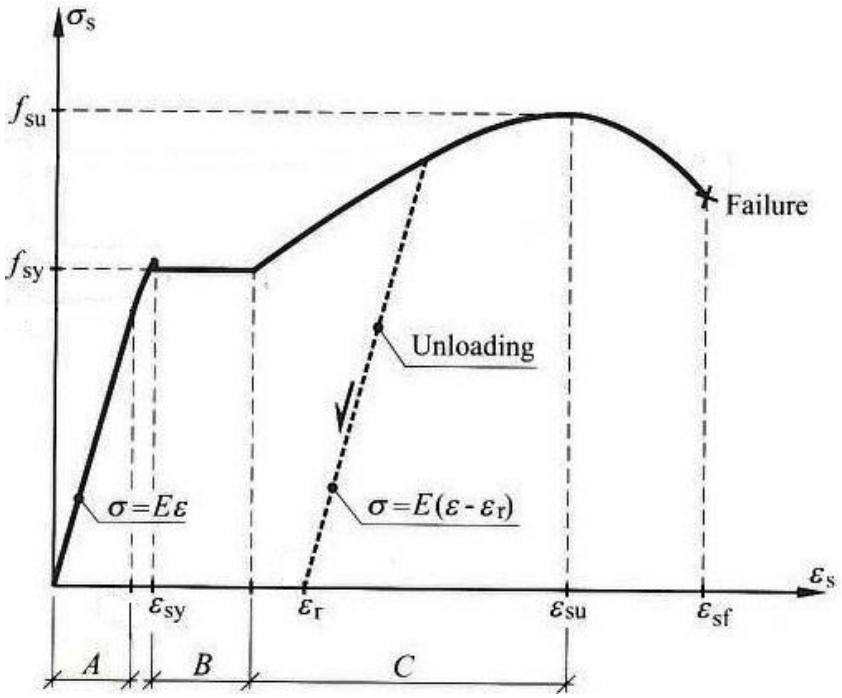

Figure 2.6 Schematic stress-strain diagram for hot-rolled steel. A=elastic interval, B=flow interval, C=consolidation interval (Holmgren et al., 2010).

The reinforcing steel, in concrete structures, can be assumed elastic to the yield limit and during compression, the ultimate limit can be assumed equal to the tensile yield limit (Holmgren et al., 2010).

2.2.3 Interaction between concrete and reinforcement

Reinforced concrete combines the compressive strength of the concrete with the tensile strength of the reinforcement to form a structure capable of taking up all kinds of forces in the form of tension and compression stress components.

When subjected to compression, the concrete and the compression reinforcing steel (if needed) will absorb the stresses at the section. The compression capacity of the steel can be utilized by protecting it against buckling using the surrounding concrete. The tension reinforcing steel will absorb the tensile stresses after the concrete has cracked. This maintains the tensile capacity of the section and also limits the crack width in the concrete for the durability and the aesthetical function of the structure.

The structure can have different types of reinforcement depending on the type and magnitude of the forces. Bending reinforcement consists of tension reinforcement mainly. In some cases compression reinforcement is also added, and it carries the tension and some of the compression stresses resulting from the bending moments and any eccentric forces. Compression reinforcement can also be used to absorb some of the compression stresses in the concrete when it is not possible to increase the area of the concrete. Shear reinforcement carries the tensile stresses resulting from the shear forces acting on the structure. The torsion reinforcement can carry the tensile forces caused by torsional moment. Shrinkage reinforcement is used to limit the shrinkage of the concrete and the widths of the shrinkage cracks by induced compressive stresses in the reinforcing steel. Usually the main

reinforcement absorbs these stresses, but sometimes there is a need for extra reinforcement (especially when using pre-stressed concrete).

When loading the structure, the reinforced concrete passes through three different stages until rupture (*see Figure 2.7*).

In the first stage, the concrete is uncracked. The concrete is able to take tensile stress.

In the second stage, the tensile zones in the concrete begin to crack. The direction of the cracks is perpendicular to the tensile stresses. The tensile stress in the cracked part is taken up by the reinforcement. This stage usually corresponds to the service condition for the beam.

The third stage (ultimate stage) represents the conditions close to the bending failure of the structure. There are two types of failures. The first one occurs when the yield limit in the reinforcement is reached and the second one occurs when the ultimate limit of the concrete is reached (Holmgren et al., 2010).

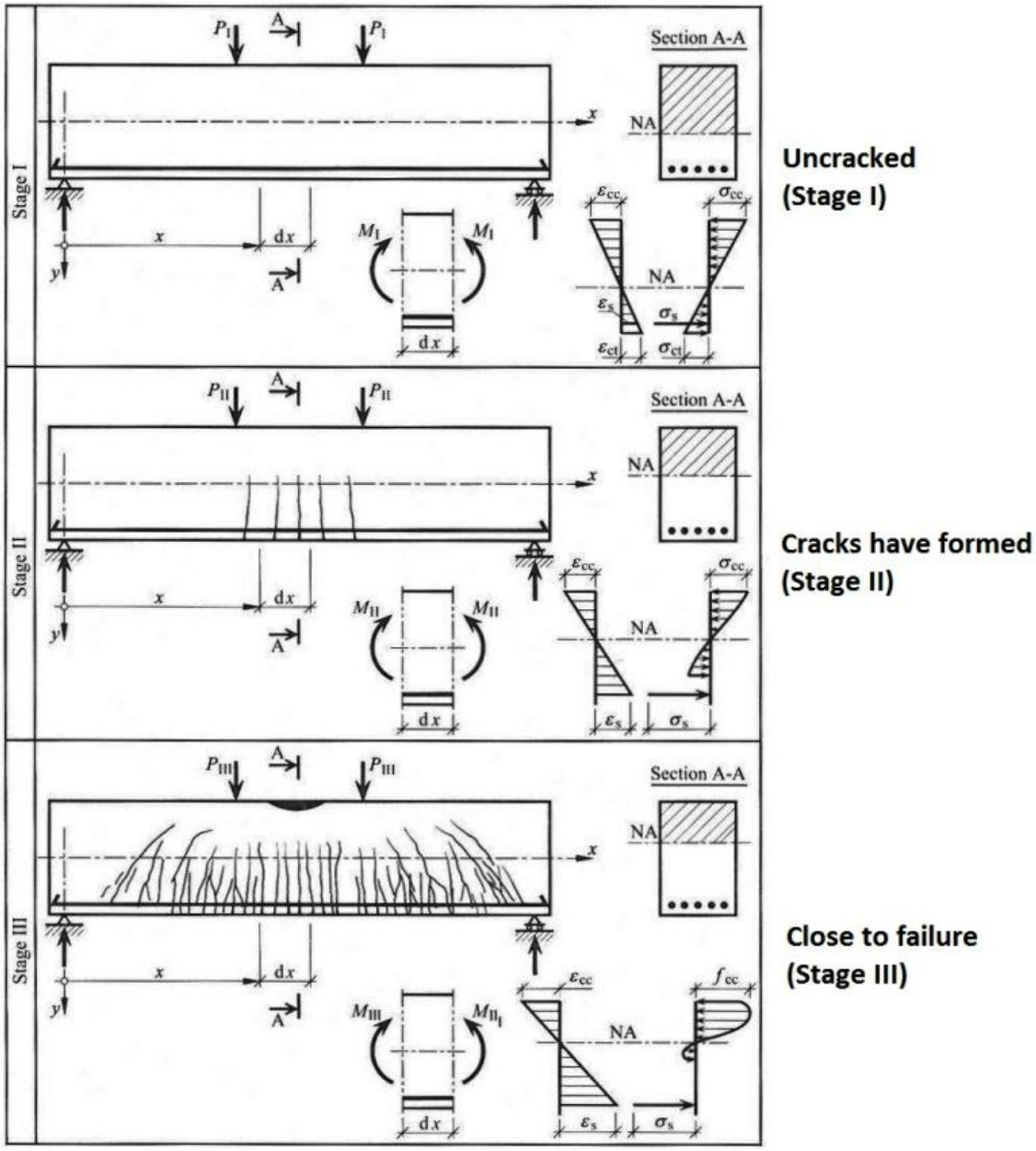

Figure 2.7 Stages in a reinforced concrete beam when subjected to increasing loading. Crack illustration, expected stress and strain distribution. NA=neutral axis (Holmgren et al., 2010).

2.3 Different Types of Cracks

Cracks in reinforced concrete have different structure and size depending on what is causing them. According to (Concrete Society, 2010) the cracks can be divided in different categories (*see Figure 2.8*).

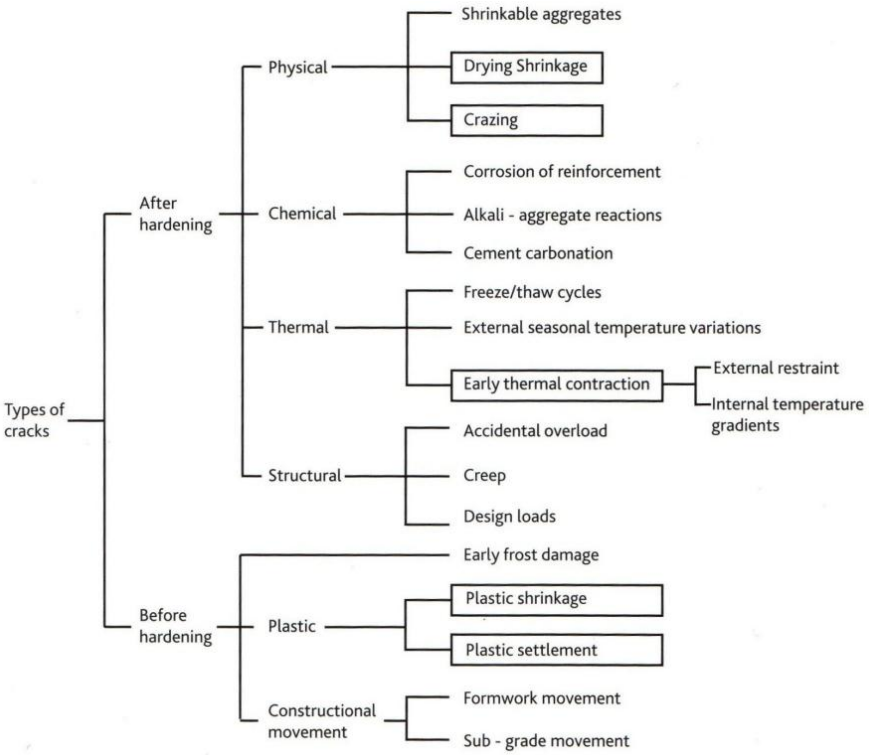

Figure 2.8 Types of cracks (Concrete Society, 2010).

Cracks can highly affect the durability and safety of a bridge and therefore it is important to know the different types of causes. The types of cracks mostly depends on the following factors (Radomski, 2002):

- Time of formation, after casting or construction
- External appearance (*see Figure 2.9*)
- Width and spreading

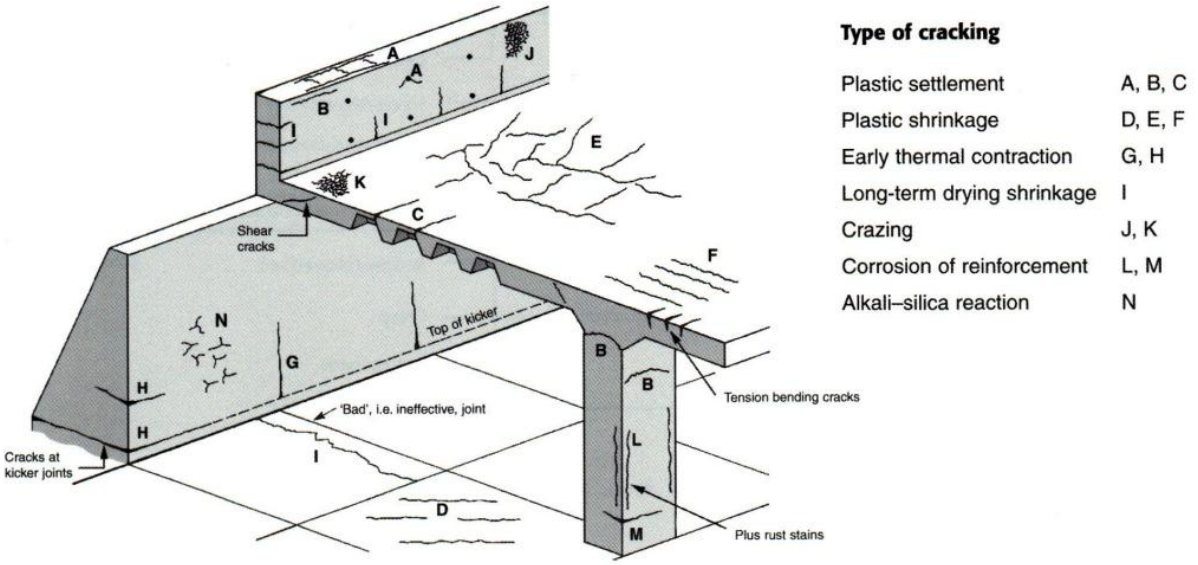

Figure 2.9 Crack location (Concrete Society, 2010).

The different causes below could have been a contributing factor for the cracking in the Ångermanälven Bridge.

- Plastic settlement
- Plastic shrinkage
- Early thermal cracks
- Shrinkage
- Service Loading
- Restraints

2.3.1 Plastic settlement

The plastic settlement cracks are caused by the difference in the restraining conditions of the concrete. When the concrete is prevented from settling at some parts (e.g. by steel reinforcement) while the adjacent concrete parts are allowed to settle, the cracks can be formed over the restraining elements, e.g. reinforcement bars.

The cracks are formed in the first hours after casting the concrete. They are distinguished by their pattern that mirrors the pattern of the restraining elements such as the steel reinforcement or the change in the section shape (*see Figure 2.10*) (Cement Concrete & Aggregates Australia, 2005).

The crack size can be larger than 1 mm. (Radomski, 2002).

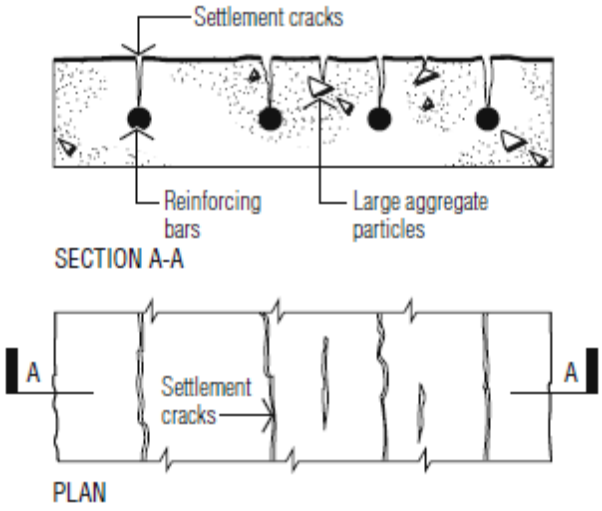

Figure 2.10 Plastic settlement cracks formed above the steel reinforcement and large aggregates particles (Cement Concrete & Aggregates Australia, 2005).

2.3.2 Plastic shrinkage

Plastic shrinkage is caused by dehydration of the fresh concrete (Burström, 2007).

The formations of the cracks appears during the first hours after casting and have a cracking pattern or long cracks on the surface (*see Figure 2.11*). The cracks can be large, (over 1 mm) (Radomski, 2002).

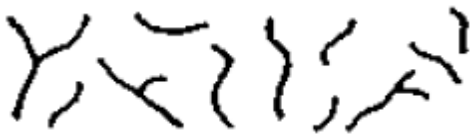

Figure 2.11 Crack illustration (Radomski, 2002).

2.3.3 Early thermal cracks

Early thermal cracks are caused by expansion and contraction of the concrete due to change in temperature (*see Figure 2.12*). The temperature change is caused by the reaction between cement and water (hydration), which generates heat. The cracks appear when the concrete is cooling during the curing process (Burström, 2007).

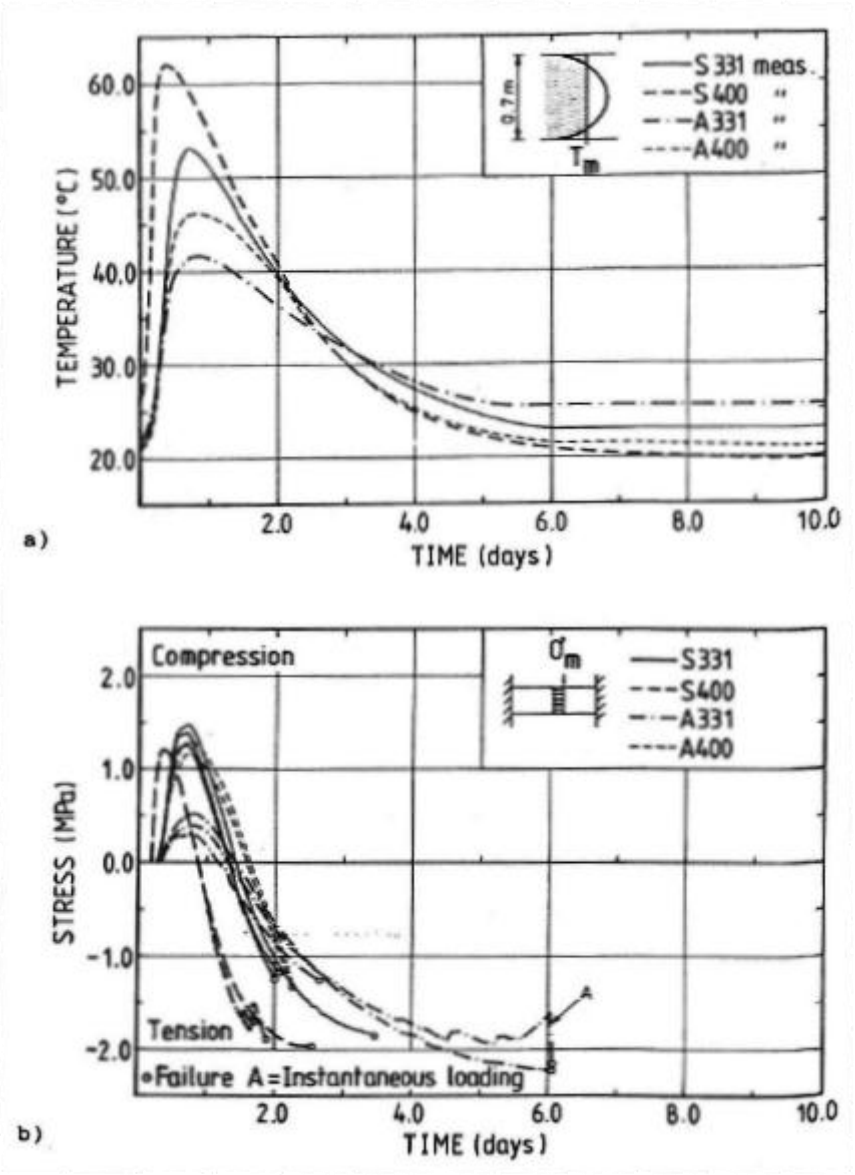

Figure 2.12 Change in mean temperature for newly cast concrete elements and laboratory test (with 100% restraint) of the stresses. S - Std Slite cement, A - Std Degerhamn cement, cement quantities 331 kg/m^3 and 400 kg/m^3 (Betongföreningen. Kommittén för sprickor i betong, 1994).

There are two different types of early thermal cracks; surface cracks and deep through cracks (*see Figure 2.13*). The surface cracks are formed during the expansion of the concrete in the first few hours after casting. They do not have a general pattern and some of the cracks close during the contraction phase, in a self-healing process (Betongföreningen. Kommittén för sprickor i betong, 1994).

The through cracks are formed during the contraction phase of concrete and might be located above the construction joints in the old concrete walls or due to other restraining condition by the old concrete. The cracks are smaller than 0.4 mm (Radomski, 2002).

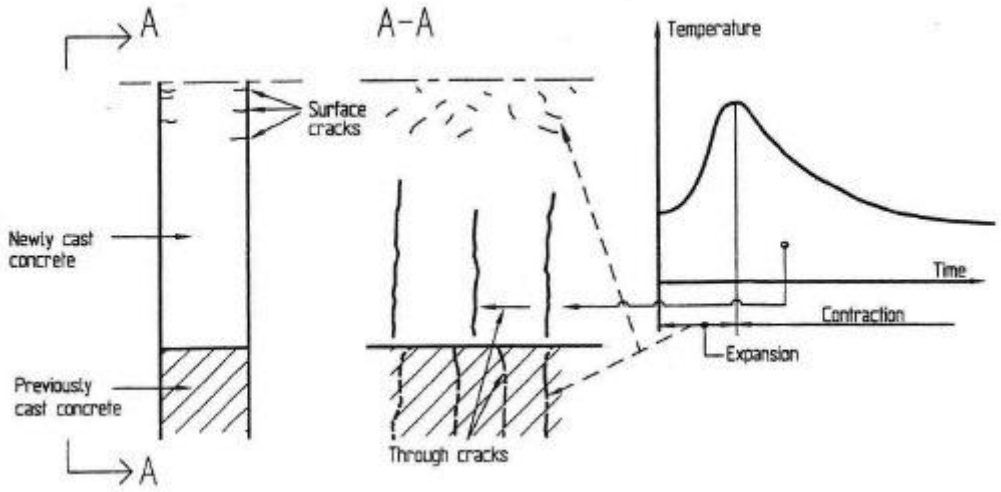

Figure 2.13 Examples of surface and through early thermal cracks in concrete (Betongföreningen. Kommittén för sprickor i betong, 1994).

2.3.4 Shrinkage

Shrinkage is caused by contraction of the concrete when the water leaves the pores in the cement paste (Burström, 2007).

The formations of the cracks appear several months after the construction work are finished and are similar to bending or tension cracks (*see Figure 2.14*). The cracks are usually smaller than 0.4 mm if the amount of reinforcement is enough (Radomski, 2002).

2.3.5 Service loading

Service loading cracks is caused by different external forces (*see Figure 2.14*). The formation of the cracks depends on the type of force and the appearance depends on the usage of the structure. The cracks are generally small, but larger cracks may occur in areas where concrete cracking is hard to asses (underestimation of the long term load etcetera). (Radomski, 2002).

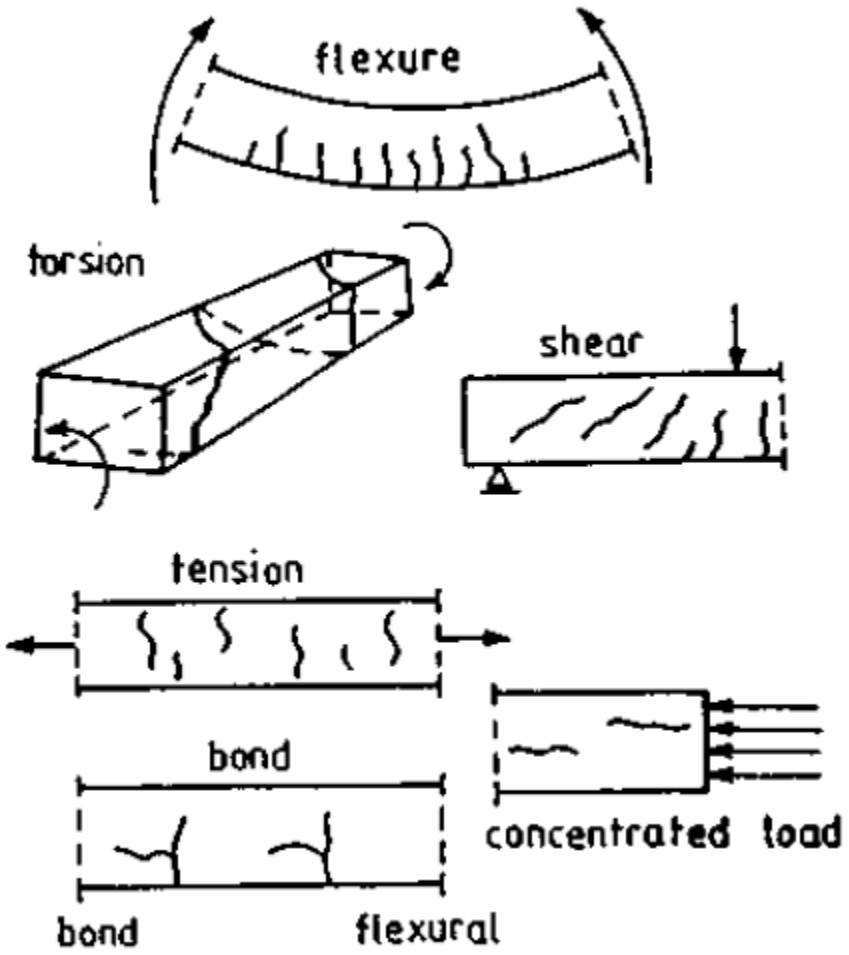

Figure 2.14 Crack illustration (Radomski, 2002).

2.3.6 Restraints

There are two types of restraints; internal and external.

The internal restraint is caused by the temperature difference, during settings, between the core and surface of a thick concrete section. This difference leads to tension at the surfaces (*see Figure 2.15*) and cracks can form in the tension zone. Internal restraint can also be caused by the temperature difference, after casting, between the reinforcement and the concrete, but only if too much reinforcement is used.

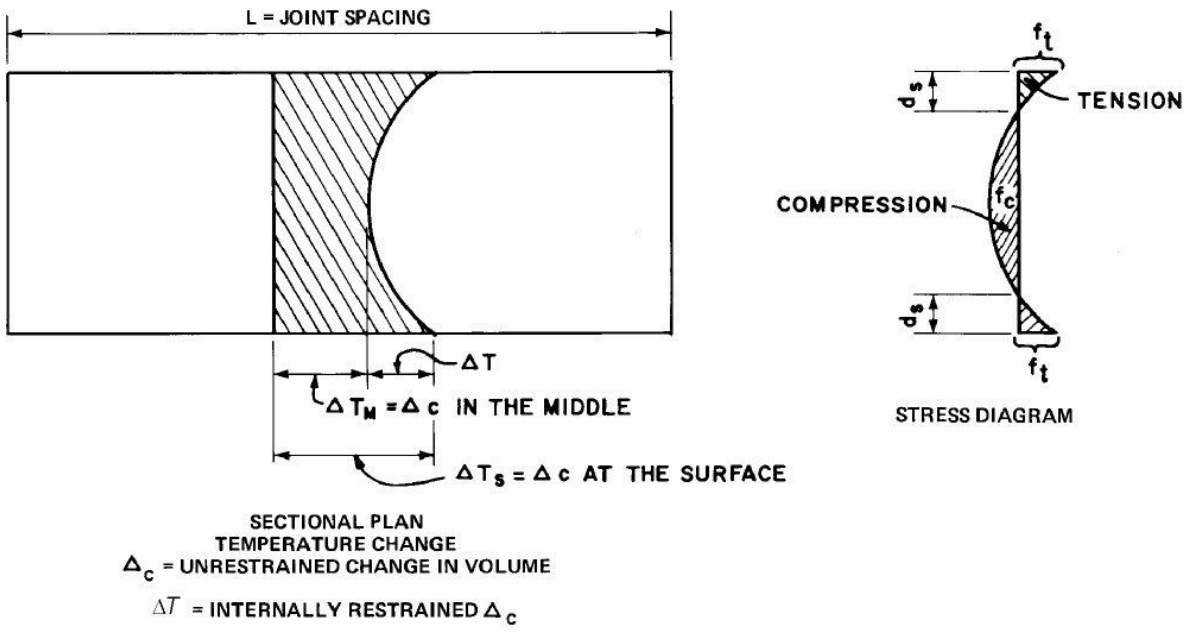

Figure 2.15 Internal restraint (ACI Committee 207, 1995).

The external restraint is caused by the boundary condition which prevents the casted concrete to move. If the structure is restrained at the ends, tension will develop along the section. There is a chance that a single primary crack will form if the longitudinal reinforcement is insufficient otherwise the crack pattern will be controlled (*see Figure 2.16*). The bond between the new and old concrete is usually smaller than the tensile strength and therefore it is likely that the first crack will form in that area. The intermediate cracks may not occur if the joint cracks are fully developed.

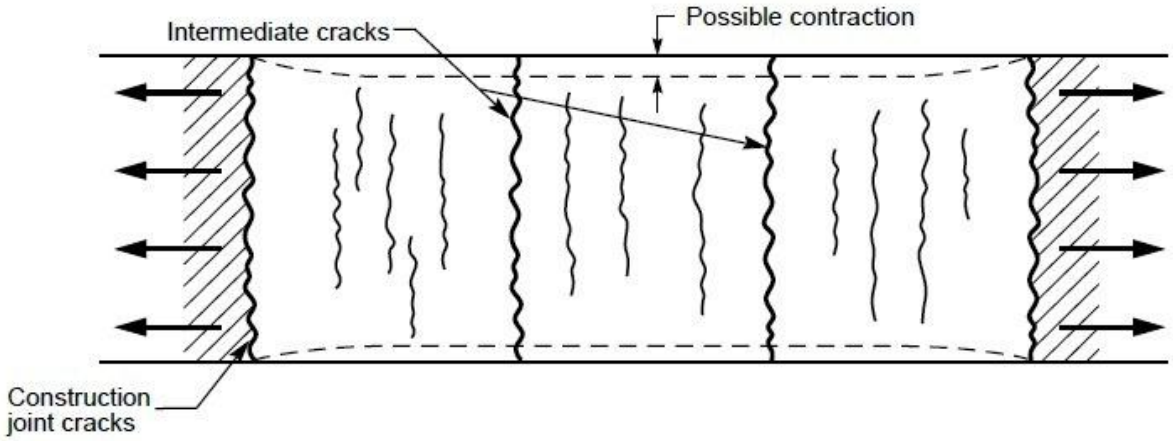

Figure 2.16 Crack formation due to external end restraint (The Highway Agency, 1987).

If the base is rigid and edges are free the concrete is not able to contract at the bases. Vertical cracks will develop in the mid-span, splayed cracks will form towards the ends and horizontal cracks may form at the ends (*see Figure 2.17*) (The Highway Agency, 1987).

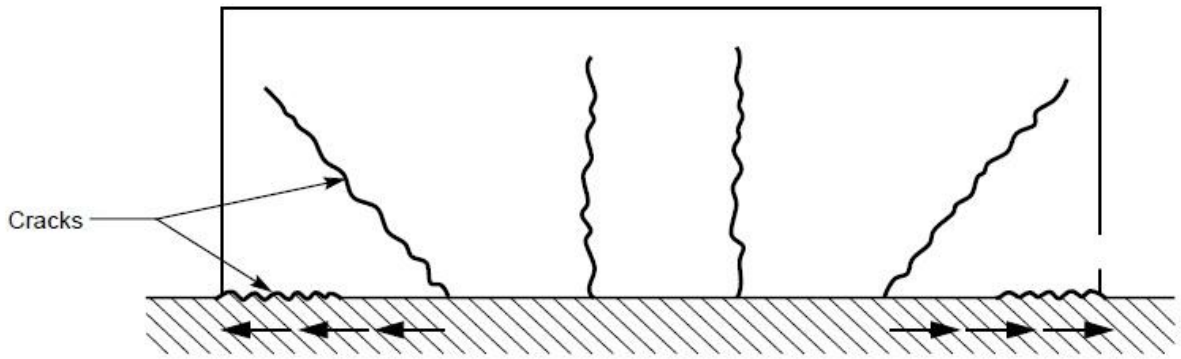

Figure 2.17 Crack formation due to external edge restraint (The Highway Agency, 1987).

If the end and edge restraint is combined, the crack pattern will be different (*see Figure 2.18*).

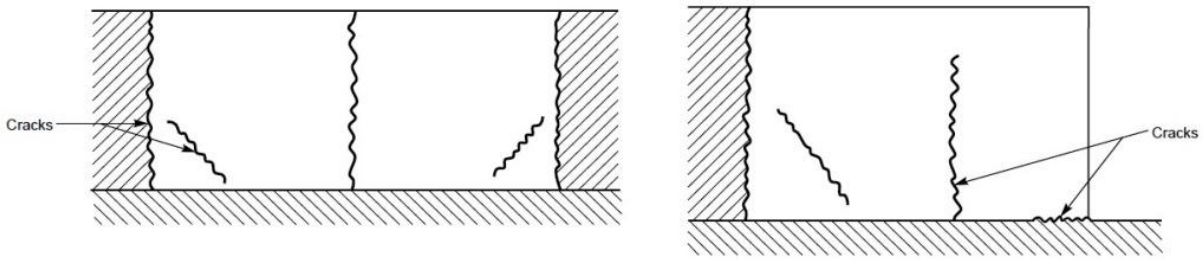

Figure 2.18 Crack formation for combined external end and edge restraints (The Highway Agency, 1987).

The cracks are generally smaller than 0.2 mm, but larger cracks can occur if the reinforcement is not sufficient (Radomski, 2002).

2.4 Crack Measurements Methods

A measuring magnifier used to measure crack width in concrete structures. The recommendation is to use a loupe with a 10 times magnifier and a measure scale of 0.1 mm step (Vägverket, 1994a).

2.5 Repair Methods

Cracks due to load, shrinkage temperature etcetera can be rehabilitated by protection against aggressive substances using the following methods:

- Hydrophobic impregnation
- Sealing
- Cover of cracks with local membrane
- Filling of cracks

- Changing crack into a joint
- Structural shielding and cladding
- Surface protection with paint

They can also be rehabilitated by strengthening of the structure component using the following methods (Danish Standards Association, 2004):

- Replacing/supplementing reinforcement
- Reinforcement in bored holes
- Adhering flat-rolled steel or fiber-composite material as external reinforcement
- Application of mortar or concrete
- Injection of cracks, voids and interstices
- Filling of cracks, voids and interstices
- Post-tensioning with external cables

The repair method for fixing cracks depends on if the crack is dormant or live. Dormant crack is unlikely to change in size after the repair. Live cracks are cracks which are expected to move (change in size) after the repair, for example due to loading. The repair method also depends on if the cracks are multiple or not.

For live multiple cracks, it is recommended, according to (Concrete Society, 2010), to use either liquid membrane or preformed membrane (bonded or unbounded sheets) as a repair method. The preformed membrane is to prefer if further cracking is expected. The advantage of using fully bonded sheets is that water has a lower chance to enter the structure in case of a damage membrane (Concrete Society, 2010).

2.6 Cracks in the Ångermanälven Bridge

According to the crack investigation report (Carlsson, 2008), the cracks are located in the edge beam, around the supports. The cracks are probably through the edge beam with a direction transverse to the bridge direction (*see Figure 2.19*).

Figure 2.19 Cracks at support 16, left side (Carlsson, 2008).

The crack widths and location have been documented by (Peab AB, 2011). The measurements of the cracks width was done as follows:

- A picture of the crack and a ruler was taken. The cracks were measured in the program EasyEL, using the ruler as a reference.
- The cracks on the top, middle and side (*see Figure 2.20*) of the right and left edge beam was measured in 2007. The biggest cracks at the top were 0.38 mm at crack number 6 for the left beam and 0.44 mm at crack number 7 for the right beam (*see Table 2.1*). In 2011, the top was documented again and some new cracks had appeared (*see Figure 2.21*). The biggest cracks at the top were now 0.26 mm at crack number 7 for the left beam and 0.36 mm at crack number 5 for the right beam. The cracks at the top, which was assumed to belong to the same section, were added to see if the development of new cracks were decreasing the old cracks.

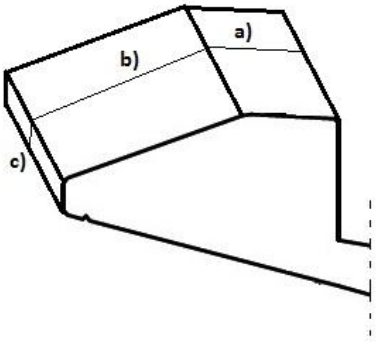

Figure 2.20 Crack location on edge beam. a) Top, b) Middle, c) Side.

Table 2.1 Crack number, location and width (mm) for the right and left edge beam at support 16 (Peab AB, 2011).

Support 16, Left Side (West)						
No.	Section	Year 2007				Year 2011
			Top	Middle	Side	Top
1	484+783,6		-	0,45	0,41	-
	484+785,7			0,28	-	-
2	484+787,6		0,32	0,27	0,38	0,24
3	484+787,9					-
4	484+788,1		0,21	-	0,27	0,22
5	484+788,6					0,16
		Σ 2,4:	0,53		0,65	Σ 2-5: 0,46
6	484+789,7		0,38	0,35	0,43	0,2
	484+790,1			-	0,28	
7	484+790,3		0,36		0,34	0,26
8	484+791,3		0,35	0,28	0,2	0,2
		Σ 6-8:	1,09			Σ 6-8: 0,66
9	484+793,9		-	-	0,35	0,19

Support 16, Right Side (East)						
No.	Section	Year 2007				Year 2011
			Top	Middle	Side	Top
1	484+783,2		0,42	0,35	0,23	0,32
2	484+787,5					0,1
3	484+787,7		0,35	0,36	0,48	0,18
						Σ 2-3: 0,28
4	484+788,9		0,34	-	0,42	0,18
5	484+789,3		0,39	0,37	0,27	0,36
6	484+789,6					0,17
7	484+790,3		0,44	0,35	-	0,27
		Σ 4,5,7:	1,17			Σ 4-7: 0,98
8	484+792,1		-	0,34	-	0,21

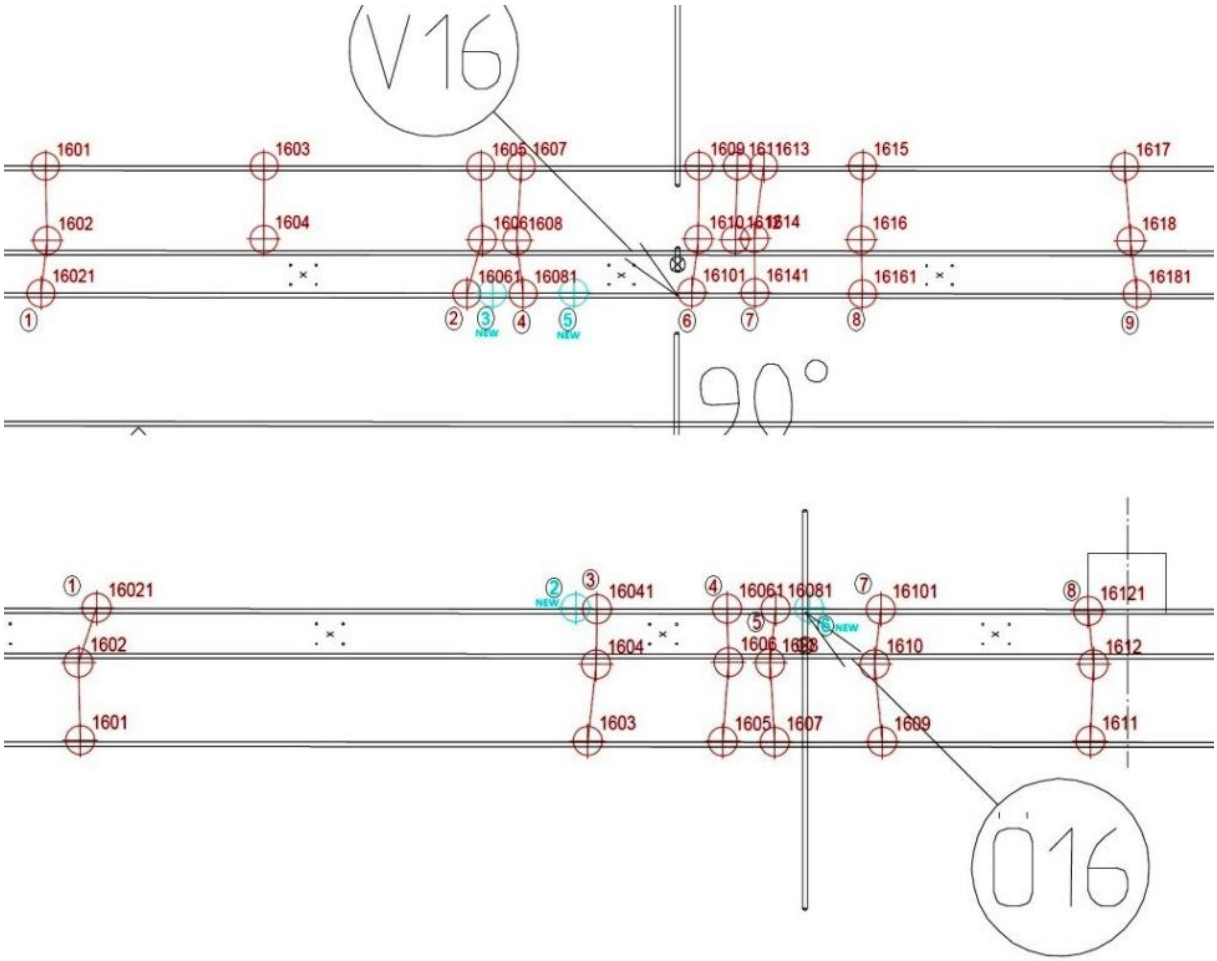

Figure 2.21 Location of the cracks on the left (above) and right (below) edge beam at support 16 (Peab AB, 2011).

3 Methods used in the Thesis

3.1 Literature Study

The project started with a literature study on the properties of reinforced concrete, regarding strength and cracking. The study also included an introduction to composite bridges. The cause, formation and time of different types of cracks were also studied for the crack investigation. Parts in BBK 94, BRO 94 including supplement nr 4 and BV Bro, utgåva 5 regarding maximum crack widths and required reinforcement area, were studied. A study of different repair methods was performed to see how the cracks could be repaired.

3.2 Design According to Swedish Standards.

The crack width in the edge beam was calculated according to BRO 94 (bridge code) with supplement nr 4, BV Bro, utgåva 5 (railway bridge code) and BBK 94 (concrete code). The stresses used in the calculations were based on the forces from the FEM-model. This was done to see if the lack of reinforcement was causing the cracks.

3.2.1 BV Bro, utgåva 5

The requirements of the design of railway bridges are according to (Banverket, 1999). The sections of BV Bro are mentioned within the parenthesis.

Crack width and exposure class

The acceptable crack width allowed in a concrete structure (*see Table 3.1*) is depending on the exposure class (*see Table 3.2*) and bridge lifetime.

Table 3.1 Maximum crack width w_k in mm and minimum crack safety factor ζ (Vägverket, 1999b).

Reinforcement type	Corrosion sensitive			Low corrosion sensitive					
Lifetime class	L0	L1	L2	L0		L1		L2	
Environmental class	ζ	ζ	ζ	ζ	w_k	ζ	w_k	ζ	w_k
A1	-	-	-	-	-	-	-	-	-
A2	1,0	1,2	1,5	0,9	0,45	1,0	0,40	1,0	0,30
A3	1,2	1,5	2,0	1,0	0,40	1,2	0,30	1,5	0,20
A4	-	2,0	2,0		-	1,5	0,20	1,5	0,20

Table 3.2 Environmental classes (Banverket, 1999).

Part of structure	Environmental class Concrete		Environmental class Reinforcement	
	L0	L1/L2	L0	L1/L2
Substructure and retaining wall	B3	B3	A2	A2
Substructure and retaining wall in seawater	B3	B3	A2	A3
Slab (used for road traffic)	B3	B4	A2	A3
Superstructure	B3	B3	A2	A2

Ångermanälven Bridge is designed for a lifetime of 120 years. The concrete slab belongs to environmental class L2 because it is part of the superstructure.

Loads

Due to assumptions, load coefficients in *Table 3.3* are the ones considered in this case (for full table see Appendix B).

Table 3.3 Load coefficients ψγ for load combination I, V:A and V:B, extraction from (BV 222-1), (Banverket, 1999).

Load combination	I Serv. build.	V:A Serv.	V:B Crack width
PERMANENT LOADS			
Own weight	1	0,95/1,05	1
Ballast		0,8/1,25	0,8/1,25
Shrinkage		0/1	0/1

Dimensions of the edge beam

Edge beams with casted balusters should be designed with a width of at least 400 mm.

The top of the edge beam should at least slope 1:20 towards the middle.

The height of the edge beam should be designed for a future track lifting of at least 150 mm (BV 441.25).

Crack width limitation

All concrete surfaces, except the edge of the bottom slabs, should use mesh as surface reinforcement with a diameter of at least 12 mm and a maximum spacing of 200 mm, if the crack width calculation does not require more reinforcement. Control of the minimum required reinforcement ratio (*see Equation (3.1)*) according to BBK 94 is not needed.

$$A_s * f_{st} \geq A_{ef} * f_{cth} \qquad (3.1)$$

Where

A_s is the reinforcement area.
f_{st} is the tensile strength of the reinforcement steel ≤ 420 MPa.
A_{ef} is the effective concrete area.
f_{cth} is a high value of the concrete strength.

If *Equation (3.1)* is used to calculate the minimum required reinforcement ratio in the edge beams, it will result in 1 % reinforcement ratio. Which is the same as the recommended reinforcement ratio according to Bro 94 (see 3.2.2).

Crack width limitation according to Bro 94 (*see Table 3.1*) is not valid in the construction stage. However *Equation (3.2)* still has to be fulfilled.

$$\frac{1}{3} * W_{k,load\ comb.I} + \frac{2}{3} * W_{k,load\ comb.V:B} < W_k \quad in\ Table\ 3.1. \qquad (3.2)$$

This specially regards bridges which in the construction stage have a different moment distribution than in the final stage (BV 442.321) (Banverket, 1999).

3.2.2 Bro 94

Requirements for the design of the reinforcement in the slab and edge beam according to (Vägverket, 1994b) and (Vägverket, 1999a). The sections of Bro 94 are mentioned within the parenthesis.

Crack width limitation

The distance between the studs in the longitudinal direction can be used instead of the crack spacing s_{rm} (*see Equation (3.7)*) in the concrete slab in the serviceability limit state. This is only valid if the studs have been placed in pair in the longitudinal direction (53.32).

The spacing in the edge beam is calculated according to *Equation (3.7)* because the distance from the studs to the edge beam is considered to be too far to have an effect on the cracking.

Design of longitudinal reinforcement in a steel-concrete composite bridge slab

Longitudinal reinforcement should be added in the concrete slab so that the total amount of reinforcement is at least 0.50 % of the concrete cross-section area. This requirement also applies to compressed concrete.

In parts of the slab which are cracked due to load combination V:A (serviceability limit state), the longitudinal reinforcement together with additional reinforcement should be at least 1.0 % of the concrete cross-section area. The maximum allowed reinforcement diameter is 16 mm (53.341).

In the concrete casting joints in the transverse direction should have longitudinal reinforcement of at least 0.70 % of the concrete cross section area (53.342) (Vägverket, 1999a).

Crack width control in concrete structures

Additional surface reinforcement should be used in structural members where shrinkage and temperature cracks usually are common (42.321).

The reinforcement should be installed so that concrete with a gravel size of 32 mm could be used in the pouring process. Processing of the concrete should also be possible (44.311).

Injection of cracks

Cracks with a width larger than 0.2 mm should be injected (44.55) (Vägverket, 1994a).

3.2.3 BBK 94

Relevant sections are mentioned within parenthesis.

Cracking criteria

These crack criteria can be used in both in serviceability and ultimate limit state. The limitation of the case depends on the boundary condition in the cracking section.

A plate, beam, column or similar part subjected to a bending moment and normal force, the concrete subjected to tensile force is considered uncracked if *Equation (3.3)* is fulfilled.

$$k\sigma_n + \sigma_m \leq k\frac{f_{ct}}{\zeta} \qquad (3.3)$$

Where

σ_n is the stress caused by normal forces (positive during tensile).
σ_m is the stress caused by moment (positive during tensile).
f_{ct} is the concrete strength.
ζ is the crack safety factor, can be varied and provided specifically for various applications of the cracking criteria (*see Table 3.1*).
k is a dimension dependent coefficient which depends on the cross-section total height h (*see Figure 3.1*).

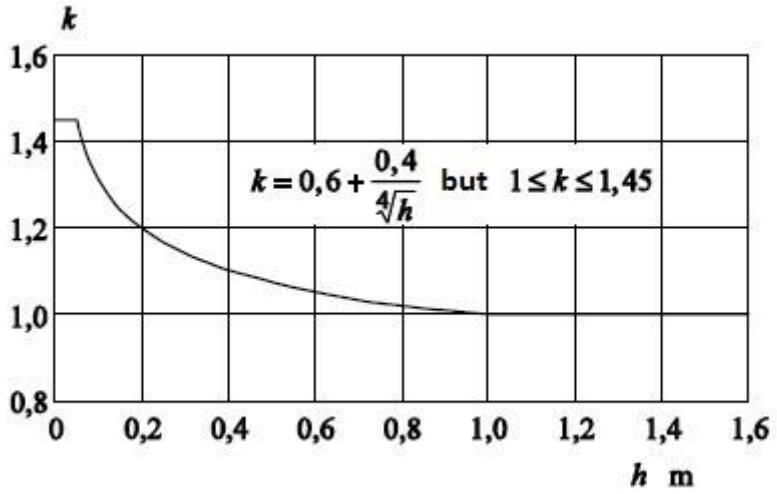

Figure 3.1 Coefficient k as a function of the cross-section total height h (Boverket, 1994).

If an incorrect assessment of the density or bending deformation does not involve personal injury, serious damage or substantial financial loss for other reasons the coefficient ζ can be set equal to 1.0 (4.5.3) (Boverket, 1994).

Calculation of the crack width

This method can be used to calculate the crack width close to the reinforcement for cracks caused by moment and/or normal force. With this method it is assumed that the minimum amount reinforcement is satisfied (*see Equation* (*3.1)*).

The characteristic crack width w_k and mean crack width w_m can be calculated according to *Equation (3.4)* and *Equation (3.5).*

$$w_k = 1.7 w_m \tag{3.4}$$

$$w_m = \nu \frac{\sigma_s}{E_s} s_{rm} \tag{3.5}$$

$$\nu = 1 - \frac{\beta}{2.5\kappa_1} * \frac{\sigma_{sr}}{\sigma_s} \geq 0.4 \tag{3.6}$$

Where

E_s is the modulus of elasticity of the reinforcement $E_s = E_{sk} = 200$ GPa.

s_{rm} is the mean crack spacing according to *Equation (3.7).*

β is a coefficient that considers the effect of the long-term load and repeated load, with
$\beta = 1.0$ at first loading.
$\beta = 0.5$ for long-term or repeated load.

κ_1 is a coefficient that accounts for bond of the reinforcement, where
$\kappa_1 = 0.8$ for ribbed bars.
$\kappa_1 = 1.2$ for intended bars.
$\kappa_1 = 1.6$ for plain bars.
For intended bars κ_1 could be set equal to 0.8, if the bar's nominal specific rib area $\geq 0.15d$ for a nominal bar diameter $d \leq 10$ mm and $\geq 0.20d$ for $d > 10$ mm.

ν is a coefficient that accounts for tension stiffness in the concrete between cracks.

σ_s is the stress in the non-prestressed reinforcement at a crack.

σ_{sr} is the value of σ_s at the load causing cracking, i.e. immediately after the formation of the crack. Long-term load ($\beta = 0.5$) and ribbed bars ($\kappa_1 = 0.8$) were used in the calculation.

The mean crack spacing s_{rm} in mm is determined according to *Equation (3.7).*

$$s_m = 50 + \kappa_1 \kappa_2 \frac{\phi}{\rho_r} \tag{3.7}$$

Where

A_{ef} is the effective area (*see Figure 3.2*), i.e. the part of the tension zone with the same center of gravity as the bonded reinforcement.

A_s is the area of bonded tensile reinforcement.

ρ_r is the effective reinforcement ratio. $\rho_r = A_s/A_{ef}$.

κ_1 is a coefficient (*see Equation (3.6)*).

κ_2 is a coefficient which accounts for the strain distribution (*see Equation (3.8) and Equation (3.9)*).

ϕ is the bar diameter in mm.

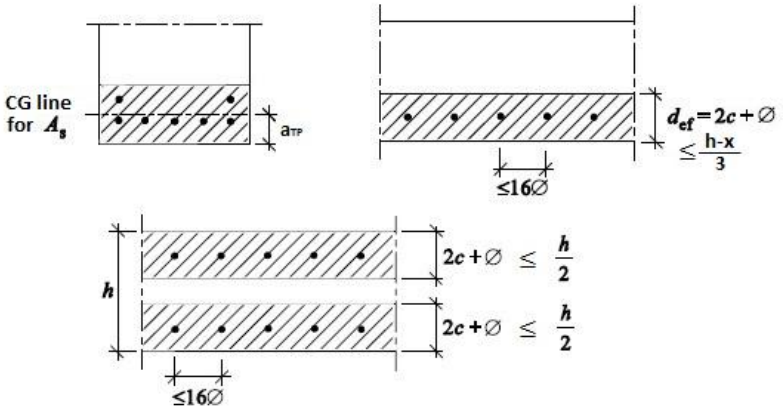

Figure 3.2 Determination of the effective concrete area A_{ef} for beam in bending (top left), slab in bending (top right) and member in tension (bottom) (Boverket, 1994).

The whole edge beam at the supports is in tension (bottom figure is used).

$$\kappa_2 = 0.125\frac{\varepsilon_1 + \varepsilon_2}{\varepsilon_1} \tag{3.8}$$

Where ε_1 and ε_2 are the strain (*see Figure 3.3*). $\varepsilon_1 > \varepsilon_2$. If the strain distribution is according to figure and the height is according to *Figure 3.2*, *Equation (3.9)* can be used to determine κ_2 (Boverket, 1994).

$$\kappa_2 = 0.25 - \frac{d_{ef}}{8(h-x)} \tag{3.9}$$

Where

d_{ef} is the height of the effective concrete area.

c is the thickness of the concrete cover.

h is the total height of the member.

x is the distance from the compressed edge to the neutral axis.

a_{TP} is the distance from the bottom edge to the CG line.

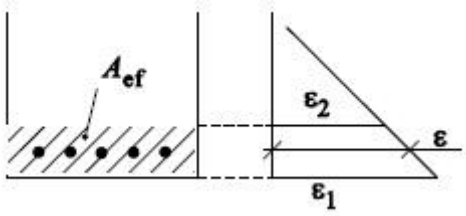

Figure 3.3 Strain ε_1 and ε_2 for determination of the coefficient κ_2 (Boverket, 1994).

3.3 Crack Investigation

3.3.1 Crack measurements

A visual inspection of the bridge was performed (as part of the thesis) first to determine different types of cracks on the edge beams, their distribution along the different spans and general locations of the cracks with the large widths. The continuity of the cracks through the edge beams and if the cracks are continuous through the whole depth of the edge beams or not were also observed. Since the noise barriers are installed, only the inner part of the edge beams are accessible for measurements.

The locations of the cracks are determined by using the provided marks on the rail track every 20 m along the bridge and transferring them to the noise barriers to have closer references to measure the crack locations. The crack locations were then determined using hand held laser rangefinder or a tape meter.

The cracks were classified to two categories according to their apparent visible width:

- Small cracks with width smaller than 0.2 mm.
- Big cracks with width greater than or equal to 0.2 mm. For which the widths were measured, recorded, and pictured for further references.

The crack widths were measured using a crack width magnifier or a crack width ruler. The width of the largest opening of the crack was recorded as the crack width.

For the transverse cracks, only the cracks that are continuous through the width and the depth of the edge beam were considered. As for the longitudinal cracks, the biggest width of the cracks was recorded along with the length of the cracks. The different casting stages of the concrete left the edge beams with casting joints which were considered as transverse cracks and measured with the same procedures.

The measurement works were more focused on the supports number 2, 3, 16 and 17 so as to compare the results with the previous investigation reports. Same procedures were adopted between supports 10 and 18. For the rest of the bridge, a quick investigation was performed recording the locations and widths of the cracks.

The spacing of a transversal crack was calculated based on its relative location to the two adjacent cracks, before and after. The average of the two distances was considered as the spacing of the crack.

3.4 FEM-Modelling

It was decided to study the cracks at support number 16 by creating a finite elements model Using LUSAS (LUSAS, 2011). As the support is only two spans from the end abutment, these 2 spans are modeled along with 3 spans length on the other side of the support (see *Figure 3.4*) this will closely model the 17 spans bridge for the load cares at hand.

Since all the supports taken into account are roller supports, one of them had to be changed into a hinged support to gain the required stability of the bridge. The final from the inner side of the bridge (support number 13) is chosen to be the hinged support.

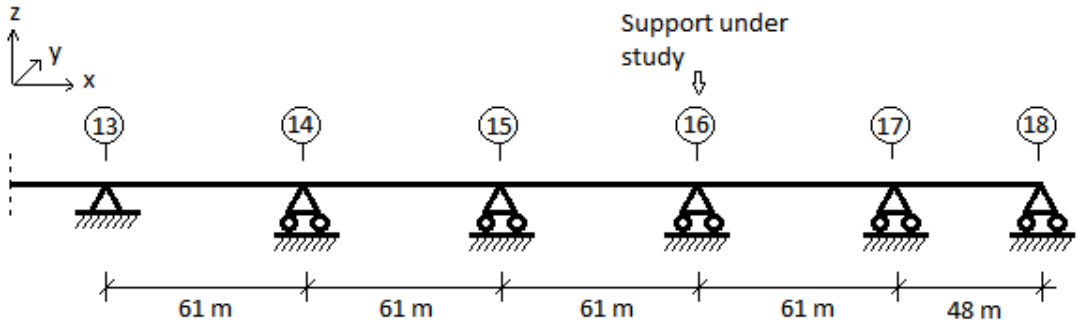

Figure 3.4 Sketch of the total spans modelled around the support under study (support number 16) and the support condition of each.

Loads on the bridge were calculated based on the concrete, steel and ballast cross sections according to the calculations by (Tyréns AB, 2004) (*see Table 3.4*).

Three load cases are applied to the bridge, dead loads of the bridge (concrete and steel own weights), ballast load and a combination of the own material weight and the ballast load with appropriate loading factor (*see Table 3.3*) to be able to study the effects of each of the cases on the bridge (*see Equation* (*3.10*)).

All the loads are applied as global distributed loads and assigned to the appropriate elements.

Loads assigned to the full section are distributed per unit area and the loads applied to the 2-D beam are distributed per unit length (see *Table 3.4*).

$$w_{tot} = \psi\gamma * w_c + \psi\gamma * w_s + \psi\gamma * w_{bal} \qquad (3.10)$$

Table 3.4 The own weight of the different materials used and the total combination of the different loads.

Material	**Concrete** w_c	**Steel** w_s	**Ballast** w_{bal}	**Total combination** w_{tot} **(min/max)**
Own weight (kN/m)	77,47	33	76,64	171,78/206,27
Own weight (kN/m^2)	11,63	4,95	12,71	26,75/32,47

3.4.1 2-D Beam model

A 2-D model was created as to have a primary idea about the internal forces in the bridge before further detailing of the bridge at the support and the spans around it. It is used also to determine points of the zero moments at which the connection between the 2-D beam and the full section detailed model is to be modeled.

The section used in the 2-D model is an I-Beam section with the same moment of inertia as the original bridge section.

3-D thick beam elements were chosen to mesh the model to include the transversal effects of the loading as well as the longitudinal ones, to include the effects of the transverse shear deformations and also because it is the most effective type of beam elements in modeling straight, constant section structures.

Quality assurance of the model was performed by four means:

- The total own weight of the bridge length was checked against the total summation of reactions from LUSAS and was found to be exactly matching (*see Table 3.5*).

Table 3.5 The results of the hand calculated total loads of the materials and the counteracting reactions of the model for quality assurance checking.

	Total load of materials
Hand calculated Loads (MN)	54,64
LUSAS Reaction summation (MN)	54,64

- Convergence analysis of the elements size was performed for the vertical displacement, longitudinal bending moment and vertical shear forces (see Appendix F). The optimum mesh size was determined based on the vertical shear force Fz convergence to be 2 m (*see Figure 3.5*).

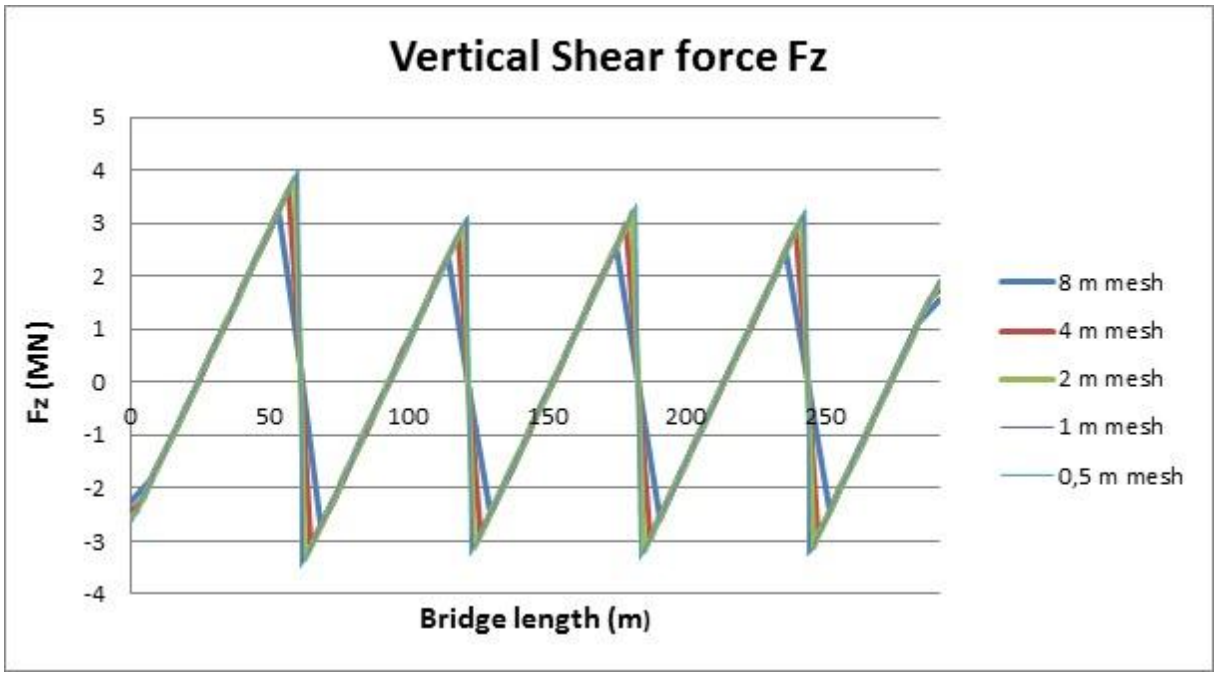

Figure 3.5 Vertical shear force along the bridge length drawn for mesh sizes 8, 4, 2, 1, and 0.5 m to for the convergence of mesh size.

- The longitudinal bending moment M_y due to own weight of the bridge was calculated with the empirical values according to (Sundquist, 2010a). The results are compared to the model output results (*see Table 3.6*). The results are similar.

Table 3.6 Longitudinal bending moment results from hand calculations and LUSAS model due to own weight of the bridge.

Position	M_{13-14}	M_{14}	M_{14-15}	M_{15}	M_{15-16}	M_{16}	M_{16-17}	M_{17}	M_{17-18}
LUSAS results (MNm)	32,28	-42,58	14,17	-32,08	17,16	-35,15	17,65	-32,29	17,72
Hand calculations (MNm)	31,65	-43,98	14,8	-29,18	14,8	-29,18	14,8	-34,42	18,2

3.4.2 Full model

A more detailed straight section of the bridge is modeled between the boundaries, determined from the 2-D model between the zero longitudinal moment points around the support 16, and is connected to the 2-D model at the same positions.

The steel section is modeled as surfaces for the different plates with assigning the thickness to each one of them. The concrete slab is modeled as four surfaces, for the four slopes of the

slab, representing the mid line of each surface and assigning a variation of the thickness to each one of them using the surface grid variation option with the appropriate thicknesses (*see Figure 3.6*).

The edge beam is modeled as a predefined I-beam section with the same properties as the edge beam. It is assigned to the edge lines of the concrete surface with an eccentricity as the distance between the concrete edge and the edge beam center of gravity. By doing this, the full connection between the edge beams and the concrete section is achieved (*see Figure 3.7*).

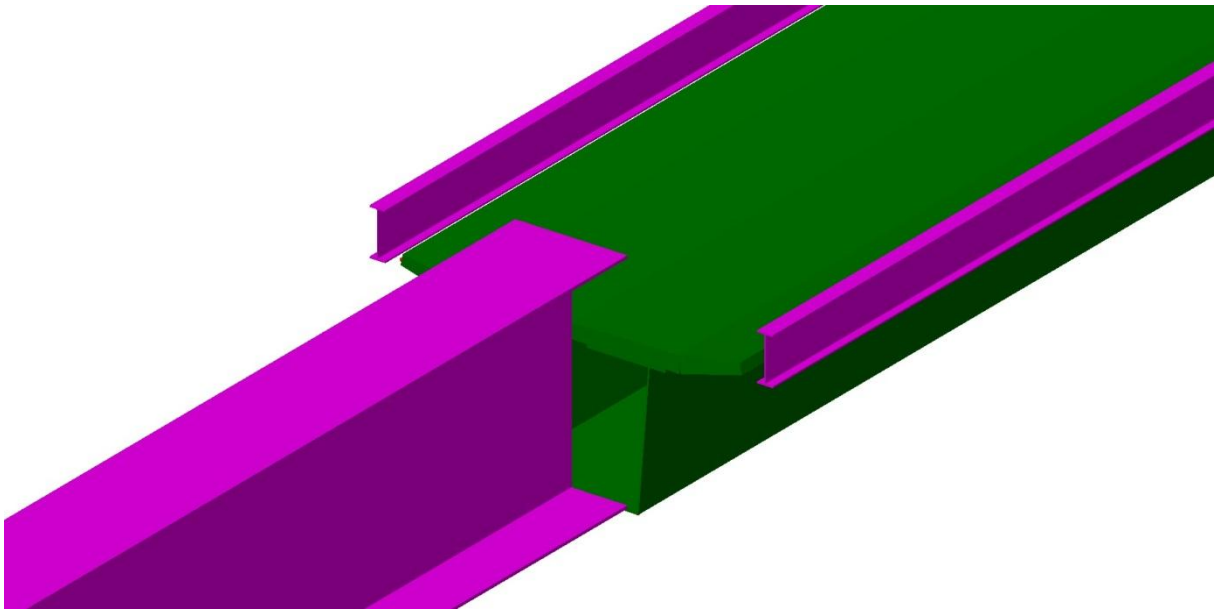

Figure 3.6 The full section and the 2-D beam section isometric view.

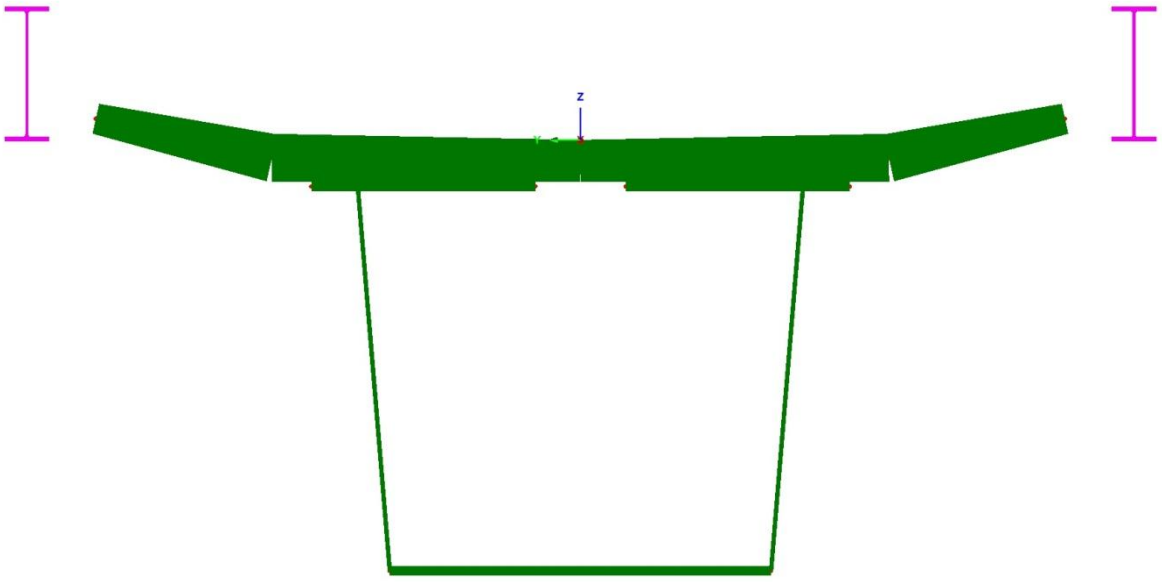

Figure 3.7 Full section of the bridge with the edge beams assigned to the edge lines of the concrete surface with the appropriate eccentricity.

Section connection (between concrete and top steel flanges)

The connection between the concrete surface and the top flanges of the steel section is modeled using a constraint equation. A tied mesh is used with a normal constraint type to fully connect them rigidly and achieve the full composite action of the whole section by maintaining the original relative position of the two surfaces after loading with the same displacements and rotations for both surfaces under all the loading cases and conditions.

The tied mesh is chosen since it does not require the matching of the mesh from both surfaces, which gives more freedom to assigning the mesh size independently to each of the surfaces. The normal constraint type of the tied mesh is chosen because it automatically defines the search direction normal to the master/slave surfaces to detect the mesh to which it is tied. By assigning the concrete surface to be the master, it is guaranteed that the steel section will only follow the displacement of the concrete section and that the forces will be transferred with the required arrangement from the concrete section, which is loaded first, to the steel flanges which will follow the behavior of the concrete as they are assigned to be the slaves of the tied mesh (*see Figure 3.8*).

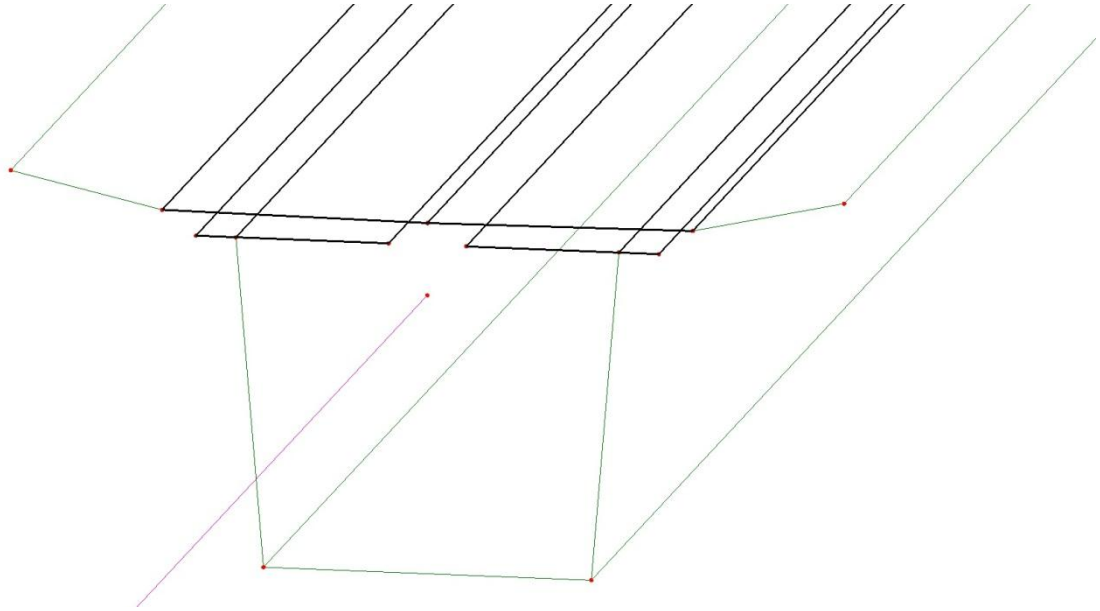

Figure 3.8 The concrete surfaces (masters) and the steel top flanges (slaves) assigned to the tied mesh constraint equation.

Model connection (between beam and full 3-D section)

The 2-D beam was inserted in the model at the point of the center of gravity of the full section to eliminate any possible extra effects due to eccentricity. The end of the beam is tied with a constraint equation to the full section to guarantee the continuity of the model with the same displacements and rotations at the connection. The geometric rigid links was the most suitable constraining equation choice for this connection since we are connecting the edge points of the full section to the end point of the 2-D beam (*see Figure 3.9*).

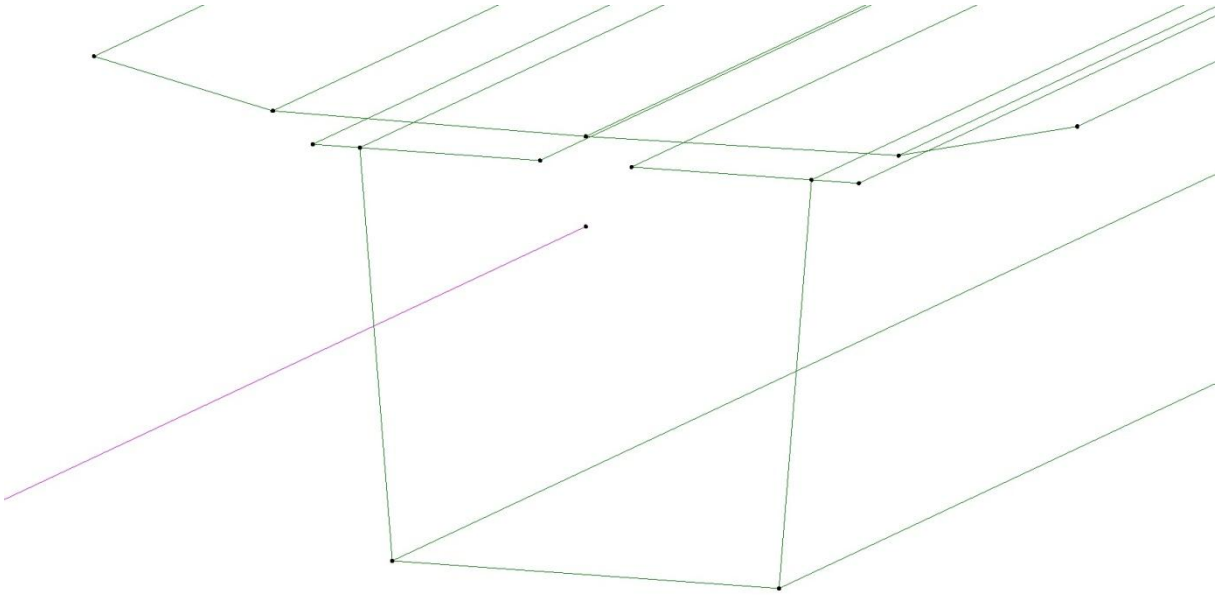

Figure 3.9 The end of the 2-D beam and the edge points of the full section assigned to the rigid links connection.

Only the edge points of the full section are linked to the end of the 2-D beam (*see Figure 3.9*) to avoid the double constraining of the top flanges as they are already linked as slaves to the concrete section (masters) with the tied mesh constraint equation. The continuity of the model after loading is checked by the shape of the deformed mesh and the final displacements (*see Figure 3.10* and *Figure 3.11*).

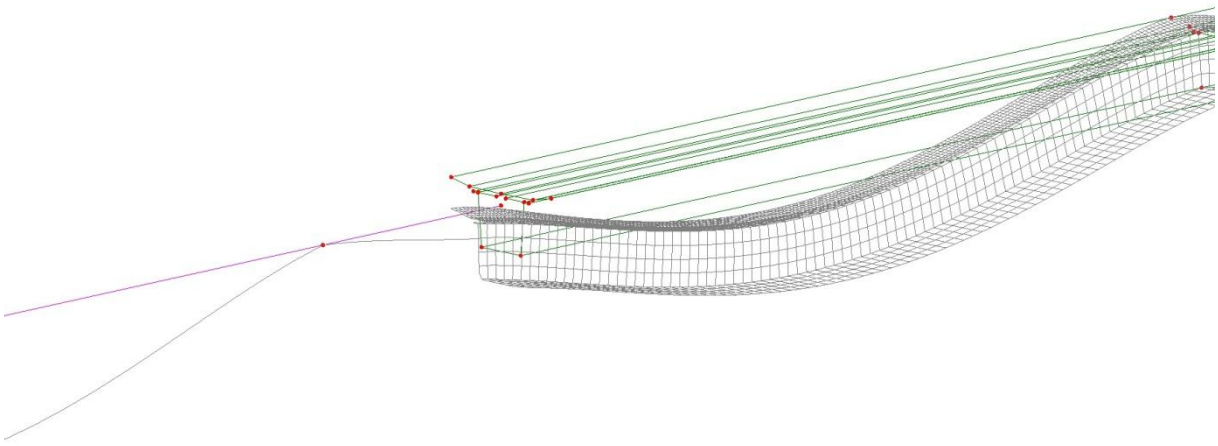

Figure 3.10 The original and deformed mesh after loading assuring the continuity of the connections before and after the loading.

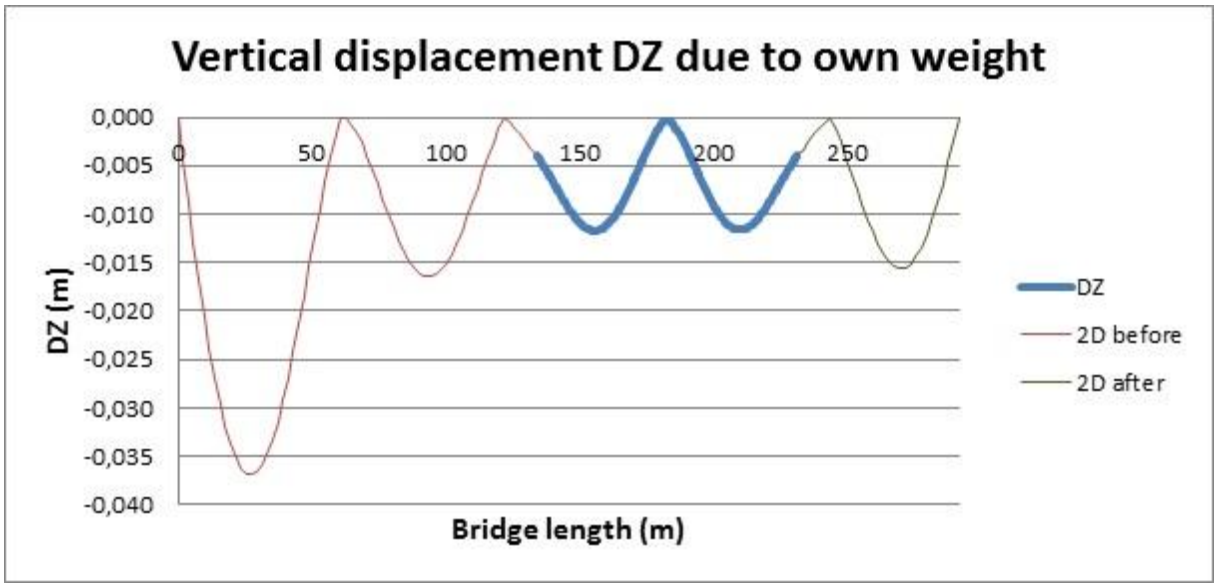

Figure 3.11 The vertical displacement due to the bridge's own weight along the bridge assuring the continuity of the model at the connections between the full section and the 2-D beam.

3.4.3 Comparison between the two models

To compare the 2-D beam model and the full model, the displacements of both are compared at the nodes with the maximum values in each span calculated for the own weight of the structure only. The general shape of the deformed model is considered as well (*see Table 3.7*). The displacement results of the 2-D model and the full model are similar.

Table 3.7 Comparison of the displacement values between 2-D and full model calculated for the own weight of the bridge at the maximum nodes of each span.

Position	Maximum (span 13-14)	span 14-15	span 15-16	span 16-17	span 17-18
Distance from origin (m)	27,50	94,50	155,80	210,30	270,00
2-D model displacement (cm)	3,80	1,30	1,80	1,80	1,30
Full model displacement (cm)	3,70	1,60	1,20	1,20	1,50

4 Calculations

4.1 Construction Method

The bridge has a composite section consisting of a steel box section and a concrete slab with edge beams. A box section for the steel beam is used as it is better suited for curved bridges since it has more warping and torsion resistance than regular I-beam sections.

The steel section was installed first using launching technique. The launching process is to prepare a launching area behind one or both abutments where the work shop manufactured steel box sections are welded together before launching. Also the areas close to the welds are painted before launching. Temporary supports are used before the abutment to hold the sections before launching and also temporary bearings are used on the intermediate supports. A so called launching nose is used to help the steel girder up on the next support because of the relatively large vertical deflection of the cantilevering girder (*see Figure 4.1*) and also to reduce the steel stresses during the launching process. After the steel section of the whole bridge is erected, it is then used to support the formwork for casting the concrete slab. The steel section is fabricated with an upwards cumber to compensate for the steel girder deflection when the concrete is poured (*see Figure 4.2*) (Sundquist, 2010b).

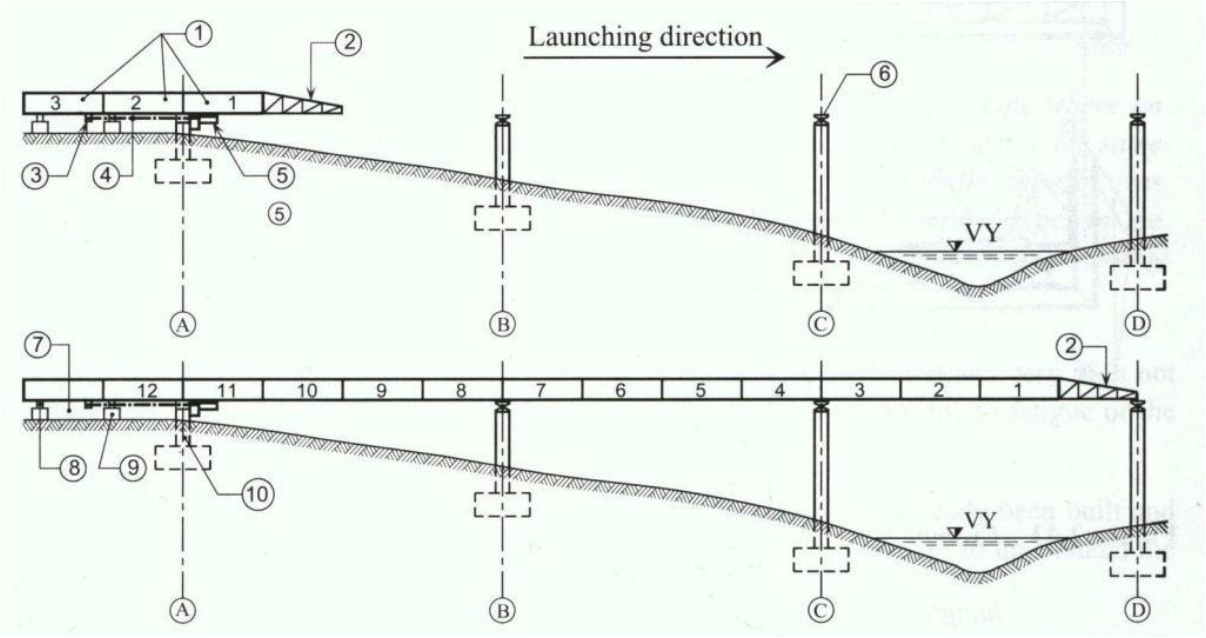

Figure 4.1 Launching technique and procedures showing 1- the welded steel parts. 2- launching nose. 4- Tensile rods. 5- Hydraulic jacks. 6- Temporary bearings. 8,9- temporary supports for launching (Sundquist, 2010b).

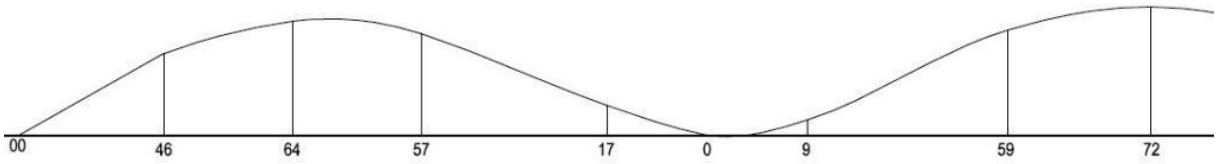

Figure 4.2 Camber in the steel section to compensate for the steel girder deflection from concrete (see Appendix A).

The steel section is varied between the supports to give the most efficient and economic use of the steel. The height of the section and the width of the bottom flange are kept constant, while the width of the top flanges increases gradually towards the support along 7 m distance from both sides. Each span consists of three different steel sections along the span length, a section for the mid-span, another section over the supports and one is used between the mid-span and the support sections. The section with the largest stiffness and area is the support section (*see Figure 4.3*).

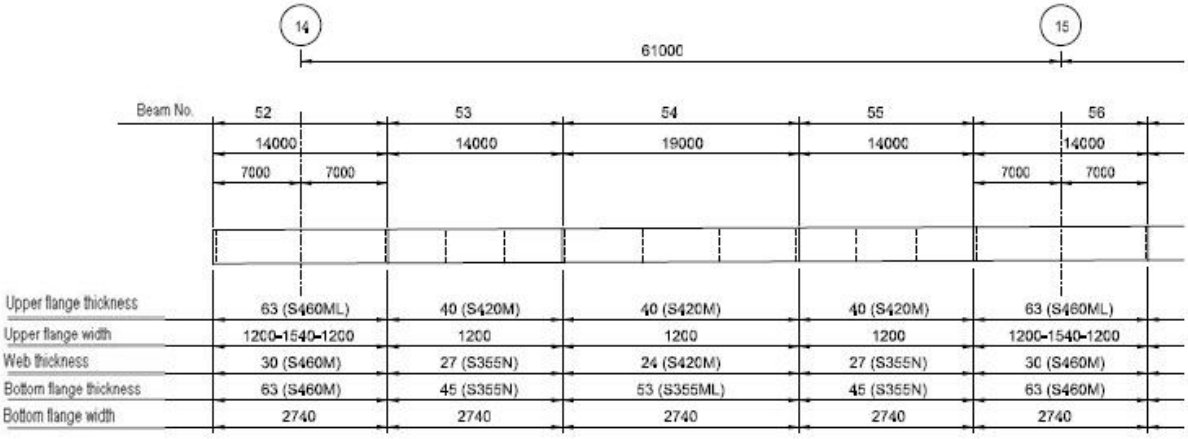

Figure 4.3 Difference in the steel plates thickness and width along the span (see Appendix A).

The bridge is divided into many segments where the concrete section is casted in a predefined sequence to decrease the tensile stresses at top of the section over the support due to the own weight of the concrete. The casting sequence is depending on casting the mid-spans segments before casting the segments over the supports (*see Figure 4.4*). By casting the mid-span segments first, the strain of the steel section is enforced to develop all along the span. When casting the concrete slab of the segment over the support, after the elongation of the top steel flanges has almost fully developed, the tensile stresses in the concrete over the supports decreases due to the own weight of the concrete. This reduces the risk for concrete cracking.

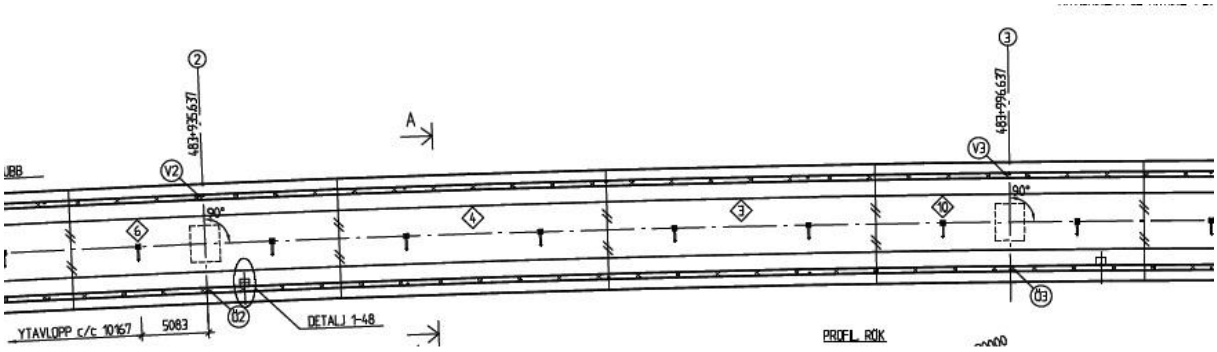

Figure 4.4 The predefined sequence of casting concrete segments showing the mid-span sections with lower numbers (3, 4) indicating earlier casting than the support segments (6, 10) (see Appendix A).

After the hardening and the curing process of the concrete is finished, the top of the concrete slab is water proofed, then the ballast is laid over, leveled and the track is installed using some equipment like a track layer. A ballast regulator is then used to form the ballast slopes and adjust their levels. After that the installation of different parts of the railway bridge like noise barriers takes place.

4.2 Creep and Shrinkage

4.2.1 Creep

For the calculation of moment of inertia, the ratio α between the modulus of elasticity for steel and concrete is used. The modulus of elasticity of concrete differs depending on the short-term or long-term effects. If the short term effect is considered the ratio α is according to *Equation (4.1)*.

$$\alpha = \frac{E_s}{E_c} \tag{4.1}$$

In the long-term effect the creep of the concrete is considered and the ratio α is according to *Equation (4.2)*.

$$\alpha = \frac{E_s}{E_{c.eff}} \tag{4.2}$$

Where

$$E_{c.eff} = \frac{E_c}{(1 + \varphi_{eff})} \tag{4.3}$$

Where φ_{eff} is the effective creep coefficient (*see Table 4.1*) (Collin et al., 2008).

Table 4.1 Creep coefficient φ in different environments (Boverket, 1994).

Environment	RH %	φ
Indoors (heated areas)	55	3
Normally outdoors and indoors (unheated areas)	75	2
Very humid environment	≥ 95	1

The effective creep coefficient used in *Table 4.1* is valid for regular concrete and if loading occurs at such an age that the compressive strength has reached the required value.

The environment at the Ångermanälven Bridge is "normally outdoors".

If loading occurs before this age and the concrete have a compressive strength which is a % of the required value, then the creep coefficient is multiplied by a factor (*see Table 4.2*) (Boverket, 1994).

Loading is assumed to occur after the compressive strength is fully reached.

Table 4.2 Correction factor at a % of the required compressive strength (Boverket, 1994).

a %	Factor
40	1,4
70	1,3
85	1,1

4.2.2 Shrinkage

The shrinkage effect in the concrete is counteracted by a compressive force, at the middle of the concrete slab, which is according to *Equation (4.4)* for the short-term load and according to *Equation (4.5)* for the long-term load (Collin et al., 2008).

$$N = \varepsilon_{cs} E_c A_c \tag{4.4}$$

$$N = \varepsilon_{cs} E_{c.eff} A_c \tag{4.5}$$

Where ε_{es} is final shrinkage (*see Table 4.3*) (Collin et al., 2008).

Table 4.3 Mean value for the final shrinkage ε_{cs} for normal concrete at normal conditions (Boverket, 1994).

Environment	RH %	ε_{cs}
Indoors (heated areas)	55	$0{,}40 \cdot 10^{-3}$
Normally outdoors and indoors (unheated areas)	75	$0{,}25 \cdot 10^{-3}$
Very humid environment	≥95	$0{,}10 \cdot 10^{-3}$

The mean value for the final shrinkage refers to free shrinkage after long time. Normal condition refers to members with at least 100 mm thickness, maximum 16-64 mm gravel size and viscous to plastic consistency.

If the shrinkage is uneven, the maximum shrinkage is $1.25\varepsilon_{cs}$ and the minimum shrinkage is $0.75\varepsilon_{cs}$ (*see Figure 4.5*) (Boverket, 1994).

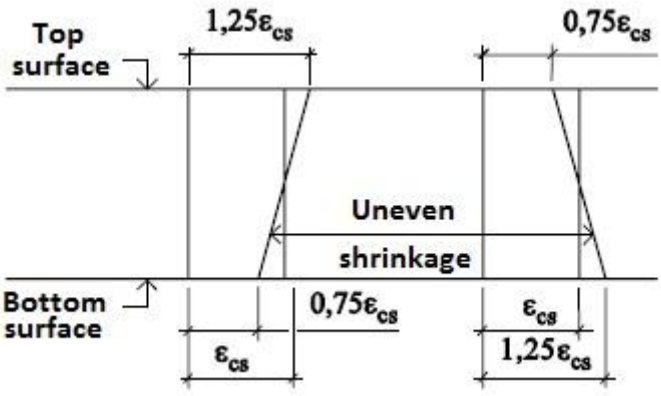

Figure 4.5 Two cases of uneven shrinkage in normal concrete (Boverket, 1994).

4.3 Section Properties

4.3.1 Simplifications

The section of the superstructure (*see Figure 4.6*) has more details than needed for the analysis of the edge beam. By making the model simpler, the calculation time can be shortened without affecting the result.

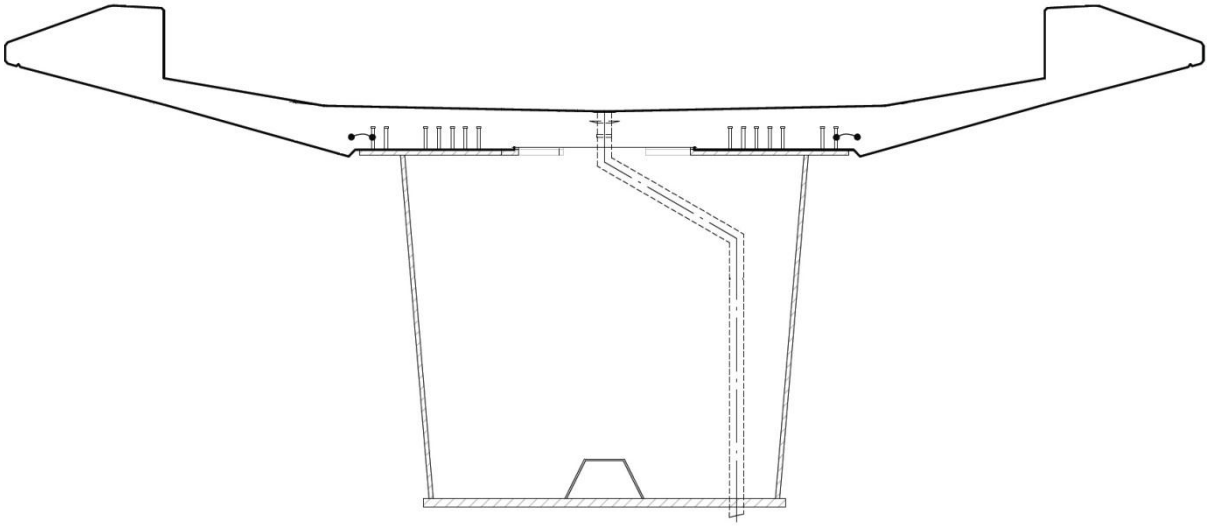

Figure 4.6 Section of the superstructure (mid-span).

The following simplifications have been made to the model (*see Figure 4.7*):

- No holes for drainage pipe in concrete and steel.
- Simplification of the concrete section near the upper flanges.
- Sharp edges instead of smooth ones.
- No studs between the steel and concrete.
- No stiffening plate at the bottom flange.
- The concrete has the same level between the two upper steel flanges
- Assuming continues slope between the edge beam and the bottom edge of the slab.
- Neglecting the outer parts of the lower steel flange.

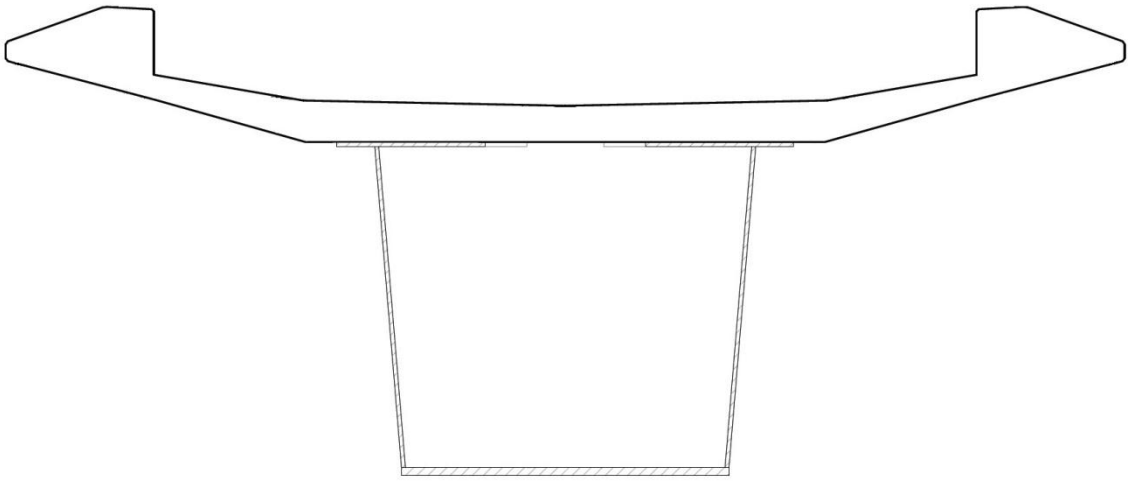

Figure 4.7 Simplified section.

4.3.2 Coordinate systems and moment of inertia calculation

Two different coordinate systems were created; one used 3-D model and one for the calculations of the moment of inertia (see Appendix C). The moment of inertia for the cross-section was calculated to get the stiffness for the 2-D model.

Due to the complexity of the cross-section, the moment of inertia was calculated with Arbitrary section property calculator (see Appendix D) in LUSAS (LUSAS, 2011).

5 Own Measurement

The investigation results for the edge beams of the bridge at the support number 16 were recorded (see *Table 5.1*). The measurements are compared to the previously done measurements in section 6.3.

The largest crack width is 0.5 mm at 484+788 at the left side edge beam. The smallest spacing of a crack is 0.2 m for the crack at 484+788.5 at the left side edge beam of the bridge also (see *Table 5.1*).

The largest casting joint is 5 mm wide at 484+779.5 just 10 m away from the support at the left side edge beam. Three other casting joints have widths of 0.5 mm at 484+758.8, and 484+799.9 at the left side edge beam, and at 484+788 at the right side edge beam (see *Table 5.1*).

Widest cracks are found closer to the support, but smaller cracks are found along the whole span as well (see *Table 5.1*).

Table 5.1 Edge beam crack measurements at support number 16. The cracks without any shown width in the table have crack width smaller than 0.2 mm.

Support 16, Left Side (West)			
Location (484+)	Width (mm)	Spacing (m)	Type
758,8	0,5		Joint
771,5		6,75	
772,3		1	
773,5		0,85	
774	0,2	0,65	
774,8		0,65	
775,3		1,1	
777	0,2	1,05	
777,4		0,3	
777,6		0,25	
777,9		0,4	
778,4		0,35	
778,6		0,2	
778,8		0,45	
779,5	5	1	Joint
780,8	0,2	0,8	
781,1		0,25	
781,3	0,3	0,45	
782		0,55	
782,4		0,45	
782,9	0,2	0,35	
783,1	0,2	0,35	
783,6		0,35	
783,8	0,4	0,4	
784,4		0,55	
784,9		0,5	
785,4		0,6	
786,1	0,3	0,9	
787,2		0,7	
787,5		0,4	
788	0,5	0,4	
788,3	0,3	0,25	
788,5	0,4	0,2	
788,7		0,55	
789,6	0,3	0,6	
789,9		0,25	
790,1	0,4	0,3	
790,5		0,3	
790,7	0,4	0,25	
791		0,5	
791,7	0,2	0,55	
792,1		0,8	
793,3		0,9	
793,9		0,45	
794,2	0,2	0,6	
795,1		0,55	
795,3		0,15	
795,4		0,35	
796		0,8	
797		0,7	
797,4		0,55	
798,1		0,55	
798,5		0,45	
799		0,7	
799,9	0,5	5,5	Joint
810			

Support 16, Right Side (East)			
Location (484+)	Width (mm)	Spacing (m)	Type
758,8			Joint
779,2		11,28	Joint
781,4	0,3	3,38	
785,9		3,13	
787,7		0,93	
787,8	0,3	0,59	
788,8	0,3	0,58	
789,0		0,29	
789,4	0,4	0,39	
789,8		0,58	
790,6	0,4	1,38	
792,5	0,3	1,72	
794,0		3,57	
799,7	0,5		Joint

6 Results

6.1 Model Results

Only the 2-D model results are used in the calculations of the stresses. Bending moment results are the only values included in the performed calculations.

Since the model is straight and horizontal, the applied loads are only vertical load. The developed section forces are only the longitudinal bending moment (My) and the vertical shear force (Fz). The vertical displacement (DZ) for long and short term loading is presented as well (see Appendix F).

The maximum section forces and displacement considered in the calculations are only according to the ballast loads. The bending moment at support number 16 is -30.5 MNm due the considered load (*see Figure 6.1*).

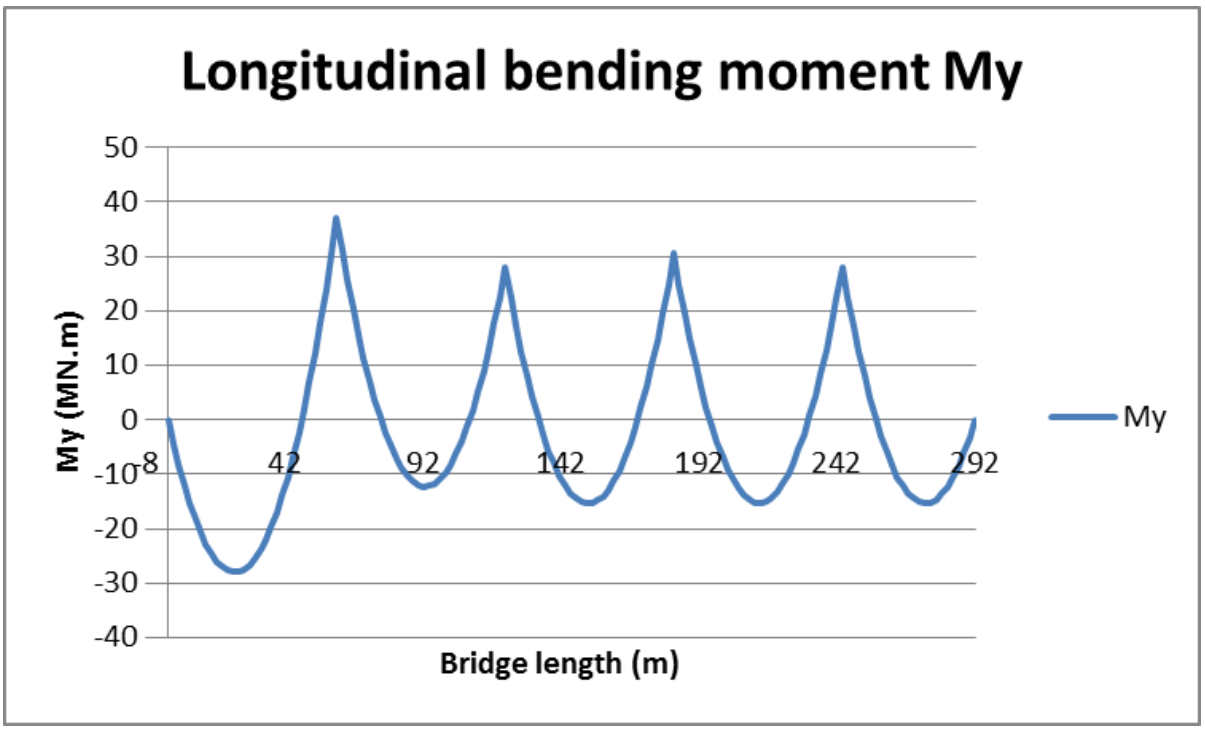

Figure 6.1 Bending moment distribution (My) along the bridge due to ballast load with the appropriate load factor.

6.2 Expected Crack Width

The amount of reinforcement needed in the edge beam (*see Table 6.1*) is designed for both 0.5 % and 1.0 % reinforcement ratio (see Appendix D).

Table 6.1 Amount of reinforcement in edge beam.

Reinforcement ratio (%)	Reinforment area (mm^2)	Design
0.5	2965	15ϕ16
1.0	5991	30ϕ16

The moment at support 16 due to shrinkage of the concrete and external loads (ballast) results in tensile stresses at the top reinforcement (*see Table 6.2*). The tensile stress results in an expected crack width in the edge beam (*see Table 6.3*).

Table 6.2 Maximum tensile stress in the top reinforcement.

Reinforcement ratio (%)	Maximum tensile stress at top reinforcemnt (MPa)
0.5	92
1.0	88

Table 6.3 Expected maximum crack width

Reinforcement ratio (%)	Crack width (mm)
0.5	0,12
1.0	0,08

6.3 Measured Cracks Width Comparison

The cracks in the edge beams measured in 2012 (own measurements) is generally bigger than the cracks measured in 2007 and 2011 (*see Table 6.4*). More cracks in range 0.2-0.4 mm were found between the cracks from the old measurements.

Table 6.4 Crack width measurement of the edge beams at support 16. The summation of the crack width in 2012 is not considering cracks smaller than 0.2 mm.

Support 16, Left Side (West)				
No.	Section	Year 2007	Year 2011	Year 2012 (section)
		Top	Top	Top
1	484+783,6	-	-	0,4 (783,8)
2	484+787,6	0,32	0,24	< 0,2 (787,5)
3	484+787,9		-	
4	484+788,1	0,21	0,22	0,5 (788,0)
5	484+788,6		0,16	0,4 (788,5)
		Σ 2,4: 0,53	Σ 2-5: 0,46	Σ: 0,9
6	484+789,7	0,38	0,2	0,3 (788,6)
7	484+790,3	0,36	0,26	0,4 (791,0)
8	484+791,3	0,35	0,2	
		Σ 6-8: 1,09	Σ 6-8: 0,66	Σ: 0,7
9	484+793,9	-	0,19	< 0,2 (793,3)

Support 16, Right Side (East)				
No.	Section	Year 2007	Year 2011	Year 2012 (section)
		Top	Top	Top
1	484+783,2	0,42	0,32	
2	484+787,5		0,1	< 0,2 (787,6)
3	484+787,7	0,35	0,18	0,3 (787,8)
			Σ 2-3: 0,28	Σ: 0,3
4	484+788,9	0,34	0,18	0,3 (789,9)
5	484+789,3	0,39	0,36	0,4 (789,4)
6	484+789,6		0,17	< 0,2 (789,7)
7	484+790,3	0,44	0,27	
		Σ 4,5,7: 1,17	Σ 4-7: 0,98	Σ: 0,7
8	484+792,1	-	0,21	

7 Conclusions and Discussion

The cracking of the edge beams were studied according to bridge codes requirements. The bridge was modeled in 2-D and the crack width was calculated and compared to the measured ones. From that the following conclusions were drawn:

7.1 Conclusions

- The calculated crack width is smaller than the measured ones.
- 1.1 % reinforcement ratio in the edge beams is believed to limit the crack width to the code limitations (0.3 mm).
- Cracks at the support may be initiated due to tensile shrinkage stresses in the concrete section.
- Other factors, related to the construction process, may have increased the tensile stresses in the edge beams at the supports and thus contributing to open the cracks to the measured cracks width values.
- Nonstructural factors (shrinkage and temperature variation) have significant effect on the edge beam cracking, since cracks are also found near to the mid-span where the concrete section is compressed due to the structural loads.
- 2-D modeling is sufficient to acquire reasonable results of the bending moment distribution, shear forces and displacements for the performed calculations.
- 3-D modeling is not needed for the studied case.
- The edge beams should have been checked for crack widths limitations according to the code requirements.

7.2 Discussion

7.2.1 Calculation and Swedish Bridge Code

The problem with the code in this case is if the edge beam on the Ångermanälven Bridge should be designed as an edge beam or as part of the slab. The code is clear on the minimum dimensions of an edge beam but there is no limitation in how big it could be.

In the original calculation, the edge beam is not structurally contributing to the slab and therefore using 0.5 % instead of 1.0 % as the longitudinal reinforcement ratio, according to 53.341 in Bro 94. But the code says that if the slab is cracked for V:A loads then 1.0% of the concrete area should be used as reinforcement area. Our calculations, which consider the edge

beams as part of the structural slab, shows that the edge beams is cracked due to shrinkage at the supports and therefore 1.0 % should have been used instead of 0.5 % in those locations.

The expected crack width in the edge beam was not checked in the original calculation. The calculations of the slab shows expected crack width of 0.162 mm in the slab directly over the top flanges. The crack width in the edge beam should, due to stress distribution of the cross-section and the fact that the top of the edge beam is located 0.8 m higher than the slab, be greater than this value.

There was no extra surface reinforcement added to the edge beams, although section 42.321 in Bro 94 states that extra surface reinforcement should be used in structural members where shrinkage and temperature cracks are common. Because of the size of the edge beam the risk for temperature cracks is relatively high.

Based on simple comparison between the reinforcement ratio and the developed crack width in our calculations, 1.1 % reinforcement in the edge beams is believed to decrease the crack width from 0.5 mm (measured) to 0.3 mm (code limit).

7.2.2 Reasons for Cracks

The shrinkage of the concrete is most likely the reason for the cracks initiation. The tensile stresses, developed due to that, are usually higher than the concrete tensile strength. Other factors will contribute to further increase of the cracks width by creating tensile stresses at the crack locations.

The external loading (for example ballast, test traffic load) will develop more tensile stresses in the concrete section over the supports increasing the width of cracks. The temperature difference between the adjacent concrete segments during curing phase (due to different hydration of concrete especially in the first hours of casting a new segment) can cause cracking. A non-homogenous joint will be created across the section which is more likely to develop cracks when the tensile loading exceeds the concrete tensile strength.

The large volume of the edge beams will lead to high temperature difference between the inside of the concrete and the outer atmosphere during the curing phase. A rapid rate of heat emissions, depending on the weather conditions and production methods, will develop through the section which is more likely to develop through cracks.

The complicated geometry of the edge beams probably caused some difficulties in their casting process, resulting in non-homogenous surfaces at some parts which can easily develop cracks under tensile loading.

7.2.3 Measurements

Using the picture of crack and ruler method (described in section 2.6), it is hard to get precise measurement due to the resolution of the pictures. The risk for human error is also bigger.

Adopting the measurement procedures described in section 3.3.1, more precise measurements are achieved. More transversal cracks were found and wider cracks were measured at the same locations of the previous investigations.

Longitudinal cracks were found on the edge beams with large widths, which can indicate a large non-structural cracking effect.

Surface spread cracks are observed with very small widths (smaller than 0.1 mm) at some locations indicating plastic shrinkage cracking and/or surface cracks from the curing process.

7.2.4 FEM Modeling

The 3-D modeling of the bridge section is very difficult and time consuming. The real behavior of the connections between adjacent surfaces is hard to model. The complicated non-linear section geometry of the bridge is difficult to represent in the model without making a lot of simplifications and so deviating from the real behavior of the section under loading. The full section modeling in 3-D is unnecessary for the studied case.

For the studied bridge, the simple 2-D model results were compared to the full section 3-D model and no significant changes in the required results were observed. Therefore a 2-D beam model of the bridge, using 3-D thick beam elements, is considered efficient enough for calculating the internal forces distribution and displacement along the bridge.

Bibliography

ACI COMMITTEE 207 1995. Effect of Restraint, Volume Change, and Reinforcement on Cracking of Mass Concrete. Farmington Hills, Michigan.

ALFREDSSON, H. & SPÅLS, J. 2008. *Cracking behaviour of concrete subjected to restraint forces : finite element analyses of prisms with different cross-sections and restraints,* Göteborg, Chalmers University of Technology.

BANVERKET 1999. *BV BRO, Utgåva 5 (BVH 583.10): Banverkets ändringar och tillägg till Vägverkets BRO 94,* Borlänge, Banverket.

BETONGFÖRENINGEN. KOMMITTÉN FÖR SPRICKOR I BETONG 1994. *Cracks in concrete structures - specially thermal cracks : report,* Stockholm, Svenska betongföreningen.

BOTNIABANAN. 2010. *Korta fakta* - [Online]. Available: http://www.botniabanan.se/Forstasidan-Historia/Om-Botniabanan/Korta-fakta/ [Accessed 2012-01-31 2012].

BOTNIABANAN. 2012. *Akvarellkarta* [Online]. Available: http://www.botniabanan.se/upload/bilder/karta/akvarellkarta.jpg [Accessed 2012-01-31 2012].

BOVERKET 1994. *Boverkets handbok om betongkonstruktioner, Band 1, Konstruktion: BBK 94,* Karlskrona, Boverket.

BURSTRÖM, P. G. 2007. *Byggnadsmaterial : uppbyggnad, tillverkning och egenskaper,* Lund, Studentlitteratur.

CARLSSON, C. 2008. Botniabanan, Långa broar i Ångermanland - Bro över ångermanälven och Nätraån, sprickor i farbanekonsol. Kontroll efter inmätning. TYRÉNS AB, Stockholm, Sweden.

CEMENT CONCRETE & AGGREGATES AUSTRALIA. 2005. *PLASTIC SETTLEMENT Cracking* [Online]. Available: http://www.concrete.net.au/publications/pdf/Settlement.pdf [Accessed 2012-02-02 2012].

COLLIN, P., JOHANSSON, B. & SUNDQUIST, H. 2008. *Steel concrete composite bridges,* Stockholm, Structural design & bridges, KTH.

CONCRETE SOCIETY 2010. *Non-structural cracks in concrete : a Concrete Society report,* London, Concrete Society.

CUSSON, D. & REPETTE, W. L. 2000. Early-age cracking in reconstructed concrete bridge barrier walls. *ACI Structural Journal,* 97**,** 438-446.

DANISH STANDARDS ASSOCIATION 2004. *Repair of concrete structures to EN 1504 : a guide for renovation of concrete structures--repair materials and systems according to the EN 1504 series,* Amsterdam ; London, Elsevier.

HOLMGREN, J., LAGERBLAD, B. & WESTERBERG, B. 2010. *Reinforced concrete structures : textbook on Concrete Structures,* Stockholm, Concrete Structures, KTH.

JOHANSSON, M. 2000. *Structural Behavior in Concrete Frame Corners of Civil Defence Shelters.* Doctor of Philosophy, Chalmers University of Technology.

LUSAS 2011. *LUSAS 14.7 user's manual*, United Kingdom.
PEAB AB 2011. Sprickmätning, bro över Ångermanälven.
RADOMSKI, W. 2002. *Bridge rehabilitation*, London, Imperial College.
STANDARDISERINGSKOMMISSIONEN I SVERIGE 2008. *Eurokod 2 : Dimensionering av betongkonstruktioner = Eurocode 2 : Design of concrete structures. Del 1-1 = Part 1-1, Allmänna regler och regler för byggnader = General rules and rules for buildings*, Stockholm, SIS.
SUNDQUIST, H. 2010a. *Beam and frame structures*, Stockholm, KTH.
SUNDQUIST, H. 2010b. *Infrastructure structures*, Stockholm, Architecture and the Built Environment, KTH Royal Institute of Technology.
SÉTRA 2010. Steel - Concrete Composite Bridges - Sustainable Design Guide. France.
THE HIGHWAY AGENCY 1987. *Design Manual for Roads and Bridges, Volume 1 - Highway Structures : Approval Procedures and General Design, Section 3 - General Design, Part 14 - Early Thermal Cracking of Concrete*, London, The Highway Agency.
TYRÉNS AB 2004. Bro över Ångermanälven, Nyland - Örnsköldsvik, km 484+396. Kap. D1, Dimensionering av farbaneplatta. Stockholm.
VÄGVERKET 1994a. *Bro. Broinspektionshandbok*, Borlänge, Vägverket.
VÄGVERKET 1994b. *Bro 94 (1994:4), 4.Betongkonstruktioner: Allmänn teknisk beskrivning för broar*, Borlänge, Vägverket.
VÄGVERKET 1999a. *Bro 94 (1999:19), 5.Stål-, trä- och aluminiumkonstruktioner: Allmänn teknisk beskrivning för broar*, Borlänge, Vägverket.
VÄGVERKET 1999b. *Bro 94 (1999:21), Supplement nr 4: Allmänn teknisk beskrivning för broar*, Borlänge, Vägverket.

Appendix A Drawings

1-596-068-10 (Summary, overview)

1-596-068-46 (Concrete slab)

1-596-068-51 (Concrete casting sequence)

1-596-068-54 (Slab reinforcement at the supports)

1-596-068-106 (steel sections 52-61, summery)

1-596-068-107 (steel sections 62-67, summery)

1-596-068-144 (steel section 58 (mid-span))

1-596-068-145 (steel section 59 (middle))

1-596-068-146 (steel section 60 (support))

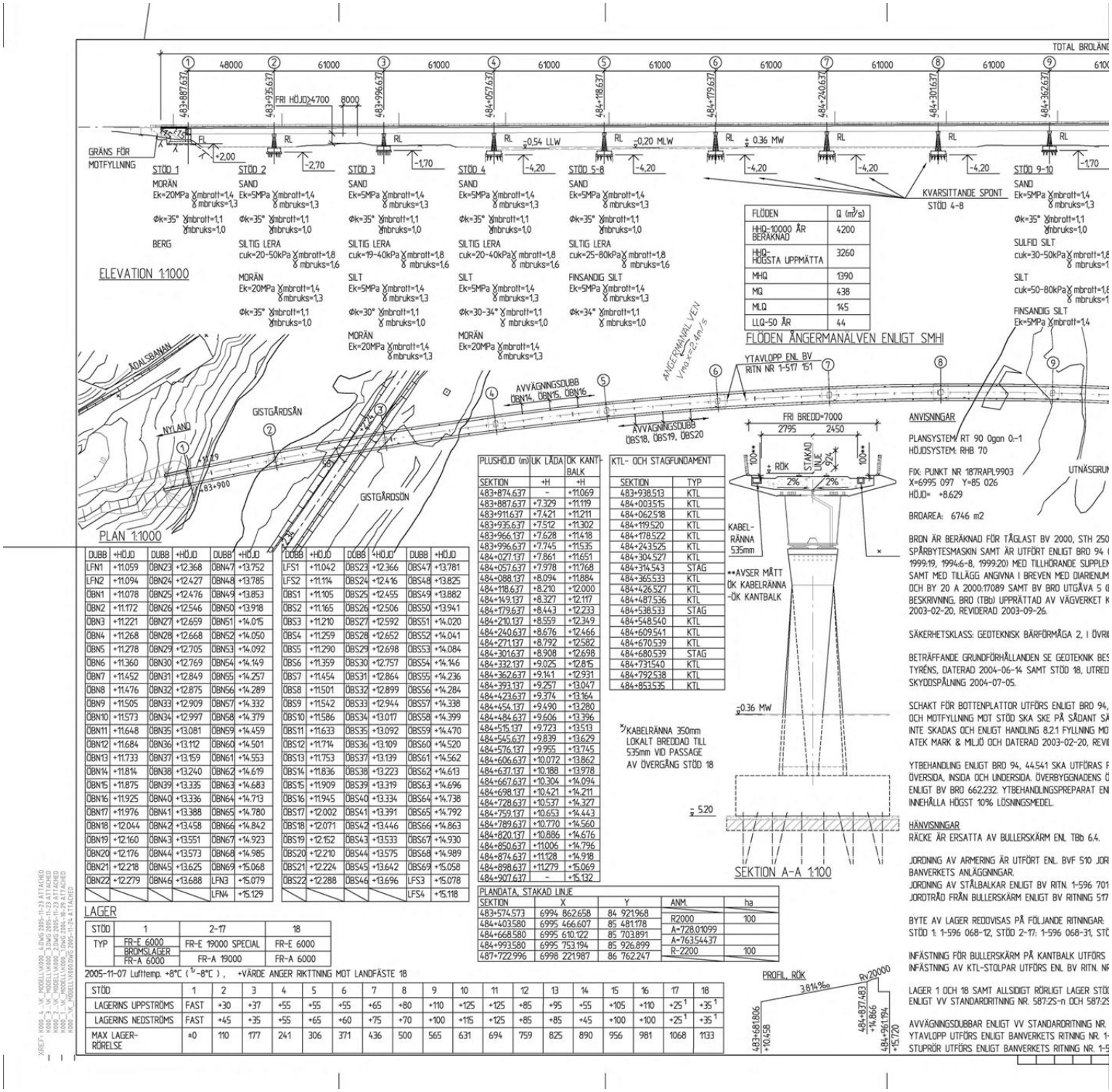

FLÖDEN	Q (m³/s)
HHQ-10000 ÅR BERÄKNAD	4200
HHQ-HÖGSTA UPPMÄTTA	3260
MHQ	1390
MQ	438
MLQ	145
LLQ-50 ÅR	44

DUBB	+HÖJD	DUBB	+HÖJD	DUBB	+HÖJD
LFN1	+11.059	ÖBN23	+12.368	ÖBN47	+13.752
LFN2	+11.094	ÖBN24	+12.427	ÖBN48	+13.785
ÖBN1	+11.078	ÖBN25	+12.476	ÖBN49	+13.853
ÖBN2	+11.172	ÖBN26	+12.546	ÖBN50	+13.918
ÖBN3	+11.221	ÖBN27	+12.659	ÖBN51	+14.015
ÖBN4	+11.268	ÖBN28	+12.668	ÖBN52	+14.050
ÖBN5	+11.278	ÖBN29	+12.705	ÖBN53	+14.092
ÖBN6	+11.360	ÖBN30	+12.769	ÖBN54	+14.149
ÖBN7	+11.452	ÖBN31	+12.849	ÖBN55	+14.257
ÖBN8	+11.476	ÖBN32	+12.875	ÖBN56	+14.289
ÖBN9	+11.505	ÖBN33	+12.909	ÖBN57	+14.332
ÖBN10	+11.573	ÖBN34	+12.997	ÖBN58	+14.379
ÖBN11	+11.648	ÖBN35	+13.081	ÖBN59	+14.459
ÖBN12	+11.684	ÖBN36	+13.112	ÖBN60	+14.501
ÖBN13	+11.733	ÖBN37	+13.159	ÖBN61	+14.553
ÖBN14	+11.814	ÖBN38	+13.240	ÖBN62	+14.619
ÖBN15	+11.875	ÖBN39	+13.335	ÖBN63	+14.683
ÖBN16	+11.925	ÖBN40	+13.336	ÖBN64	+14.713
ÖBN17	+11.976	ÖBN41	+13.388	ÖBN65	+14.780
ÖBN18	+12.044	ÖBN42	+13.458	ÖBN66	+14.842
ÖBN19	+12.160	ÖBN43	+13.551	ÖBN67	+14.923
ÖBN20	+12.176	ÖBN44	+13.573	ÖBN68	+14.985
ÖBN21	+12.218	ÖBN45	+13.625	ÖBN69	+15.068
ÖBN22	+12.279	ÖBN46	+13.688	LFN3	+15.079
				LFN4	+15.129

DUBB	+HÖJD	DUBB	+HÖJD	DUBB	+HÖJD
LFS1	+11.042	ÖBS23	+12.366	ÖBS47	+13.781
LFS2	+11.114	ÖBS24	+12.416	ÖBS48	+13.825
ÖBS1	+11.105	ÖBS25	+12.455	ÖBS49	+13.882
ÖBS2	+11.165	ÖBS26	+12.506	ÖBS50	+13.941
ÖBS3	+11.210	ÖBS27	+12.592	ÖBS51	+14.020
ÖBS4	+11.259	ÖBS28	+12.652	ÖBS52	+14.041
ÖBS5	+11.290	ÖBS29	+12.698	ÖBS53	+14.084
ÖBS6	+11.359	ÖBS30	+12.757	ÖBS54	+14.146
ÖBS7	+11.454	ÖBS31	+12.864	ÖBS55	+14.236
ÖBS8	+11.501	ÖBS32	+12.899	ÖBS56	+14.284
ÖBS9	+11.542	ÖBS33	+12.944	ÖBS57	+14.338
ÖBS10	+11.586	ÖBS34	+13.017	ÖBS58	+14.399
ÖBS11	+11.633	ÖBS35	+13.092	ÖBS59	+14.470
ÖBS12	+11.714	ÖBS36	+13.109	ÖBS60	+14.520
ÖBS13	+11.753	ÖBS37	+13.139	ÖBS61	+14.562
ÖBS14	+11.836	ÖBS38	+13.223	ÖBS62	+14.613
ÖBS15	+11.909	ÖBS39	+13.319	ÖBS63	+14.696
ÖBS16	+11.945	ÖBS40	+13.334	ÖBS64	+14.738
ÖBS17	+12.002	ÖBS41	+13.391	ÖBS65	+14.792
ÖBS18	+12.071	ÖBS42	+13.446	ÖBS66	+14.863
ÖBS19	+12.152	ÖBS43	+13.533	ÖBS67	+14.930
ÖBS20	+12.210	ÖBS44	+13.575	ÖBS68	+14.989
ÖBS21	+12.224	ÖBS45	+13.642	ÖBS69	+15.058
ÖBS22	+12.288	ÖBS46	+13.696	LFS3	+15.078
				LFS4	+15.118

PLUSHÖJD (m)	UK LÄDA	ÖK KANTBALK
SEKTION	+H	+H
483+874.637	-	+11.069
483+887.637	+7.329	+11.119
483+911.637	+7.421	+11.211
483+935.637	+7.512	+11.302
483+966.137	+7.628	+11.418
483+996.637	+7.745	+11.535
484+027.137	+7.861	+11.651
484+057.637	+7.978	+11.768
484+088.137	+8.094	+11.884
484+118.637	+8.210	+12.000
484+149.137	+8.327	+12.117
484+179.637	+8.443	+12.233
484+210.137	+8.559	+12.349
484+240.637	+8.676	+12.466
484+271.137	+8.792	+12.582
484+301.637	+8.908	+12.698
484+332.137	+9.025	+12.815
484+362.637	+9.141	+12.931
484+393.137	+9.257	+13.047
484+423.637	+9.374	+13.164
484+454.137	+9.490	+13.280
484+484.637	+9.606	+13.396
484+515.137	+9.723	+13.513
484+545.637	+9.839	+13.629
484+576.137	+9.955	+13.745
484+606.637	+10.072	+13.862
484+637.137	+10.188	+13.978
484+667.637	+10.304	+14.094
484+698.137	+10.421	+14.211
484+728.637	+10.537	+14.327
484+759.137	+10.653	+14.443
484+789.637	+10.770	+14.560
484+820.137	+10.886	+14.676
484+850.637	+11.006	+14.796
484+874.637	+11.128	+14.918
484+898.637	+11.279	+15.069
484+907.637	-	+15.132

KTL- OCH STAGFUNDAMENT	
SEKTION	TYP
483+938.513	KTL
484+003.515	KTL
484+062.518	KTL
484+119.520	KTL
484+178.522	KTL
484+243.525	KTL
484+304.527	KTL
484+314.543	STAG
484+365.533	KTL
484+426.527	KTL
484+487.536	KTL
484+538.533	STAG
484+548.540	KTL
484+609.541	KTL
484+670.539	KTL
484+680.539	STAG
484+731.540	KTL
484+792.538	KTL
484+853.535	KTL

PLANDATA, STAKAD LINJE				
SEKTION	X	Y	ANM.	ha
483+574.573	6994 862.658	84 921.968		
484+403.580	6995 466.607	85 481.178	R2000	100
484+668.580	6995 610.122	85 703.891	A=728.01099	
484+993.580	6995 753.194	85 926.899	A=763.54437	
487+722.996	6998 221.987	86 762.247	R-2200	100

LAGER

STÖD	1	2-17	18
TYP	FR-E 6000	FR-E 19000 SPECIAL	FR-E 6000
	BROMSLAGER		
	FR-A 6000	FR-A 19000	FR-A 6000

2005-11-07 Lufttemp. +8°C (▽-8°C), +VÄRDE ANGER RIKTTNING MOT LANDFÄSTE 18

STÖD	1	2	3	4	5	6	7	8	9	10	11	12	13	14	15	16	17	18
LAGERINS UPPSTRÖMS	FAST	+30	+37	+55	+55	+55	+65	+80	+110	+125	+125	+85	+95	+55	+105	+110	+25[1]	+35[1]
LAGERINS NEDSTRÖMS	FAST	+45	+35	+55	+65	+60	+75	+70	+100	+115	+125	+85	+85	+45	+100	+100	+25[1]	+35[1]
MAX LAGER-RÖRELSE	±0	110	177	241	306	371	436	500	565	631	694	759	825	890	956	981	1068	1133

ANVISNINGAR

PLANSYSTEM: RT 90 0gon 0:-1
HÖJDSYSTEM: RHB 70

FIX: PUNKT NR 187RAPL9903
X=6995 097 Y=85 026
HÖJD= +8.629

BRDAREA: 6746 m2

BRON ÄR BERÄKNAD FÖR TÅGLAST BV 2000, STH 250
SPÅRBYTESMASKIN SAMT ÄR UTFÖRT ENLIGT BRO 94 (
1999:19, 1994:6-8, 1999:20) MED TILLHÖRANDE SUPPLEN
SAMT MED TILLÄGG ANGIVNA I BREVEN MED DIARIENUM
OCH BY 20 A 2000:17089 SAMT BV BRO UTGÅVA 5 (
BESKRIVNING, BRO (TBb) UPPRÄTTAD AV VÄGVERKET K
2003-02-20, REVIDERAD 2003-09-26.

SÄKERHETSKLASS: GEOTEKNISK BÄRFÖRMÅGA 2, I ÖVRI

BETRÄFFANDE GRUNDFÖRHÅLLANDEN SE GEOTEKNIK BES
TYRÉNS, DATERAD 2004-06-14 SAMT STÖD 18, UTRED
SKYDDSPÅLNING 2004-07-05.

SCHAKT FÖR BOTTENPLATTOR UTFÖRS ENLIGT BRO 94,
OCH MOTFYLLNING MOT STÖD SKA SKE PÅ SÅDANT SÄ
INTE SKADAS OCH ENLIGT HANDLING 8.2:1 FYLLNING MO
ATEK MARK & MILJÖ OCH DATERAD 2003-02-20, REVI

YTBEHANDLING ENLIGT BRO 94, 44.541 SKA UTFÖRAS F
ÖVERSIDA, INSIDA OCH UNDERSIDA. ÖVERBYGGNADENS Ö
ENLIGT BV BRO 662.232. YTBEHANDLINGSPREPARAT EN
INNEHÅLLA HÖGST 10% LÖSNINGSMEDEL.

HÄNVISNINGAR

RÄCKE ÄR ERSATTA AV BULLERSKÄRM ENL TBb 6.4.

JORDNING AV ARMERING ÄR UTFÖRT ENL. BVF 510 JOR
BANVERKETS ANLÄGGNINGAR.
JORDNING AV STÅLBALKAR ENLIGT BV RITN. 1-596 701
JORDTRÅD FRÅN BULLERSKÄRM ENLIGT BV RITNING 517

BYTE AV LAGER REDOVISAS PÅ FÖLJANDE RITNINGAR:
STÖD 1: 1-596 068-12, STÖD 2-17: 1-596 068-31, STÖ

INFÄSTNING FÖR BULLERSKÄRM PÅ KANTBALK UTFÖRS
INFÄSTNING AV KTL-STOLPAR UTFÖRS ENL BV RITN. NR

LAGER 1 OCH 18 SAMT ALLSIDIGT RÖRLIGT LAGER STÖ
ENLIGT VV STANDARDRITNING NR. 587:2S-n OCH 587:2S

AVVÄGNINGSDUBBAR ENLIGT VV STANDARDRITNING NR.
YTAVLOPP UTFÖRS ENLIGT BANVERKETS RITNING NR. 1-
STUPRÖR UTFÖRS ENLIGT BANVERKETS RITNING NR. 1-5

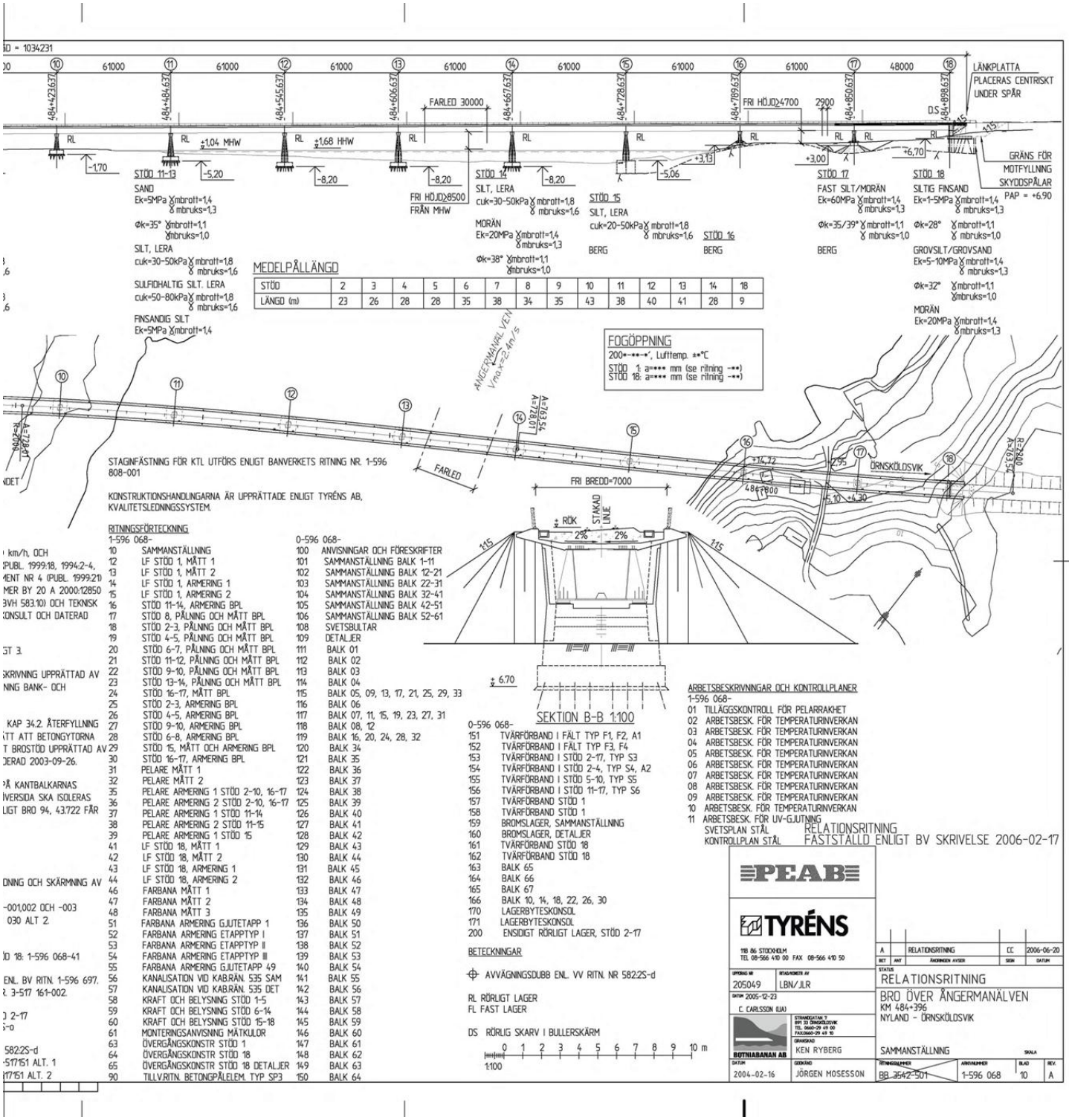
61000
48000
LÄNKPLATTA PLACERAS CENTRISKT UNDER SPÅR
FARLED 30000
FRI HÖJD≥4700
2900
GRÄNS FÖR MOTFYLLNING SKYDDSPÅLAR
PAP = +6,90
STÖD 11-13
SAND
Ek=5MPa γmbrott=1,4 γmbruks=1,3
Φk=35° γmbrott=1,1 γmbruks=1,0
SILT, LERA
cuk=30-50kPa γmbrott=1,8 γmbruks=1,6
SULFIDHALTIG SILT. LERA
cuk=50-80kPa γmbrott=1,8 γmbruks=1,6
FINSANDIG SILT
Ek=5MPa γmbrott=1,4
STÖD 14
SILT, LERA
cuk=30-50kPa γmbrott=1,8 γmbruks=1,6
MORÄN
Ek=20MPa γmbrott=1,4 γmbruks=1,3
Φk=38° γmbrott=1,1 γmbruks=1,0
STÖD 15
SILT, LERA
cuk=20-50kPa γmbrott=1,8 γmbruks=1,6
BERG
STÖD 16
BERG
STÖD 17
FAST SILT/MORÄN
Ek=60MPa γmbrott=1,4 γmbruks=1,3
Φk=35/39° γmbrott=1,1 γmbruks=1,0
BERG
STÖD 18
SILTIG FINSAND
Ek=1-5MPa γmbrott=1,4 γmbruks=1,3
Φk=28° γmbrott=1,1 γmbruks=1,0
GROVSILT/GROVSAND
Ek=5-10MPa γmbrott=1,4 γmbruks=1,3
Φk=32° γmbrott=1,1 γmbruks=1,0
MORÄN
Ek=20MPa γmbrott=1,4 γmbruks=1,3
MEDELPÅLLÄNGD
STÖD 2 3 4 5 6 7 8 9 10 11 12 13 14 18
LÄNGD (m) 23 26 28 28 35 38 34 35 43 38 40 41 28 9
FOGÖPPNING
STÖD 1: a=*** mm (se ritning -**)
STÖD 18: a=*** mm (se ritning -**)
ÄNGERMANÄLVEN
Vmax=2,1m/s
ÖRNSKÖLDSVIK
FARLED
FRI BREDD=7000
STAKAD LINJE
RÖK
SEKTION B-B 1:100
STAGNFÄSTNING FÖR KTL UTFÖRS ENLIGT BANVERKETS RITNING NR. 1-596 808-001
KONSTRUKTIONSHANDLINGARNA ÄR UPPRÄTTADE ENLIGT TYRÉNS AB, KVALITETSLEDNINGSSYSTEM.
RITNINGSFÖRTECKNING
1-596 068-
10 SAMMANSTÄLLNING
12 LF STÖD 1, MÄTT 1
13 LF STÖD 1, MÄTT 2
14 LF STÖD 1, ARMERING 1
15 LF STÖD 1, ARMERING 2
16 STÖD 11-14, ARMERING BPL
17 STÖD 8, PÅLNING OCH MÄTT BPL
18 STÖD 2-3, PÅLNING OCH MÄTT BPL
19 STÖD 4-5, PÅLNING OCH MÄTT BPL
20 STÖD 6-7, PÅLNING OCH MÄTT BPL
21 STÖD 11-12, PÅLNING OCH MÄTT BPL
22 STÖD 9-10, PÅLNING OCH MÄTT BPL
23 STÖD 13-14, PÅLNING OCH MÄTT BPL
24 STÖD 16-17, MÄTT BPL
25 STÖD 2-3, ARMERING BPL
26 STÖD 4-5, ARMERING BPL
27 STÖD 9-10, ARMERING BPL
28 STÖD 6-8, ARMERING BPL
29 STÖD 15, MÄTT OCH ARMERING BPL
30 STÖD 16-17, ARMERING BPL
31 PELARE MÄTT 1
32 PELARE MÄTT 2
35 PELARE ARMERING 1 STÖD 2-10, 16-17
36 PELARE ARMERING 2 STÖD 2-10, 16-17
37 PELARE ARMERING 1 STÖD 11-14
38 PELARE ARMERING 2 STÖD 11-15
39 PELARE ARMERING 1 STÖD 15
41 LF STÖD 18, MÄTT 1
42 LF STÖD 18, MÄTT 2
43 LF STÖD 18, ARMERING 1
44 LF STÖD 18, ARMERING 2
46 FARBANA MÄTT 1
47 FARBANA MÄTT 2
48 FARBANA MÄTT 3
51 FARBANA ARMERING GJUTETAPP 1
52 FARBANA ARMERING ETAPPTYP I
53 FARBANA ARMERING ETAPPTYP II
54 FARBANA ARMERING ETAPPTYP III
55 FARBANA ARMERING GJUTETAPP 49
56 KANALISATION VID KAB.RÄN. 535 SAM
57 KANALISATION VID KAB.RÄN. 535 DET
58 KRAFT OCH BELYSNING STÖD 1-5
59 KRAFT OCH BELYSNING STÖD 6-14
60 KRAFT OCH BELYSNING STÖD 15-18
61 MONTERINGSANVISNING MÄTKULOR
63 ÖVERGÅNGSKONSTR STÖD 1
64 ÖVERGÅNGSKONSTR STÖD 18
65 ÖVERGÅNGSKONSTR STÖD 18 DETALJER
90 TILLV.RITN. BETONGPÅLELEM. TYP SP3
0-596 068-
100 ANVISNINGAR OCH FÖRESKRIFTER
101 SAMMANSTÄLLNING BALK 1-11
102 SAMMANSTÄLLNING BALK 12-21
103 SAMMANSTÄLLNING BALK 22-31
104 SAMMANSTÄLLNING BALK 32-41
105 SAMMANSTÄLLNING BALK 42-51
106 SAMMANSTÄLLNING BALK 52-61
108 SVETSBULTAR
109 DETALJER
111 BALK 01
112 BALK 02
113 BALK 03
114 BALK 04
115 BALK 05, 09, 13, 17, 21, 25, 29, 33
116 BALK 06
117 BALK 07, 11, 15, 19, 23, 27, 31
118 BALK 08, 12
119 BALK 16, 20, 24, 28, 32
120 BALK 34
121 BALK 35
122 BALK 36
123 BALK 37
124 BALK 38
125 BALK 39
126 BALK 40
127 BALK 41
128 BALK 42
129 BALK 43
130 BALK 44
131 BALK 45
132 BALK 46
133 BALK 47
134 BALK 48
135 BALK 49
136 BALK 50
137 BALK 51
138 BALK 52
139 BALK 53
140 BALK 54
141 BALK 55
142 BALK 56
143 BALK 57
144 BALK 58
145 BALK 59
146 BALK 60
147 BALK 61
148 BALK 62
149 BALK 63
150 BALK 64
0-596 068-
151 TVÄRFÖRBAND I FÄLT TYP F1, F2, A1
152 TVÄRFÖRBAND I FÄLT TYP F3, F4
153 TVÄRFÖRBAND I STÖD 2-17, TYP S3
154 TVÄRFÖRBAND I STÖD 2-4, TYP S4, A2
155 TVÄRFÖRBAND I STÖD 5-10, TYP S5
156 TVÄRFÖRBAND I STÖD 11-17, TYP S6
157 TVÄRFÖRBAND STÖD 1
158 TVÄRFÖRBAND STÖD 1
159 BROMSLAGER, SAMMANSTÄLLNING
160 BROMSLAGER, DETALJER
161 TVÄRFÖRBAND STÖD 18
162 TVÄRFÖRBAND STÖD 18
163 BALK 65
164 BALK 66
165 BALK 67
166 BALK 10, 14, 18, 22, 26, 30
170 LAGERBYTESKONSOL
171 LAGERBYTESKONSOL
200 ENSIDIGT RÖRLIGT LAGER, STÖD 2-17
BETECKNINGAR
AVVÄGNINGSDUBB ENL. VV RITN. NR 582:2S-d
RL RÖRLIGT LAGER
FL FAST LAGER
DS RÖRLIG SKARV I BULLERSKÄRM
0 1 2 3 4 5 6 7 8 9 10 m
1:100
ARBETSBESKRIVNINGAR OCH KONTROLLPLANER
1-596 068-
01 TILLÄGGSKONTROLL FÖR PELARRAKHET
02 ARBETSBESK. FÖR TEMPERATURINVERKAN
03 ARBETSBESK. FÖR TEMPERATURINVERKAN
04 ARBETSBESK. FÖR TEMPERATURINVERKAN
05 ARBETSBESK. FÖR TEMPERATURINVERKAN
06 ARBETSBESK. FÖR TEMPERATURINVERKAN
07 ARBETSBESK. FÖR TEMPERATURINVERKAN
08 ARBETSBESK. FÖR TEMPERATURINVERKAN
09 ARBETSBESK. FÖR TEMPERATURINVERKAN
10 ARBETSBESK. FÖR TEMPERATURINVERKAN
11 ARBETSBESK. FÖR UV-GJUTNING
SVETSPLAN STÅL
KONTROLLPLAN STÅL
RELATIONSRITNING
FASTSTÄLLD ENLIGT BV SKRIVELSE 2006-02-17
PEAB
TYRÉNS
BOTNIABANAN AB
A RELATIONSRITNING CC 2006-06-20
STATUS
RELATIONSRITNING
BRO ÖVER ÅNGERMANÄLVEN
KM 484+396
NYLAND - ÖRNSKÖLDSVIK
SAMMANSTÄLLNING
205049 LBN/JLR
2005-12-23
C. CARLSSON (UA)
KEN RYBERG
2004-02-16
JÖRGEN MOSESSON
BB 3542-501
1-596 068
10
A

SITUATIONSPLAN

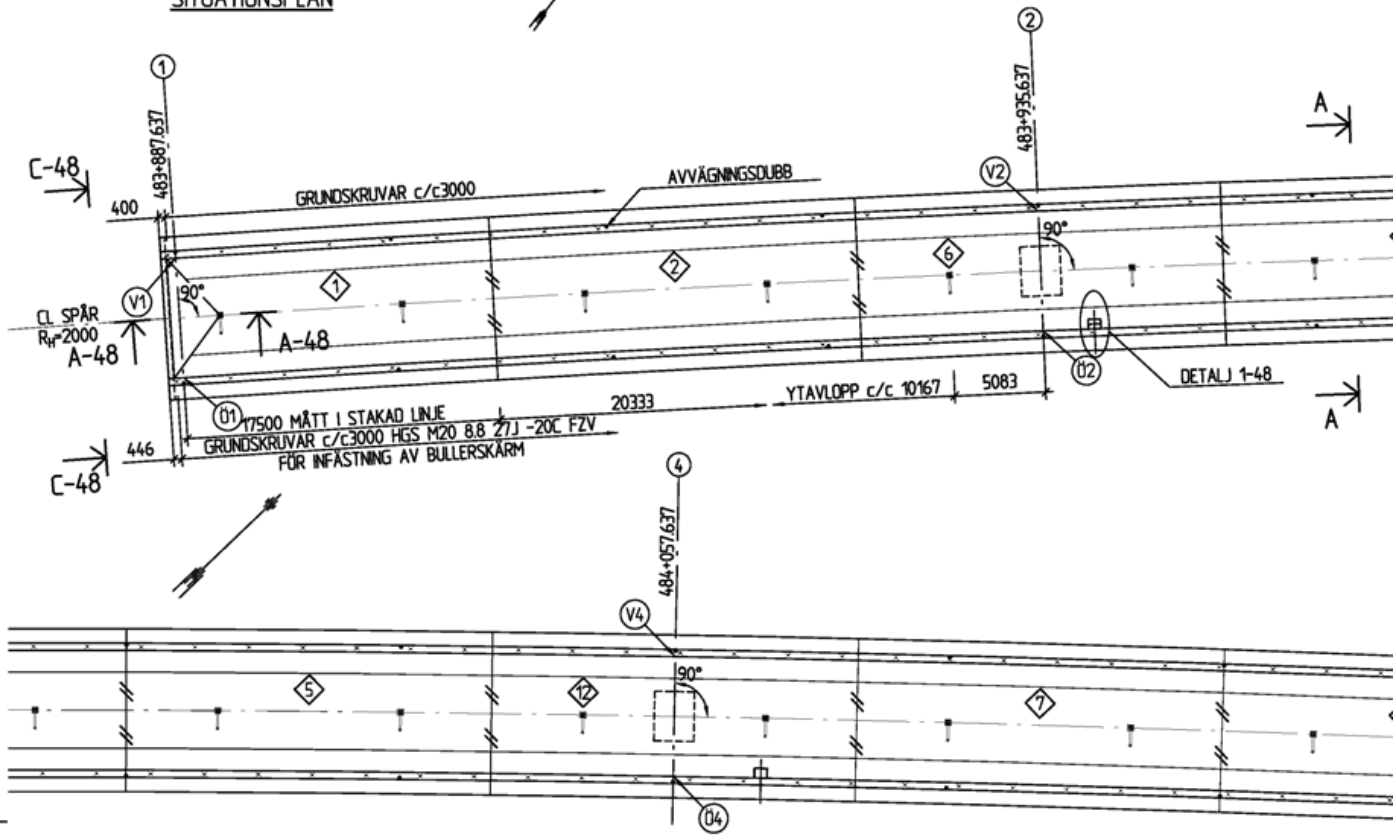

PLAN 1:200

STÖD 1-6

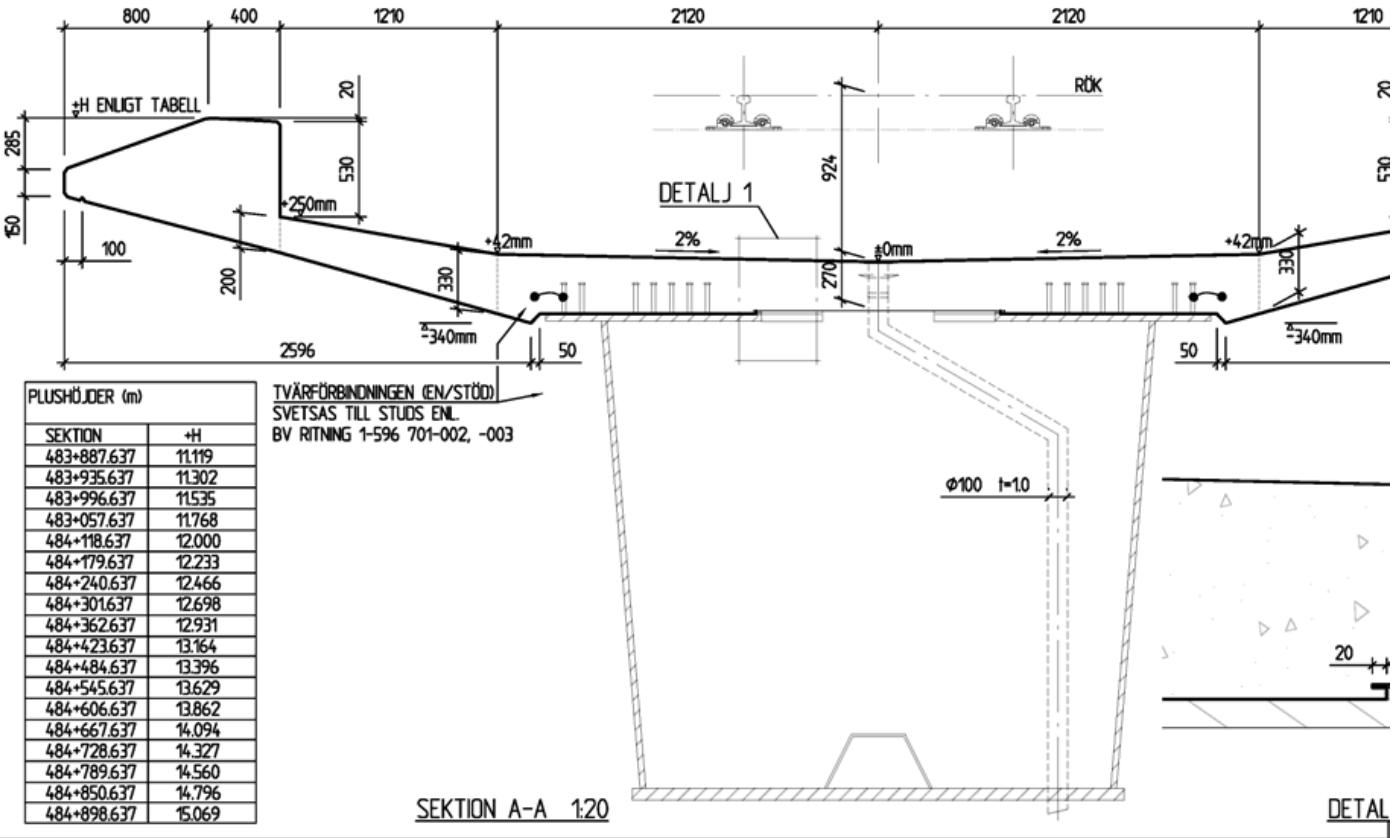

PLUSHÖJDER (m)	
SEKTION	±H
483+887.637	11.119
483+935.637	11.302
483+996.637	11.535
483+057.637	11.768
484+118.637	12.000
484+179.637	12.233
484+240.637	12.466
484+301.637	12.698
484+362.637	12.931
484+423.637	13.164
484+484.637	13.396
484+545.637	13.629
484+606.637	13.862
484+667.637	14.094
484+728.637	14.327
484+789.637	14.560
484+850.637	14.796
484+898.637	15.069

TVÄRFÖRBINDNINGEN (EN/STÖD)
SVETSAS TILL STUDS ENL.
BV RITNING 1-596 701-002, -003

SEKTION A-A 1:20

DETAL

XREF: K201_VK_MODELL VK2010WG 2004-9-2 ATTACHED

ANVISNINGAR

ALLMÄNNA ANVISNINGAR SE RITNING 1-596 068-12.

ANVISNINGAR SE RITNING 1-596 068-48.

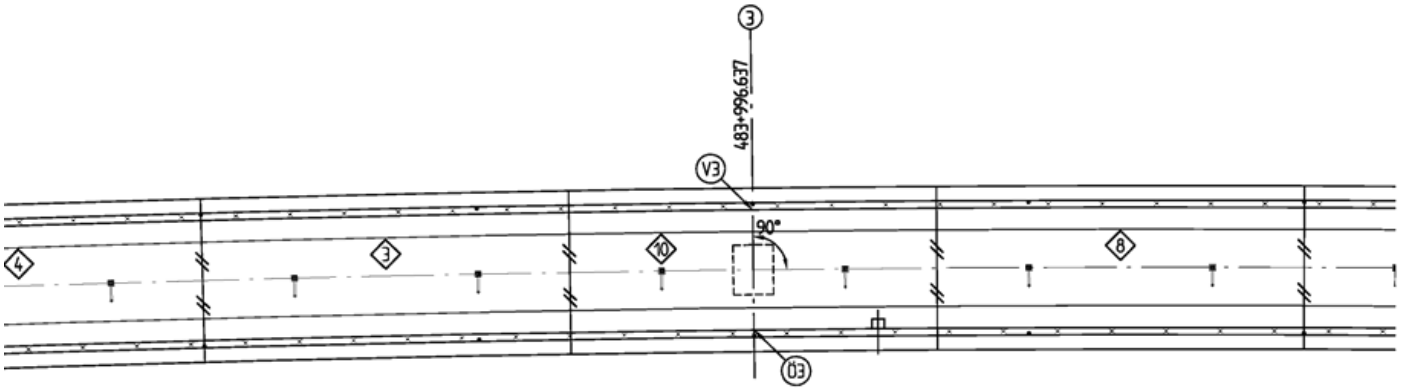

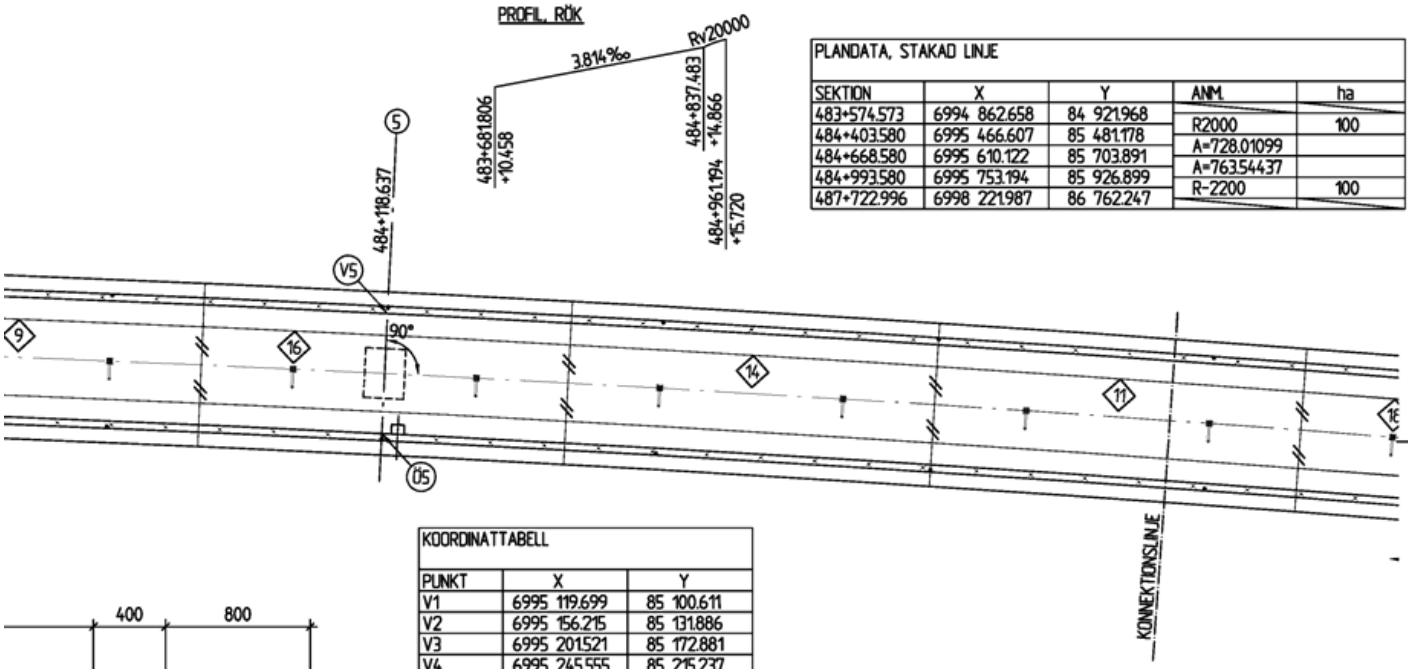

PLANDATA, STAKAD LINJE				
SEKTION	X	Y	ANM.	ha
483+574.573	6994 862.658	84 921.968		
484+403.580	6995 466.607	85 481.178	R2000	100
484+668.580	6995 610.122	85 703.891	A=728.01099	
484+993.580	6995 753.194	85 926.899	A=763.54437	
487+722.996	6998 221.987	86 762.247	R-2200	100

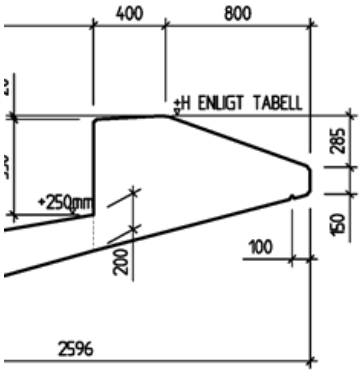

KOORDINATTABELL		
PUNKT	X	Y
V1	6995 119.699	85 100.611
V2	6995 156.215	85 131.886
V3	6995 201.521	85 172.881
V4	6995 245.555	85 215.237
V5	6995 288.277	85 258.917
V6	6995 329.647	85 303.880
V7	6995 369.627	85 350.083
V8	6995 408.179	85 397.484
V9	6995 445.268	85 446.038
V10	6995 480.871	85 495.705
V11	6995 515.039	85 546.327
V12	6995 548.133	85 597.632
V13	6995 580.491	85 649.382
V14	6995 612.467	85 701.345
V15	6995 644.417	85 753.294
V16	6995 676.686	85 805.024
V17	6995 709.596	85 856.325
V18	6995 736.137	85 896.237
Ö1	6995 115.428	85 105.721
Ö2	6995 151.823	85 136.892
Ö3	6995 196.977	85 177.750
Ö4	6995 240.865	85 219.966
Ö5	6995 283.445	85 263.501
Ö6	6995 324.678	85 308.314
Ö7	6995 364.525	85 354.364
Ö8	6995 402.949	85 401.607
Ö9	6995 439.914	85 450.000
Ö10	6995 475.386	85 499.484
Ö11	6995 509.471	85 549.981
Ö12	6995 542.507	85 601.196
Ö13	6995 574.829	85 652.889
Ö14	6995 606.790	85 704.829
Ö15	6995 638.753	85 756.799
Ö16	6995 671.055	85 808.580
Ö17	6995 704.018	85 859.964
Ö18	6995 730.634	85 899.989

REVIDERING A FASTSTÄLLD ENLIGT BV SKRIVELSE 2005-03-22

FASTSTÄLLD ENLIGT BV SKRIVELSE 2004-10-05

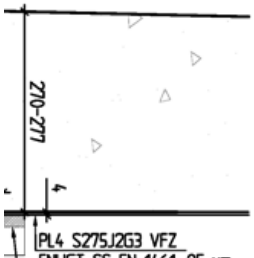

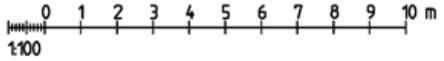

PEAB

TYRÉNS

118 86 STOCKHOLM
TEL. 08-566 410 00 FAX 08-566 410 50

STRANDGATAN 7
891 33 ÖRNSKÖLDSVIK
TEL. 0660-29 49 00
FAX.0660-29 49 10

BOTNIABANAN AB

UPPDRAG NR	RITAD/KONSTR AV
205049	LBN/JLR

DATUM 2004-09-15

C. CARLSSON (UA) R. FREDRIKSSON (KA)

GRANSKAD KEN RYBERG

DATUM	GODKÄND
2004-09-15	JÖRGEN MOSESSON

B		RELATIONSRITNING	CC	2006-06-20
A	2	KONSOLT.JOCKLEK		05-01-28
BET	ANT	ÄNDRINGEN AVSER	SIGN	DATUM

STATUS

RELATIONSRITNING

BRO ÖVER ÅNGERMANÄLVEN
KM 484+396
NYLAND - ÖRNSKÖLDSVIK

FARBANA, MÅTT 1

SKALA

RITNINGSNUMMER	ARKIVNUMMER	BLAD	REV.
BB 3542-501	1-596 068	46	B

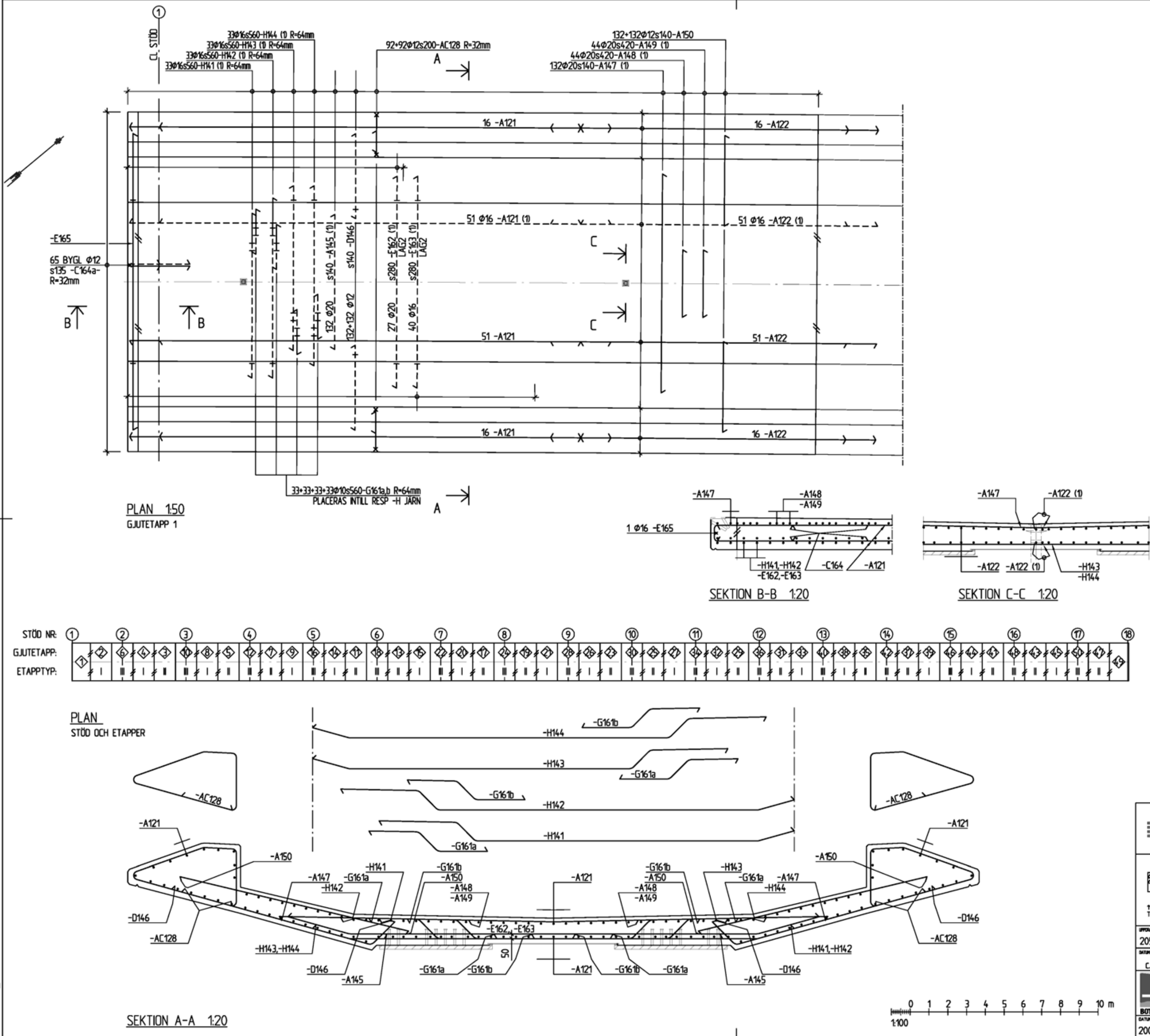

ANVISNINGAR

ALLMÄNNA ANVISNINGAR SE RITNING 1-596 068-12.

ARMERING: B500B

SPECIFICERINGEN AV ARMERINGEN ÄR I PRINCIP UTFÖRD EFTER ANVISNING 1A 1979 UTGIVEN AV BASTA. BOCKNINGSTYPER ENL. TYPBLAD 2A 1979. RAK STÅNG BETECKNAS DOCK ALLTID MED TYP A OCH NUMMER. DISTANSKLOTSAR FÖR ARMERING SKA UTFÖRAS MED BETONG AV ANLÄGGNINGSCEMENT I KULÖR SÅ LIKA ÖVRIG BETONG SOM MÖJLIGT.

TÄCKANDE BETONGSKIKT (TB): KANTBALK = 45 MM I ÖVRIGT: 40 MM DÄR EJ ANNAT FRAMGÅR I RESPEKTIVE ARMERINGSFIGUR. TB GÄLLER ÄVEN FÖR EV. MONTERINGSARMERING. MONTERINGSSTÅNG MAX Φ12.

ANVÄNDA ARMERINGSLITTERA: 121, 122, 128, 141-150, 161-165

SKARVLÄNGD: DÄR EJ ANNAT ANGES
Φ12 = 600 MM
Φ16 = 800 MM
Φ20 =1000 MM
Φ25 =1250 MM
Φ32 =1600 MM

BOCKNINGSRADIER

Φ12 = 64 MM
Φ16 = 100 MM
Φ20 = 100 MM
Φ25 = 160 MM
Φ32 = 200 MM

HÄNVISNING
JORDNING AV ARMERING SKA UTFÖRAS ENLIGT BV RITNING 1-596 701-001, -002. ARMERING KLENARE ÄN Φ16 FÅR EJ ANVÄNDAS. ARMERING SOM INGÅR I JORDSLINGA SVETSAS MELLAN ANSLUTNINGARNA OCH SKALL TYDLIGT MÄRKAS OCH ANVÄNDAS FÖR FORTSATT SLINGA TILL GJ.

BETECKNINGAR

BYGL BYGEL

GJUTFOG ENL. BRO 94, 44.424.

(1) ANPASSAS TILL YTAVLOPP

FASTSTÄLLD ENLIGT BV SKRIVELSE 2004-11-22

PEAB

TYRÉNS
118 86 STOCKHOLM
TEL 08-566 410 00 FAX 08-566 410 50

A	RELATIONSRITNING		CC	2006-06-20
BET	ÄNT	ÄNDRINGEN AVSER	SIGN	DATUM

UPPDRAG NR 205049 — HANDLÄGGARE LBN/JLR
DATUM 2004-10-19
C. CARLSSON (UA) — R. FREDRIKSSON (KA)
BOTNIABANAN AB — KEN RYBERG
DATUM 2004-10-19 — GODKÄND JÖRGEN MOSESSON

STATUS: RELATIONSRITNING
BRO ÖVER ÅNGERMANÄLVEN
KM 484+396
NYLAND - ÖRNSKÖLDSVIK
FARBANA, ARMERING GJUTETAPP 1

RITNINGSNUMMER BB 3542-501 — 1-596 068 — BLAD 51 — REV. A

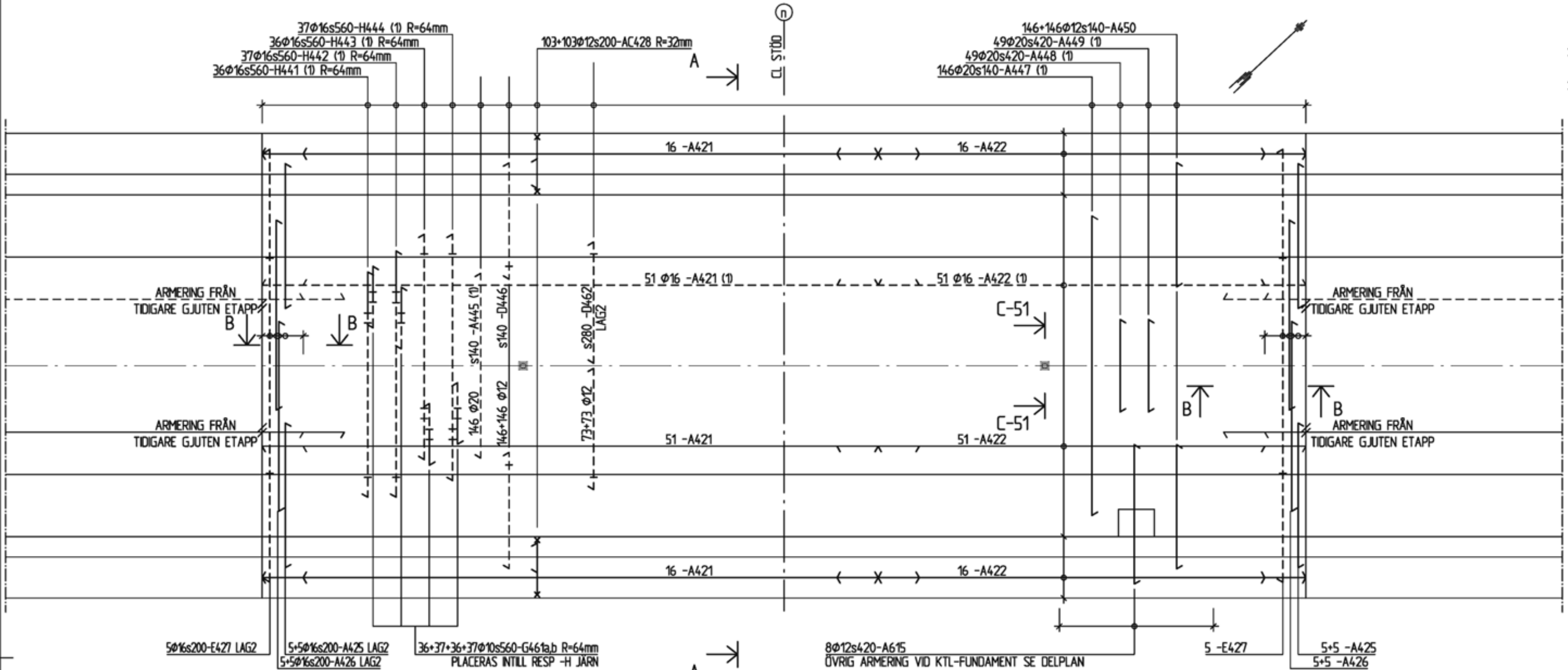

PLAN 1:50

GJUTETAPP 10

GÄLLER ÄVEN ETAPP 6, 12, 16, 18, 22, 24, 28, 30, 34, 36, 40, 42, 46, 48 OCH 50

ETAPPTYP III, PLAN -51

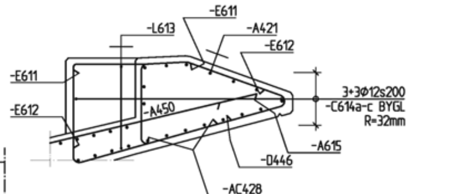

SEKTION C-C 1:20

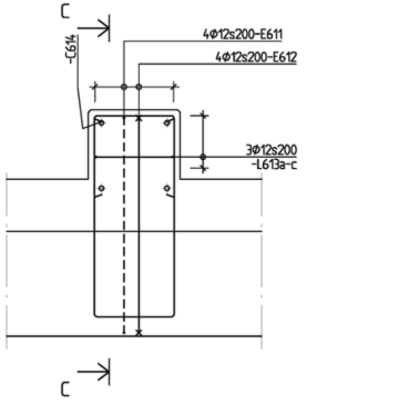

DELPLAN 1:20

KTL-KONSOL, TOTALT 19 ST

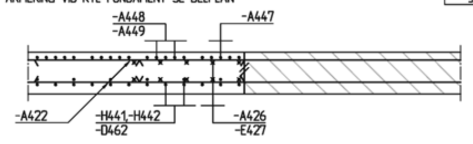

SEKTION B-B 1:20

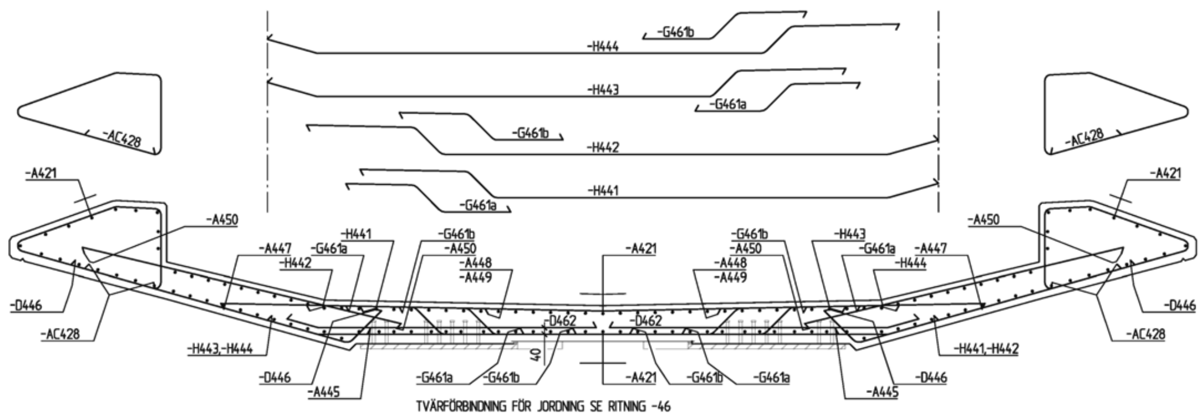

SEKTION A-A 1:20

ANVISNINGAR

SE RITNING 1-596 068-51.

ANVÄNDA ARMERINGSLITTERA: 421, 422, 425-428, 441-450, 461, 462, 611-615

JORDNING AV ARMERING SKA UTFÖRAS ENLIGT BV RITNING 1-596 701-001, -002.
ARMERING KLENARE ÄN Ø16 FÅR EJ ANVÄNDAS.

BETECKNINGAR

BYGL BYGEL

GJUTFOG ENL. BRO 94, 44.424.

(1) ANPASSAS TILL YTAVLOPP

FASTSTÄLLD ENLIGT BV SKRIVELSE 2004-11-22

0 1 2 3 4 5 6 7 8 9 10 m
1:100

PEAB

TYRÉNS

118 86 STOCKHOLM
TEL 08-566 410 00 FAX 08-566 410 50

A	RELATIONSRITNING	CC	2006-06-20

RELATIONSRITNING

BRO ÖVER ÅNGERMANÄLVEN
KM 484+396
NYLAND - ÖRNSKÖLDSVIK

UPPDRAG NR 205049 | HANDLÄGGARE LBN/JLR
DATUM 2004-10-19
C. CARLSSON (UA) R. FREDRIKSSON (KA)
BOTNIABANAN AB
STRANDGATAN 7, 891 33 ÖRNSKÖLDSVIK, TEL 0660-29 49 00, FAX 0660-29 49 10
GRANSKAD KEN RYBERG
DATUM 2004-10-19 | GODKÄND JÖRGEN MOSESSON

FARBANA, ARMERING TYPETAPP III

BB 3542-501 | 1-596 068 | BLAD 54

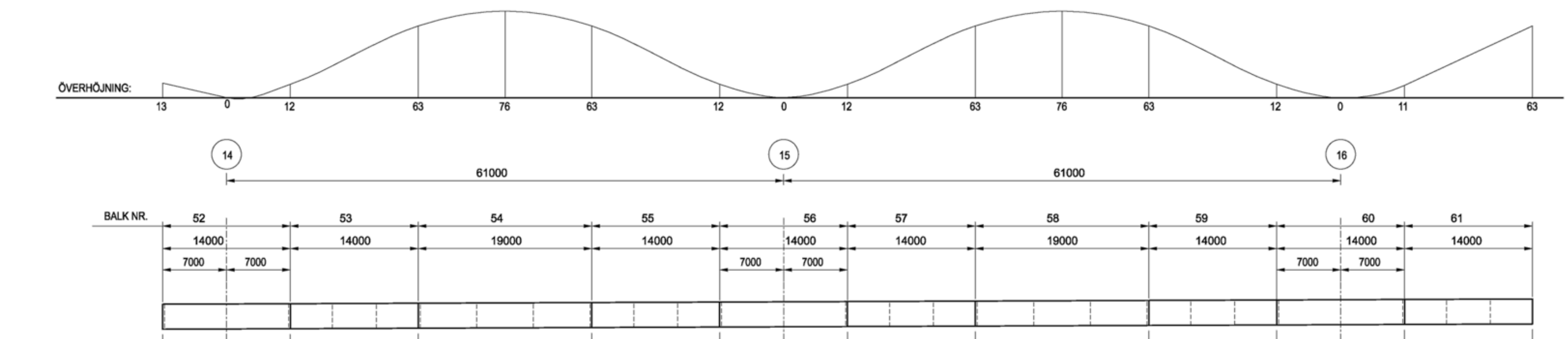

BALK NR.	52	53	54	55	56	57	58	59	60	61
Längd	14000 (7000 / 7000)	14000	19000	14000	14000 (7000 / 7000)	14000	19000	14000	14000 (7000 / 7000)	14000
ÖVERFLÄNS TJOCKLEK	63 (S460ML)	40 (S420M)	40 (S420M)	40 (S420M)	63 (S460ML)	40 (S420M)	40 (S420M)	40 (S420M)	63 (S460ML)	40 (S420M)
ÖVERFLÄNS BREDD	1200-1540-1200	1200	1200	1200	1200-1540-1200	1200	1200	1200	1200-1540-1200	1200
LIVPLÅT TJOCKLEK	30 (S460M)	27 (S355N)	24 (S420M)	27 (S355N)	30 (S460M)	27 (S355N)	24 (S420M)	27 (S355N)	30 (S460M)	27 (S355N)
BOTTENPLÅT TJOCKLEK	63 (S460M)	45 (S355N)	53 (S355ML)	45 (S355N)	63 (S460M)	45 (S355N)	53 (S355ML)	45 (S355N)	63 (S460M)	45 (S355N)
BOTTENPLÅT BREDD	2740	2740	2740	2740	2740	2740	2740	2740	2740	2740

VY
1:250

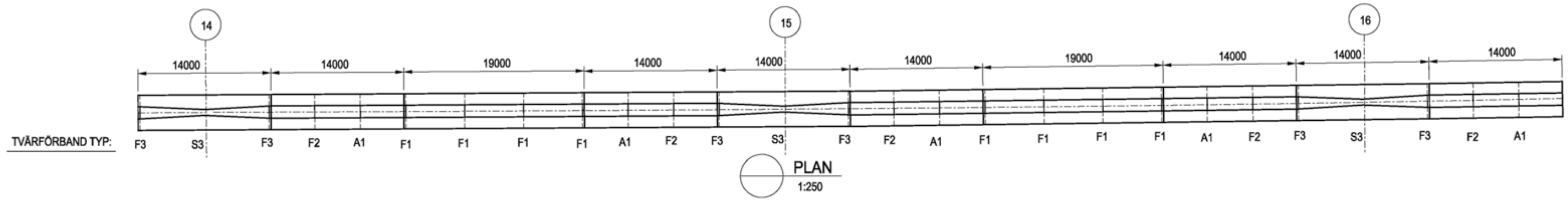

PLAN
1:250

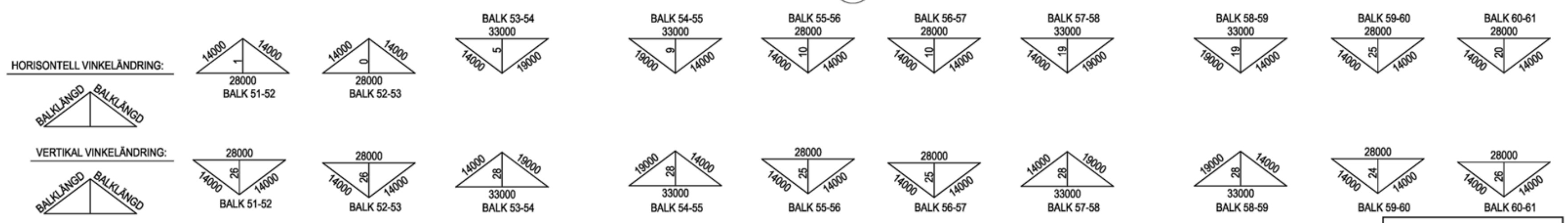

RELATIONSRITNING
FASTSTÄLLD ENLIGT BV SKRIVELSE 2004-06-07

* LÄNGDMÅTT GÄLLER I CL JÄRNVÄG.
* BRYTNING I HORISONTAL- OCH VERTIKALPLANET I ALLA BALKSKARVAR.

0 1 2 3 4 5 6 7 8 9 10 m
1:100

PEAB
SCAN BRIDGE
strukturas
UPPDRAG NR 21050 | KONSTR AV HQ | DATUM 2004-06-11 | RITAD AV AT

TYRÉNS
UPPDRAG NR 205049 | RITAD/KONSTR AV
DATUM 2004-04-21
C. CARLSSON (UA) | P.O. THOMASSON (KA)
STRANDGATAN 7, 891 33 ÖRNSKÖLDSVIK, TEL 0660-29 49 00, FAX 0660-29 49 10
BOTNIABANAN AB
GRANSKAD KEN RYBERG
DATUM 2004-04-21 | GODKÄND JÖRGEN MOSESSON

REV	ÄNDRINGEN AVSER	DATUM
A	RELATIONSRITNING	2006-06-20
–	FASTSTÄLLD ARBETSRITNING	2004-06-11

STATUS
RELATIONSRITNING
BRO ÖVER ÅNGERMANÄLVEN
KM 484 + 396
NYLAND - ÖRNSKÖLDSVIK
STÅLÖVERBYGGNAD
SAMMANSTÄLLNING BALK 52-61
SKALA 1:250
RITNINGSNUMMER BB-3542-501 | ARKIVNUMMER 1-596068 | BLAD 106 | REV. A

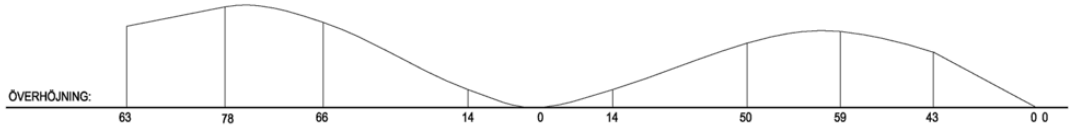

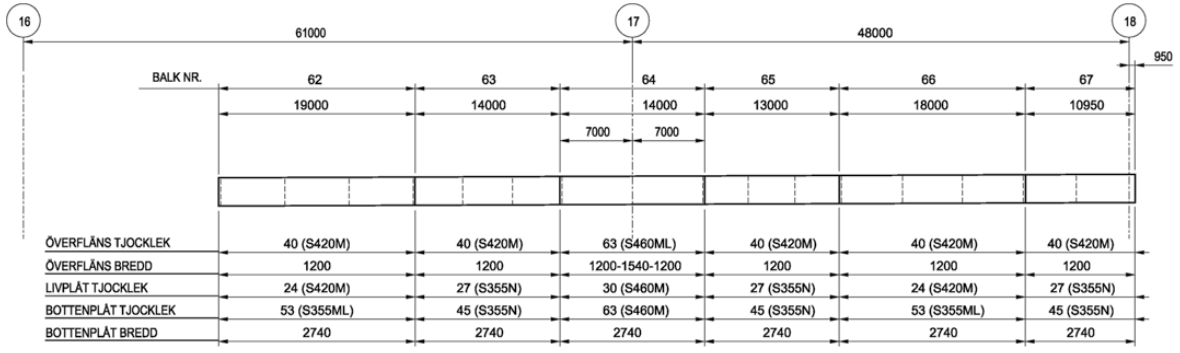

VY
1:250

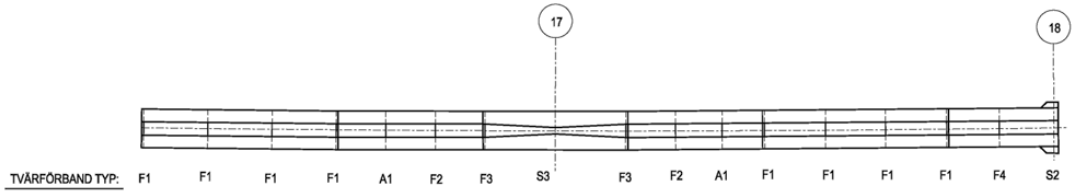

PLAN
1:250

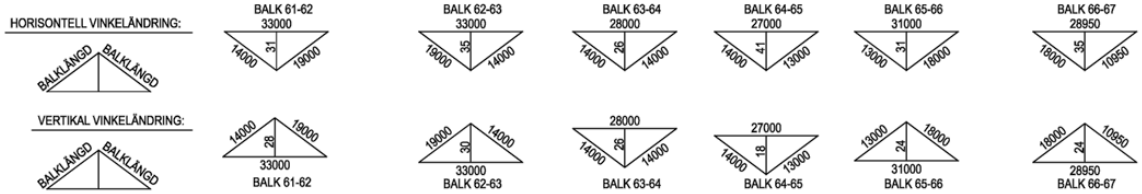

* LÄNGDMÅTT GÄLLER I CL JÄRNVÄG.

* BRYTNING I HORISONTAL- OCH VERTIKALPLANET I ALLA BALKSKARVAR.

0 1 2 3 4 5 6 7 8 9 10 m
1:100

RELATIONSRITNING
FASTSTÄLLD ENLIGT BV SKRIVELSE 2004-06-07

PEAB
SCAN BRIDGE
strukturas
KONSTR AV: HG
UPPDRAG NR: 2050
DATUM: 2004-06-11
RITAD AV: AT
TYRÉNS
UPPDRAG NR: 205049
RITAD/KONSTR AV:
DATUM: 2004-04-21
C. CARLSSON (LIA) P.O. THOMASSON (KA)
STRANDGATAN 7
BYP. 33 ÖRNSKÖLDSVIK
TEL. 0660-29 49 00
FAX.0660-29 49 10
GRANSKAD: KEN RYBERG
DATUM: 2004-04-21
GODKÄND: JÖRGEN MOSESSON

REV	ÄNDRINGEN AVSER	SIGN	DATUM
A	RELATIONSRITNING		2005-06-20
	FASTSTÄLLD ARBETSRITNING		2004-06-11

STATUS: RELATIONSRITNING

BRO ÖVER ÅNGERMANÄLVEN
KM 484 + 396
NYLAND – ÖRNSKÖLDSVIK
STÅLÖVERBYGGNAD
SAMMANSTÄLLNING BALK 62-67

SKALA 1:250

KONSTRUKTIONSNR	ARKIVNUMMER	BLAD	REV.
BB-3542-501	1-596068	107	A

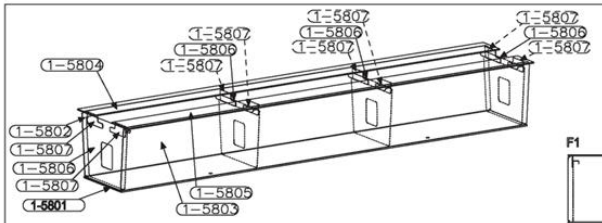

3D BALK

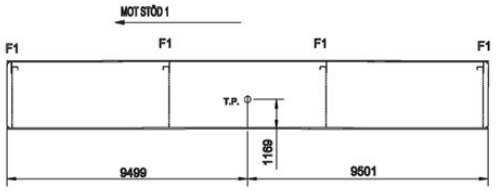

TYNGDPUNKT
1:100

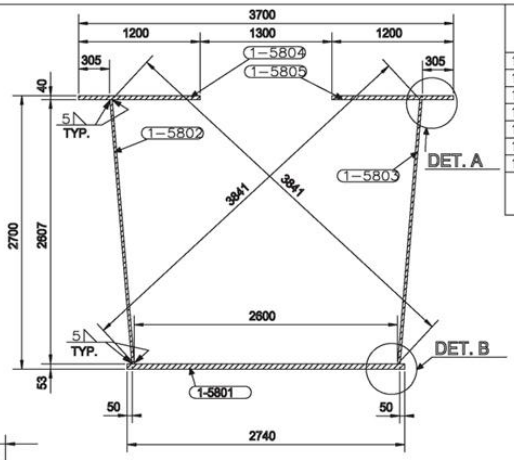

SEKTION C-C
1:25

Pos.	Ant.	Benämning	Dimension Längd mm	Dimension Bredd mm	Vikt	Kvalitet	Anm.
1-5801	1	PL53*2740	19003	2740	21645.3	S355ML	
1-5802	1	PL24*2645	19007	2631	9360.4	S420M	
1-5803	1	PL24*2645	19012	2631	9362.9	S420M	
1-5804	1	PL40*1200	18998	1200	7158.1	S420M	
1-5805	1	PL40*1200	19004	1200	7160.2	S420M	
1-5806	4	PL12*3000	2724	2994	2563.6	S355J2G3	
1-5807	8	PL20*443	1137	443	505.0	S355J2G3	
		Total stålvikt			57755.4	kg	

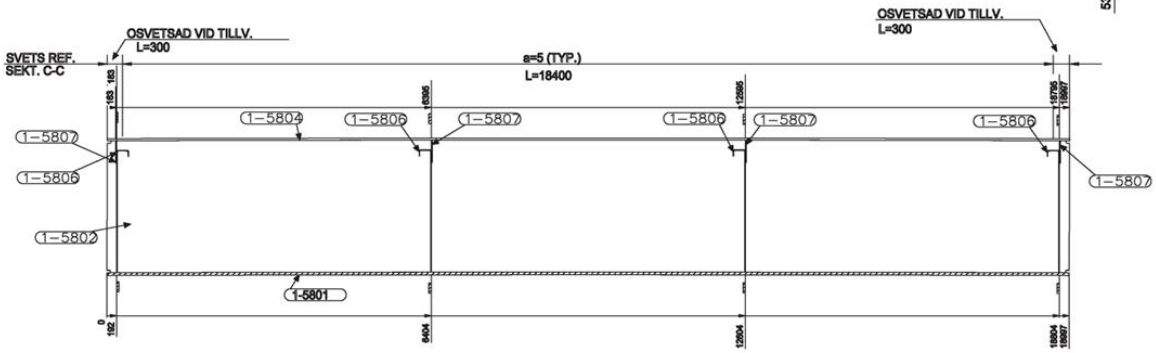

SEKTION B-B VÄNSTER SIDA
1:50

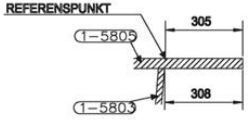

DET. A
1:10

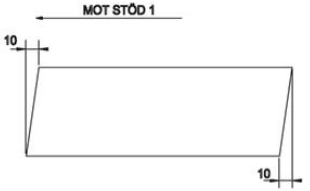

SNEDSKÄRNING AV BALKÄNDAR

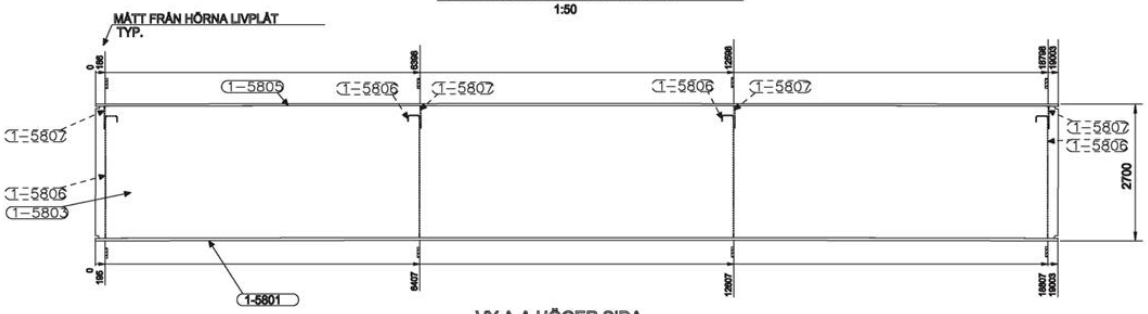

VY A-A HÖGER SIDA
1:50

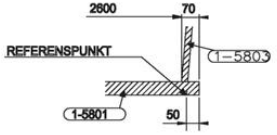

DET. B
1:10

ANVISNINGAR OCH FÖRESKRIFTER:
SE RITNING 1-596 068 100

SVETSBULTAR:
SE RITNING 1-596 068 108

TVÄRFÖRBAND OCH TVÄRAVSTYVNING:
SE RITNING 0-596 068 151

RELATIONSRITNING
FASTSTÄLLD ENLIGT BV SKRIVELSE 2004-06-07

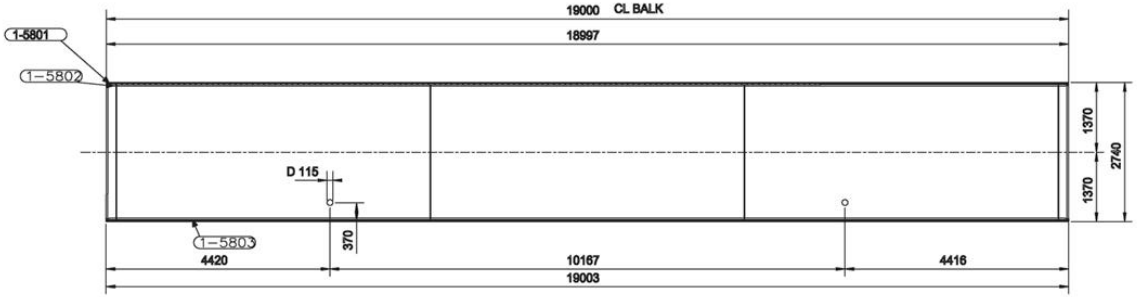

PLAN VID UNDERFLÄNS
1:50

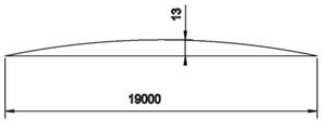

ÖVERHÖJNING

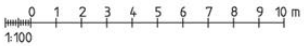

PEAB
SCAN BRIDGE
strukturas
TYRÉNS

UPPDRAG NR	21060	KONSTR AV	HJ
DATUM	2006-05-30	RITAD AV	TJO

A	RELATIONSRITNING		2006-06-20
-	FASTSTÄLLD ARBETSRITNING		2004-06-11
REV	ÄNDRINGEN AVSER	SIGN	DATUM

UPPDRAG NR	205049
RITAD/KONSTR AV	
DATUM	2004-03-25
C. CARLSSON (LIA)	P.O. THOMASSON (KA)
GRANSKAD	KEN RYBERG
GODKÄND	JÖRGEN MOSESSON
DATUM	2004-03-25

STRANDGATAN 7
BOX 53 SKELLEFTEÅ
TEL. 0660-29 49 00
FAX 0660-29 49 10
BOTHNIABANAN AB

STATUS
RELATIONSRITNING

BRO ÖVER ÅNGERMANÄLVEN
KM 484 + 396
NYLAND - ÖRNSKÖLDSVIK

STÅLÖVERBYGGNAD
BALK 58

1:50	
1:20	
1:100	
SKALA	1:10

BB-3642-001	1-596 068	144	A

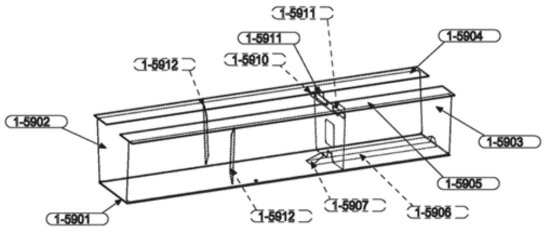

3D BALK

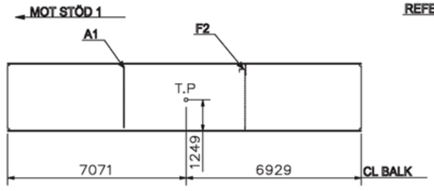

TYNGDPUNKT

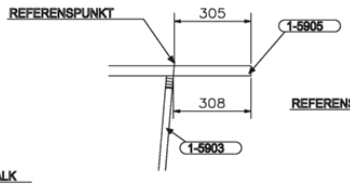

DET. A
1:10

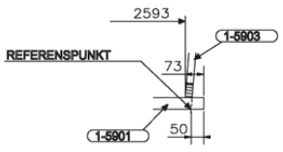

DET. B
1:10

Pos.	Ant.	Benämning	Dimension Längd mm	Bredd mm	Vikt	Kvalitet	Anm.
1-5901	1	PL45*2740	14004	2740	13547.3	S355N	
1-5902	1	PL27*2626	13996	2626	7780.3	S355N	
1-5903	1	PL27*2626	14005	2626	7784.6	S355N	
1-5904	1	PL40*1200	13998	1200	5273.9	S420M	
1-5905	1	PL40*1200	14006	1200	5276.8	S420M	
1-5906	1	PL10*970	5381		370.6	S355J2G3	TRP 10
1-5907	1	PL6*570	742	570	13.6	S355J2G3	
1-5910	1	PL12*3000	2733	2988	627.3	S355J2G3	
1-5911	2	PL20*443	1137	443	126.2	S355J2G3	
1-5912	2	PL25*275	2424	275	226.3	S355J2G3	
				Total stålvikt	41026.8	kg	

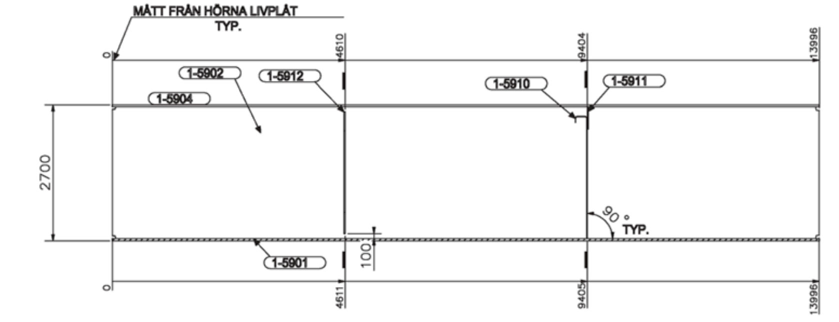

SEKTION B-B VÄNSTER SIDA
1:50

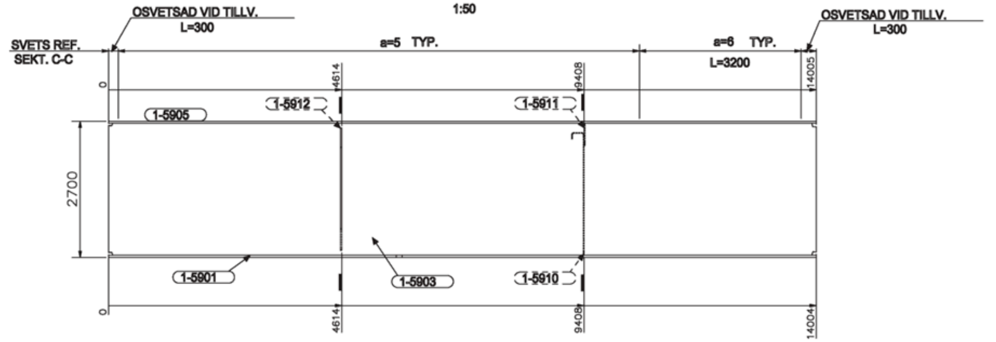

VY A-A HÖGER SIDA
1:50

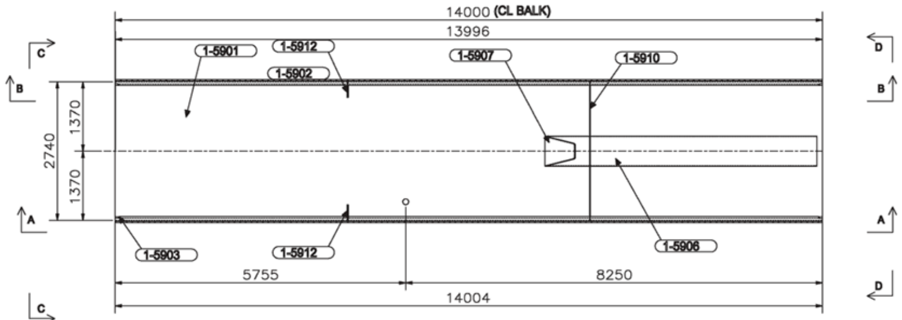

PLAN VID UNDERFLÄNS
1:50

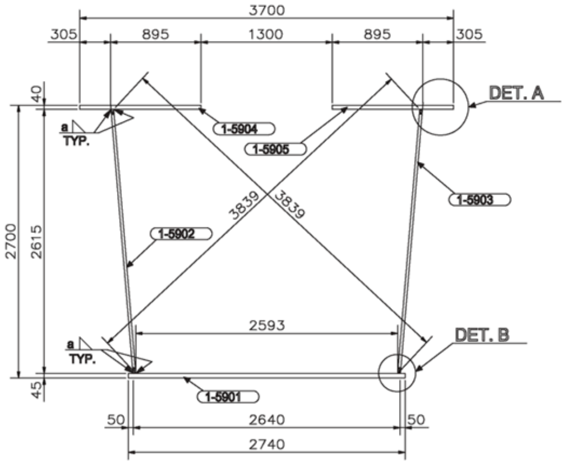

SEKTION C-C
1:25

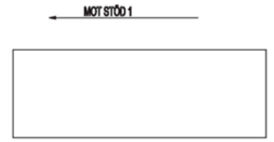

INGEN SNEDSKÄRNING AV BALKÄNDAR

ANVISNINGAR OCH FÖRESKRIFTER:
SE RITNING 1-596 068 100

SVETSBULTAR:
SE RITNING 1-596 068 108

TVÄRFÖRBAND OCH TVÄRAVSTYVNING:
SE RITNING 1-596 068 151

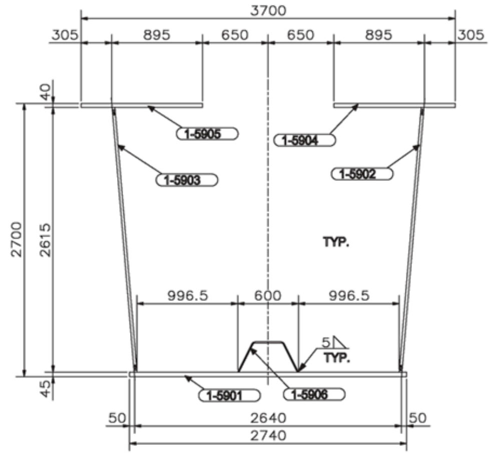

SEKTION D-D
1:25

0 1 2 3 4 5 6 7 8 9 10 m
1:100

RELATIONSRITNING
FASTSTÄLLD ENLIGT BV SKRIVELSE 2004-06-07

PEAB
SCAN BRIDGE
strukturas
TYRÉNS

UPPDRAG NR 21050	KONSTR AV HQ	
DATUM 2006-06-20	RITAD AV AT	

REV	ÄNDRINGEN AVSER	SIGN	DATUM
A	RELATIONSRITNING		2006-06-20
-	FASTSTÄLLD ARBETSRITNING		2004-06-11

UPPDRAG NR 205049
DATUM 2004-03-25
C. CARLSSON (UA) P.O. THOMASSON (KA)
STRANDGATAN 7, 891 33 ÖRNSKÖLDSVIK, TEL. 0660-29 49 00, FAX.0660-29 49 10
GRANSKAD KEN RYBERG
BOTTNIABANAN AB
DATUM 2004-03-25
GODKÄND JÖRGEN MOSESSON

STATUS
RELATIONSRITNING
BRO ÖVER ÅNGERMANÄLVEN
KM 484 + 396
NYLAND - ÖRNSKÖLDSVIK
STÅLÖVERBYGGNAD
BALK 59

SKALA 1:50 1:25 1:100 1:10

RITNINGSNUMMER BB-3542-501 | ARKIVNUMMER 1-596 068 | BLAD 145 | REV. A

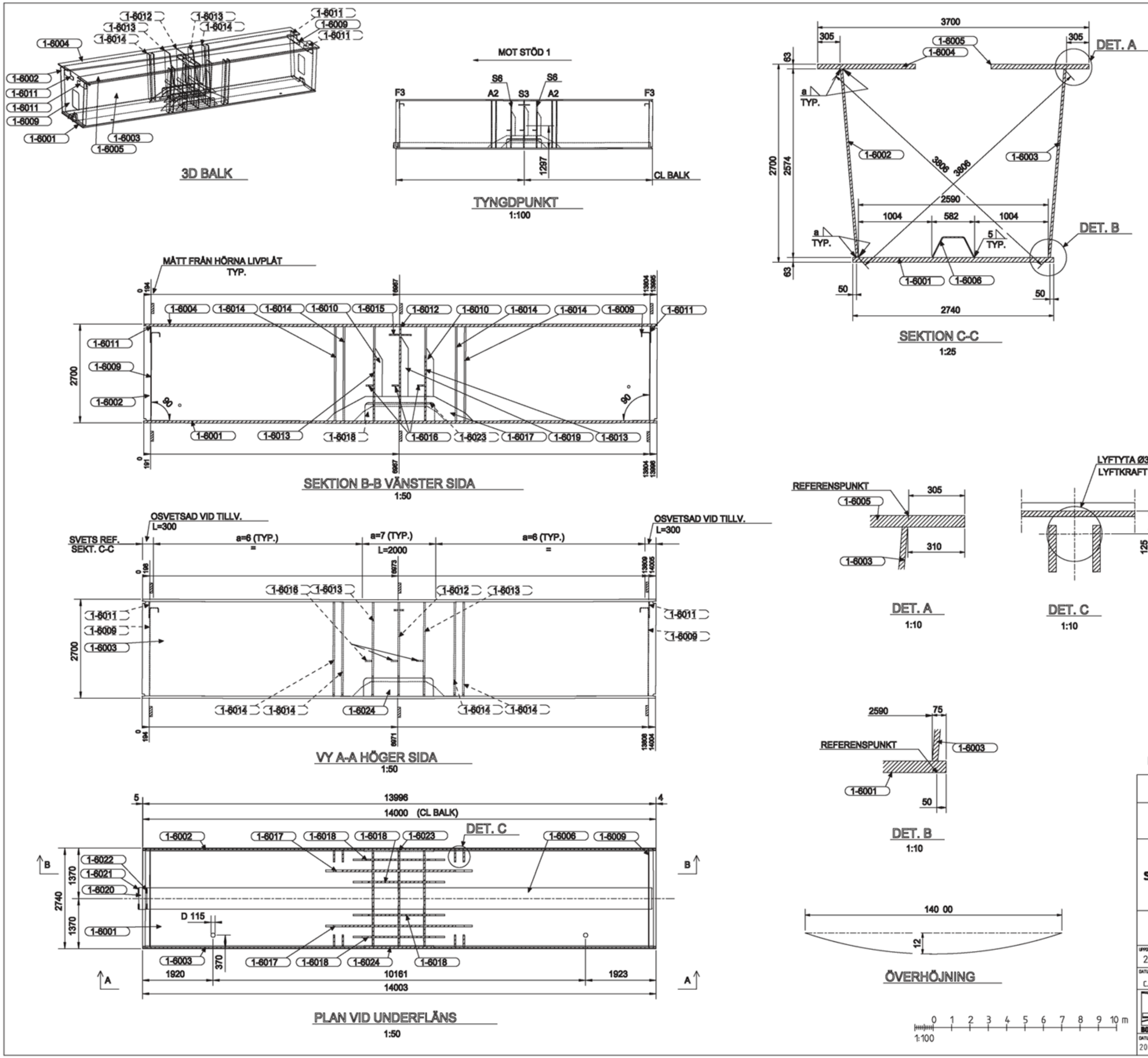

Pos.	Ant.	Benämning	Dimension Längd mm	Bredd mm	Vikt	Kvalitet	Anm.
1-6001	1	PL63*2740	14005	2740	18933.2	S460M	
1-6002	1	PL30*2594	14005	2595	8285.5	S460M	
1-6003	1	PL30*2594	14014	2595	8290.2	S460M	
1-6004	1	PL63*1540	13998	1540	9461.7	S460ML	
1-6005	1	PL63*1540	14006	1540	9467.7	S460ML	
1-6006	1	PL12*930	13775		1165.3	S460M	TRP 12
1-6009	2	PL12*3000	2714	2983	1244.1	S355J2G3	
1-6010	4	PL30*200	1301	200	218.9	S355J2G3	
1-6011	4	PL20*443	1137	443	252.4	S355J2G3	
1-6012	1	PL40*3006	2793	3006	1875.8	S355N	
1-6013	2	PL40*2574	3017	2574	3051.6	S355N	
1-6014	8	PL40*300	2607	300	1941.0	S355N	
1-6015	1	PL30*600	2200	600	267.3	S355J2G3	
1-6016	3	PL30*200	2652	200	335.5	S355J2G3	
1-6017	2	PL50*670	3998	671	1612.6	S460M	
1-6018	4	PL40*400	2499	401	1036.2	S355N	
1-6019	2	PL30*200	1615	200	139.0	S355J2G3	
1-6020	1	PL10*970	223		16.2	S355J2G3	TRP 10
1-6021	2	PL5*30	300	30	0.7	S355J2G3	
1-6022	2	PL5*30	280	30	0.7	S355J2G3	
1-6023	1	PL40*503	1900	503	294.6	S460M	
1-6024	1	PL40*503	1900	503	294.6	S460M	
		Total stålvikt			68184.8	kg	

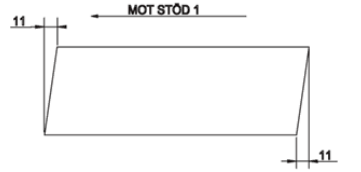

SNEDSKÄRNING AV BALKÄNDAR

ANVISNINGAR OCH FÖRESKRIFTER:
SE RITNING 1-596 068 100

SVETSBULTAR:
SE RITNING 1-596 068 108

TVÄRFÖRBAND OCH TVÄRAVSTYVNING:
SE RITNING 1-596 068 152, 153 OCH 156

RELATIONSRITNING
FASTSTÄLLD ENLIGT BV SKRIVELSE 2004-06-07

PEAB
SCAN BRIDGE
strukturas
TYRÉNS

REV	ÄRT	ÄNDRINGEN AVSER	DATUM
A		RELATIONSRITNING	2006-06-20
-		FASTSTÄLLD ARBETSRITNING	2004-06-11

RELATIONSRITNING
BRO ÖVER ÅNGERMANÄLVEN
KM 484 + 396
NYLAND - ÖRNSKÖLDSVIK
STÅLÖVERBYGGNAD
BALK 60

Uppdrag nr 205049 — Datum 2004-04-21 — C. CARLSSON (UA), P.O. THOMASSON (KA) — Granskad KEN RYBERG — Godkänd JÖRGEN MOSESSON — Datum 2004-04-21 — BOTNIABANAN AB — Uppdrag nr 21050, Konstr av HQ, Datum 2006-06-20, Ritad av TJO — Skala 1:50, 1:25, 1:100, 1:10 — BB-3542-501 — 1-596 068 — Blad 146 — Rev. A

Appendix B Load Coefficients

Table B.1 Load coefficients ψγ for different load combinations (Tabell 222-1), (Banverket, 1999).

	Lastkombination (kortf def)	I bruks bygg	II brott bygg	III öve höj	IV:A brott	IV:B	V:A bruks	V:B sprick-vidd	V:C ned-böjn.	VI ut-matt	VII egen-sväng	VIII olycks	IX maskin
Nr	PERMANENTA LASTER												
1	Egentyngd	1	1	1	0,95*/1,05	1,15	0,95/1,05	1		1	1	1	1
2	Ballast			1	0,8/1,25	1,25	0,8/1,25	0,8/1,25		1	1	1	1
3	Överfyllnad			1	0,9/1,1	1,1	0,9/1,1	1		1	1	1	1
	Jordtryck												
4	aktivt, vilo	0,9/1,1	0,9/1,1	1	0,9/1,1	0,9/1,1	0,9/1,1	0,9/1,1		1		1	
5	passivt	0,9/1	0,9/1	1	0,9/1	0,9/1	0,9/1	0,9/1		1		1	
6	Stödförskjutning				0/1	0/1	0/1	0/1					
7	Krympning			1	0/1	0/1	0/1	0/1		0,6			
8	Spännkraft t=0	1	1										1
9	Spännkraft t=t1				1	1	1	1		1	1	1	1
10	Spännkraft t=t2			1	1	1	1	1		1	1	1	1
11	Vattentryck	1	1	1	1	1	1	1		1		1	1
12	Påhängslast på påle					1		1					
	VARIABLA LASTER												
21	Tåglast BV 2000			0,2	0,7/1,4		1		1	0,8		0,8	
22	Tåglast Malm 2000			0,2	0,7/1,4		1		1	1		1	
23	Spårbytesmaskin				0,8/1,2		1						
24	Renhållningsfordon				0,7/1,4		1						
25	Utryckningsfordon				0,7/1,4		1						1
26	Broms- och acc-kraft				0,8/1,2		0,8						
27	Sidokraft				0,6/1,4		0,6						
28	Gångbanelast				0,7/1,4		1	0,3					
29	Jordtryck av överlast				0,6/1,4		1	0,3	1	1			
30	Temp (21.262+21.263)				0,6/1,3		0,6	0,6					1
31	Temp (21.262+21.264)				0,6/1,3		0,6	0,6					1
32	Temp (21.262+21.265)				0,6/1,3		0,6	0,6					1
33	Vindlast		0,4/1		0,6/1,3		0,6		0,4	0,6			1
34	Is- och strömtryck		0,4/1		0,6/1,3		0,6						
35	Snölast		0,4/1		0,6/1,3		0,6	0,2					1
36	Last på insp.-brygga				0,7/1,4		0,7						
37	Arbetsfordon	1	1/1,3										
38	Last från övergångs-konstruktion				0,6/1,4		0,6						
39	Olikformig last												1
40	Last på räcke				0,7/1,4		0,7						
41	Vattentryck		0,6/1		0,8/1,3		0,8	0,3					
42	Last på lådbotten				0,7/1,5		0,7						
43	Temp spänningar i räler				0,6/1,3		0,6						
	OLYCKSLASTER												
51	Påkörningskraft (21.31)											1	
52	Påseglingskraft (21.32)											1	
53	Avslagen hängare(21.34)											1	
54	Avslagen påle (21.35)											1	
55	Urspårning (221.36)											1	
56	Explosion (221.38)											1	
57	Brott i kabel (21.33)											1	
58	Brott i spännkabel(21.37)											1	

* Vid dimensionering för hydrauliskt upplyft sätts det lägre värdet till 0,9.

Appendix C Section Properties

Coordinate System for the FEM-Model

The simplified model is divided in to points (*see Figure C.1*) and given coordinates in the y- and z-direction (*see* Table C.1).

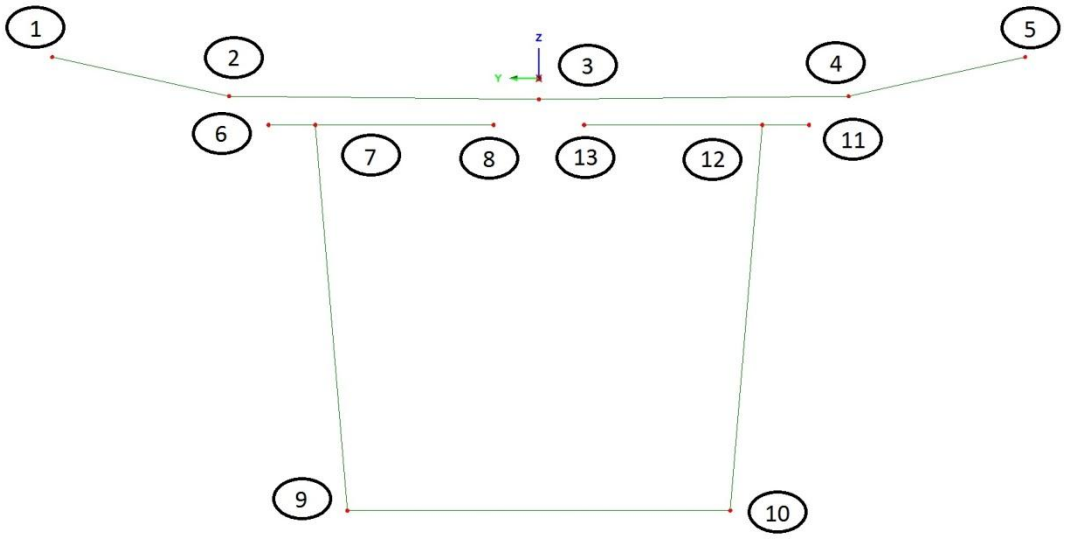

Figure C.1 Coordinate location for FEM 3-D model.

Table C.1 Coordinates of the section used in the FEM 3-D model

Steel Section		
Point	Y	Z
6	1,85	-0,3195
7	1,53	-0,3195
8	0,31	-0,3195
9	1,31	-2,9565
10	-1,31	-2,9565
11	-1,85	-0,3195
12	-1,53	-0,3195
13	-0,31	-0,3195

Concrete Section		
Point	Y	Z
1	3,33	0,145
2	2,12	-0,123
3	0	-0,144
4	-2,12	-0,123
5	-3,33	0,145

Section Model for Moment of Inertia Calculation

Due to limitations in LUSAS, a new more precise coordinate system was used to calculate the moment of inertia for the concrete section and the four different steel sections (*see Figure C.2, Figure C.3 and Table C.2*).

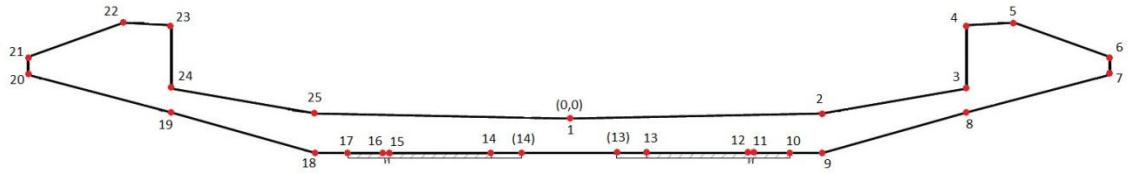

Figure C.2 Coordinate location on concrete slab, for moment of inertia calculation.

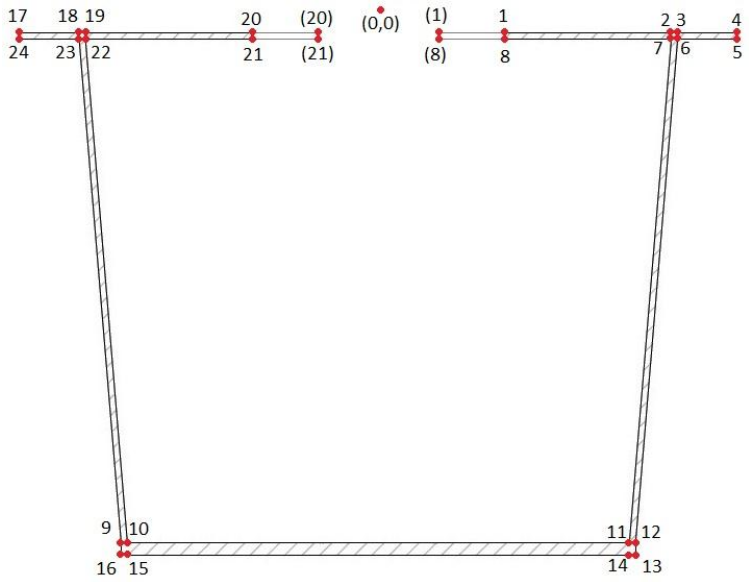

Figure C.3 Coordinate location on steel box, for moment of inertia calculation. (The points within parenthesis are only used for the support section.)

Table C.2 Coordinates for moment of inertia calculation.

Steel							Concrete		
Support/Support end			Middle		Mid-span		Slab and edge beams		
Point	Coordinates (m)		Coordinates (m)		Coordinates (m)		Point	Coordinates (m)	
No.	x	y	x	y	x	y	No.	x	y
(1)	0,31	-0,288					1	0	0
1	0,65	-0,288	0,65	-0,288	0,65	-0,288	2	2,12	0,042
2	1,51	-0,288	1,515	-0,288	1,518	-0,288	3	3,33	0,25
3	1,54	-0,288	1,542	-0,288	1,542	-0,288	4	3,33	0,78
4	1,85	-0,288	1,85	-0,288	1,85	-0,288	5	3,73	0,8
5	1,85	-0,351	1,85	-0,328	1,85	-0,328	6	4,53	0,515
6	1,54	-0,351	1,542	-0,328	1,542	-0,328	7	4,53	0,365
7	1,51	-0,351	1,515	-0,328	1,518	-0,328	8	3,33	0,0398548*
8	0,65	-0,351	0,65	-0,328	0,65	-0,328	9	2,12	-0,288
(8)	0,31	-0,351					10	1,85	-0,288
9	-1,325	-2,925	-1,324	-2,943	-1,324	-2,935	11	1,54	-0,288
10	-1,295	-2,925	-1,297	-2,943	-1,3	-2,935	12	1,51	-0,288
11	1,295	-2,925	1,2965	-2,943	1,3	-2,935	13	0,65	-0,288
12	1,325	-2,925	1,3235	-2,943	1,324	-2,935	(13)	0,31	-0,288
13	1,325	-2,988	1,3235	-2,988	1,324	-2,988	(14)	-0,31	-0,288
14	1,295	-2,988	1,2965	-2,988	1,3	-2,988	14	-0,65	-0,288
15	-1,295	-2,988	-1,297	-2,988	-1,3	-2,988	15	-1,51	-0,288
16	-1,325	-2,988	-1,324	-2,988	-1,324	-2,988	16	-1,54	-0,288
17	-1,85	-0,288	-1,85	-0,288	-1,85	-0,288	17	-1,85	-0,288
18	-1,54	-0,288	-1,542	-0,288	-1,542	-0,288	18	-2,12	-0,288
19	-1,51	-0,288	-1,515	-0,288	-1,518	-0,288	19	-3,33	0,0398548*
20	-0,65	-0,288	-0,65	-0,288	-0,65	-0,288	20	-4,53	0,365
(20)	-0,31	-0,288					21	-4,53	0,515
(21)	-0,31	-0,351					22	-3,73	0,8
21	-0,65	-0,351	-0,65	-0,328	-0,65	-0,328	23	-3,33	0,78
22	-1,51	-0,351	-1,515	-0,328	-1,518	-0,328	24	-3,33	0,25
23	-1,54	-0,351	-1,542	-0,328	-1,542	-0,328	25	-2,12	0,042
24	-1,85	-0,351	-1,85	-0,328	-1,85	-0,328			

* 1,21*(653/2410)-0.288

Appendix D Thesis Calculations

Moment of Inertia

Due to limitations in LUSAS, the moment of inertia for the whole composite section could not be calculated directly. The concrete section and the steel section is therefore created separately and analyzed in the Arbitrary section property calculator (*see Figure D.1, Figure D.2, Figure D.3, Figure D.4 and Figure D.5*). The moment of inertia of the composite sections; mid-span, middle (section between mid-span and support end), support end (end of the support section) and support, is then calculated by hand. The Arbitrary section property calculator was also used to calculate the area of the edge beam (*see Figure D.6*).

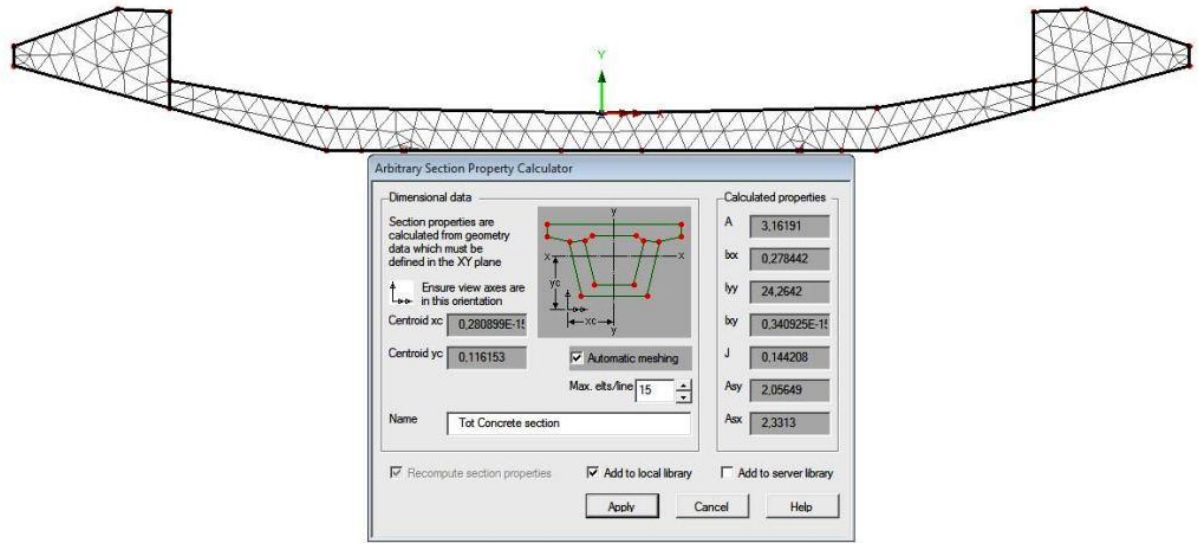

Figure D.1 Output data from LUSAS, for the concrete section.

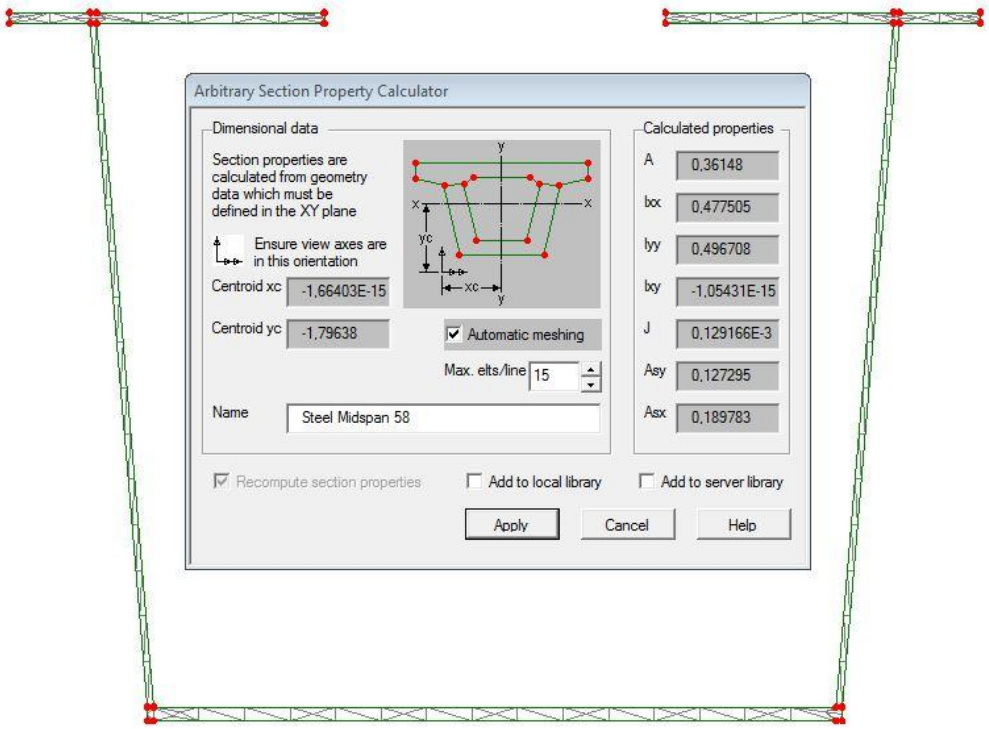

Figure D.2 Output data from LUSAS, for the steel section at mid-span.

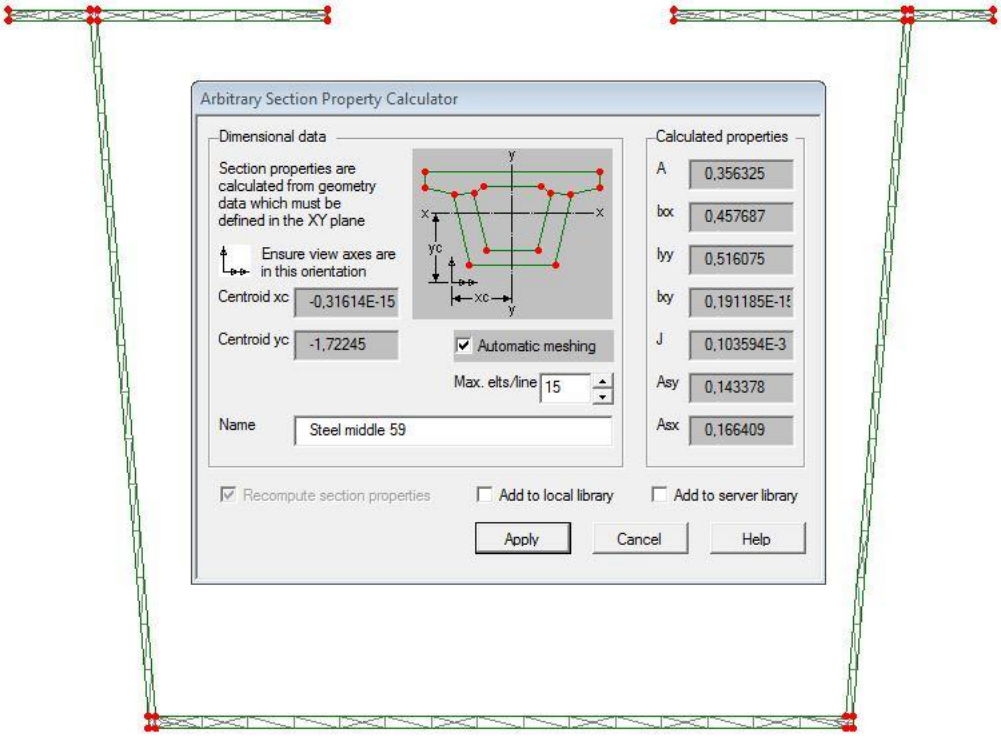

Figure D.3 Output data from LUSAS, for the steel section at middle.

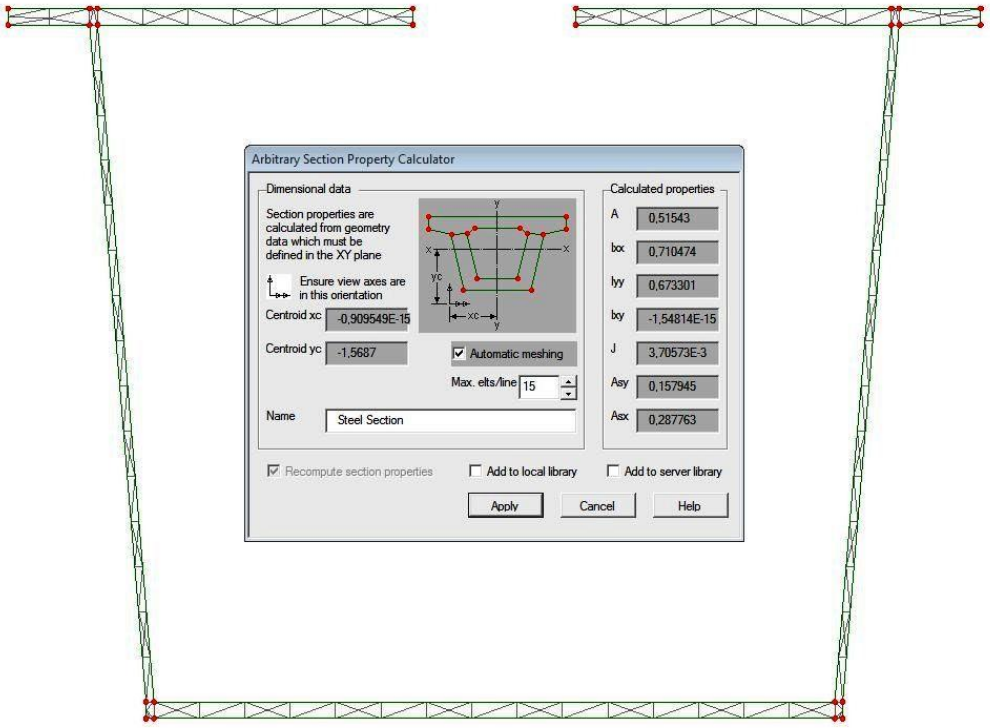

Figure D.4 Output data from LUSAS, for the steel section at supports.

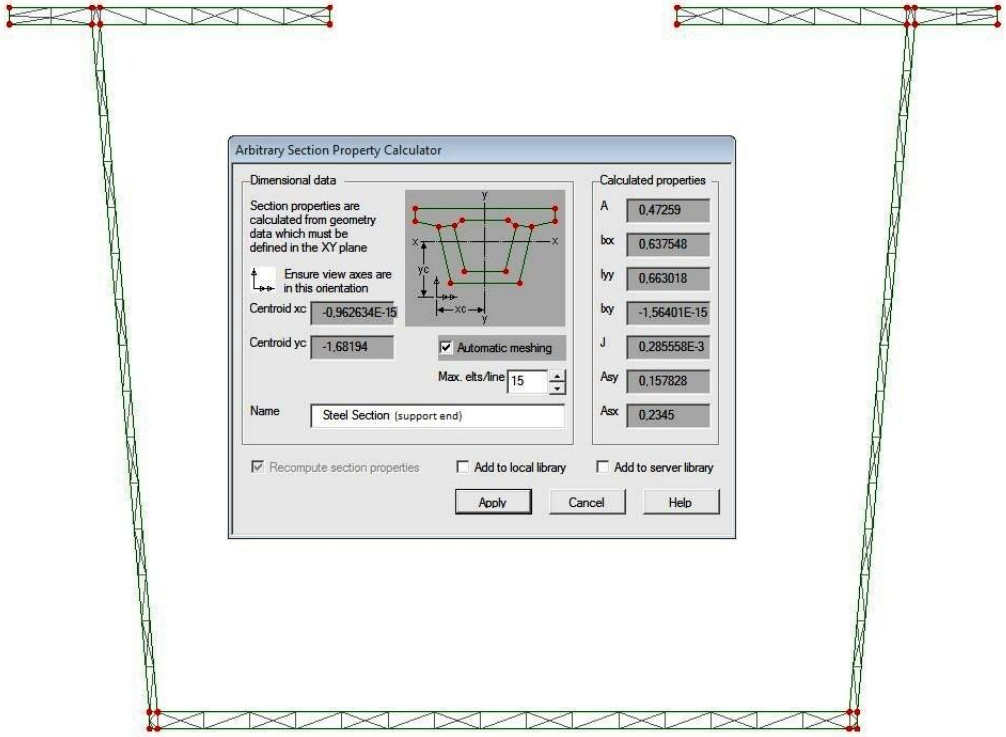

Figure D.5 Output data from LUSAS, for the steel section at support end.

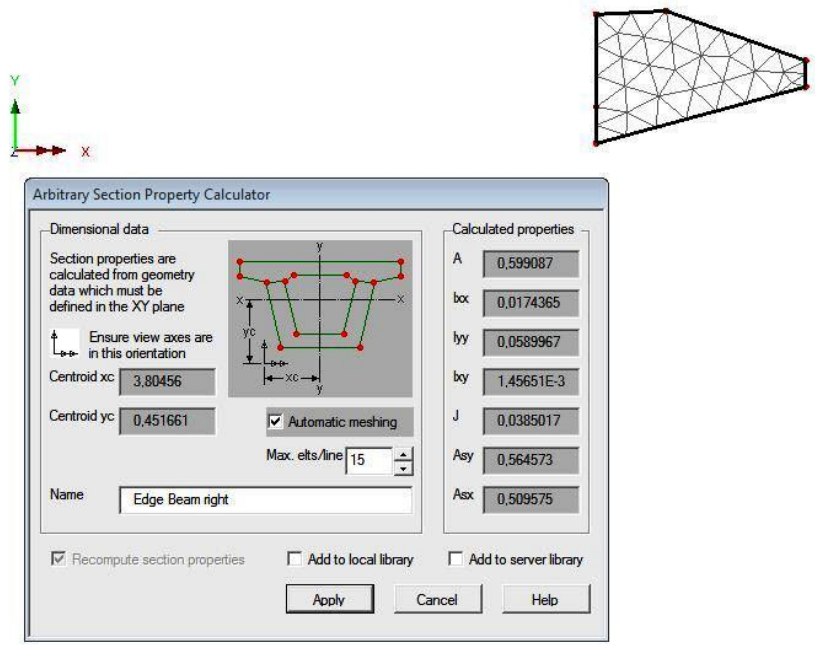

Figure D.6 Output data from LUSAS, for the right edge beam section.

The moment of inertia for the four different composite sections are calculated for both short- and long-term loading according to section 2.5.1 in (Collin et al., 2008). *Figure D.7* is showing the distances used in the calculation. The stresses due to shrinkage for three composite sections (mid-span, middle and support) are calculated according to section 2.4.1 in (Collin et al., 2008). The values of the moment of inertia for the "support end" section are close to the ones for the "support" section. The moments of inertia for the "support end" are therefore assumed to be same as the "support" section. The bending caused by the shrinkage stress is also calculated.

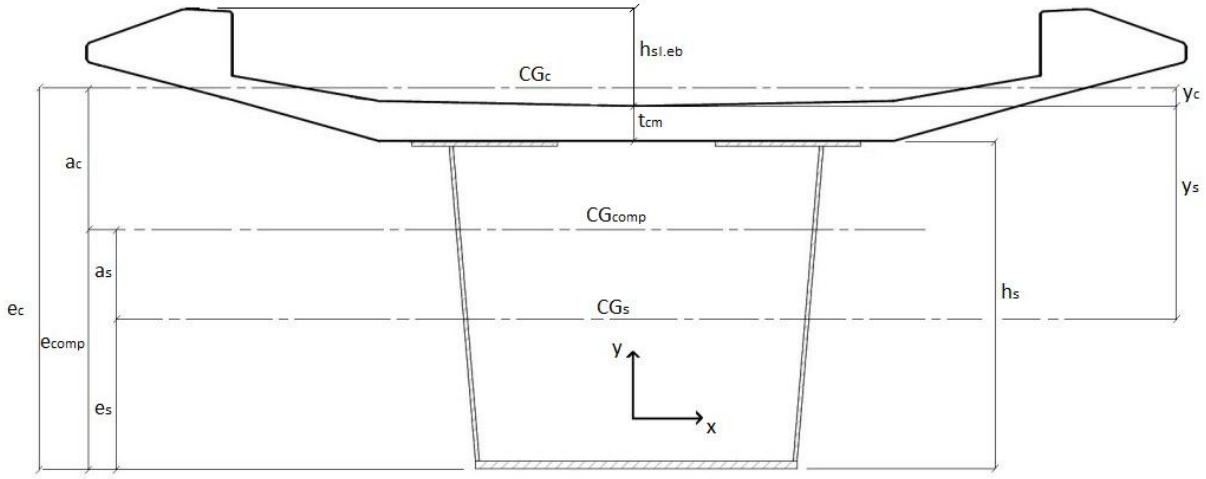

Figure D.7 Composite section with explanations of the distances to the center of gravity, CG_c, CG_s, CG_{comp}, for the concrete, steel and composite section, used in the calculation.

Moment of inertia and stress due to shrinkage for mid-span section

Concrete Properties

$E_{ck} := 32 \cdot GPa$

$t_{cm} := 288 \cdot mm$

$h_{sl.eb} := 0.8 \cdot m$

$\varphi_{eff} := 2$ BBK 94, 2.4.7

$E_{c.eff} := \frac{E_{ck}}{(1 + \varphi_{eff})} = 10.667 \cdot GPa$ Effect of creep, (long term)

Input from Lusas (Concrete)

$y_c := 0.116153 \cdot m$

$A_c := 3.16191 \cdot m^2$

$I_{c.xx} := 0.278442 \cdot m^4$

Steel Properties at Mid-span (Beam 54, 58, 62, 66)

$E_{sk} := 210 \cdot GPa$

$h_s := 2700 \cdot mm$

Input from Lusas (Mid-span)

$y_s := 1.79638 \cdot m$

$A_s := 0.36148 \cdot m^2$

$I_{s.xx} := 0.477505 \cdot m^4$

Composite Calculation at Mid-span (Beam 54, 58, 62, 66)

$\alpha_s := \frac{E_{sk}}{E_{ck}} = 6.563$ Short term load

$\alpha_l := \frac{E_{sk}}{E_{c.eff}} = 19.688$ Long term load

$\alpha := \begin{pmatrix} \alpha_s \\ \alpha_l \end{pmatrix}$

$A_{c.eff} := \frac{A_c}{\alpha} = \begin{pmatrix} 0.482 \\ 0.161 \end{pmatrix} m^2$

$A_{comp} := A_{c.eff} + A_s = \begin{pmatrix} 0.843 \\ 0.522 \end{pmatrix} m^2$

$e_c := h_s + t_{cm} + y_c = 3.104\,m$

$e_s := h_s + t_{cm} - y_s = 1.192\,m$

$e_{comp} := \frac{A_s \cdot e_s + A_{c.eff} \cdot e_c}{A_{comp}} = \begin{pmatrix} 2.284 \\ 1.78 \end{pmatrix} m$

$a_s := e_{comp} - e_s = \begin{pmatrix} 1.093 \\ 0.588 \end{pmatrix} m$

$a_c := e_c - e_{comp} = \begin{pmatrix} 0.82 \\ 1.324 \end{pmatrix} m$

$I_{comp} := I_{s.xx} + A_s \cdot a_s^2 + \frac{I_{c.xx}}{\alpha} + \overrightarrow{\left(A_{c.eff} \cdot a_c^2\right)} = \begin{pmatrix} 1.275 \\ 0.898 \end{pmatrix} m^4$

The moment of inertia for the composite section at the mid-span is:
1.275 m^4 for a short-term load
0.898 m^4 for a long-term load

Stress Distrubution due to shrinkage

$E_{sr} := 200 \cdot GPa$ Reinforcement

$\varepsilon_{cs} := 0.025 \cdot \%$ Final concrete shrinkage

$L := 19 \cdot m$ Length of the steel beam 54, 58, 62

$L_{66} := 18 \cdot m$ Length of the steel beam 66

Force

$$N := \begin{pmatrix} \varepsilon_{cs} \cdot E_{ck} \cdot A_c \\ \varepsilon_{cs} \cdot E_{c.eff} \cdot A_c \end{pmatrix} = \begin{pmatrix} 25.295 \\ 8.432 \end{pmatrix} \cdot MN$$ Force in concrete due to shrinkage

Distances

$$y_{ceb.top} := a_c - y_c + h_{sl.eb} = \begin{pmatrix} 1.504 \\ 2.008 \end{pmatrix} m$$ Distance, CGcomp to top edge beam

$$y_{cs.top} := a_c - y_c = \begin{pmatrix} 0.704 \\ 1.208 \end{pmatrix} m$$ Distance, CGcomp to top slab center

$$y_{c.bot} := a_c - y_c - t_{cm} = \begin{pmatrix} 0.416 \\ 0.92 \end{pmatrix} m$$ Distance, CGcomp to bottom slab

$$y_{s.bot} := e_{comp} = \begin{pmatrix} 2.284 \\ 1.78 \end{pmatrix} m$$ Distance, CGcomp to bottom steel

Stresses (As a simply supported beam)

$$\sigma_1 := -\frac{N}{\overrightarrow{(\alpha \cdot A_{comp})}} - \frac{\overrightarrow{(N \cdot a_c \cdot y_{ceb.top})}}{\overrightarrow{(I_{comp} \cdot \alpha)}} + \frac{N}{A_c} = \begin{pmatrix} -0.296 \\ 0.579 \end{pmatrix} \cdot MPa$$

Top of edge beam

$$\sigma_2 := -\frac{N}{\overrightarrow{(\alpha \cdot A_{comp})}} - \frac{\overrightarrow{(N \cdot a_c \cdot y_{cs.top})}}{\overrightarrow{(I_{comp} \cdot \alpha)}} + \frac{N}{A_c} = \begin{pmatrix} 1.686 \\ 1.084 \end{pmatrix} \cdot MPa$$

Top of slab center

$$\sigma_3 := -\frac{N}{\overrightarrow{(\alpha \cdot A_{comp})}} - \frac{\overrightarrow{(N \cdot a_c \cdot y_{c.bot})}}{\overrightarrow{(I_{comp} \cdot \alpha)}} + \frac{N}{A_c} = \begin{pmatrix} 2.399 \\ 1.266 \end{pmatrix} \cdot MPa$$

Bottom of slab

$$\sigma_4 := -\frac{N}{A_{comp}} - \frac{\overrightarrow{(N \cdot a_c \cdot y_{c.bot})}}{I_{comp}} = \begin{pmatrix} -36.754 \\ -27.585 \end{pmatrix} \cdot MPa$$

Top steel

$$\sigma_5 := -\frac{N}{A_{comp}} + \frac{\overrightarrow{(N \cdot a_c \cdot y_{s.bot})}}{I_{comp}} = \begin{pmatrix} 7.147 \\ 5.971 \end{pmatrix} \cdot MPa$$

Bottom steel

Shrinkage effect on beam

$$r_{cs} := \frac{E_{sk} \cdot h_s}{\sigma_5 - \sigma_4}$$

$$\frac{1}{r_{cs}} = \begin{pmatrix} 7.743 \times 10^{-5} \\ 5.918 \times 10^{-5} \end{pmatrix} \frac{1}{m}$$

Bending caused by shrinkage

Output values used in: <u>Moment at supports due to shrinkage</u>

$$\theta_{cs.ms} := \frac{L}{r_{cs}} = \begin{pmatrix} 1.471 \times 10^{-3} \\ 1.124 \times 10^{-3} \end{pmatrix}$$

$$\theta_{cs.ms.66} := \frac{L_{66}}{r_{cs}} = \begin{pmatrix} 1.394 \times 10^{-3} \\ 1.065 \times 10^{-3} \end{pmatrix}$$

$$L_{ms} := L = 19\,m$$

$$L_{ms.66} := L_{66} = 18\,m$$

$$I_{comp.ms} := I_{comp} = \begin{pmatrix} 1.275 \\ 0.898 \end{pmatrix} m^4$$

Moment of inertia and stress due to shrinkage for middle section

Concrete Properties

$E_{ck} := 32 \cdot GPa$

$t_{cm} := 288 \cdot mm$

$h_{sl.eb} := 0.8 \cdot m$

$\varphi_{eff} := 2$ BBK 94, 2.4.7

$E_{c.eff} := \frac{E_{ck}}{(1 + \varphi_{eff})} = 10.667 \cdot GPa$ Effect of creep, (long term)

Input from Lusas (Concrete)

$y_c := 0.116153 \cdot m$

$A_c := 3.16191 \cdot m^2$

$I_{c.xx} := 0.278442 \cdot m^4$

Steel Properties at Middle (Beam 53, 55, 57, 59, 61, 63, 65, 67)

$E_{sk} := 210 \cdot GPa$

$h_s := 2700 \cdot mm$

Input from Lusas (Middle)

$y_s := 1.72245 \cdot m$

$A_s := 0.356325 \cdot m^2$

$I_{s.xx} := 0.457687 \cdot m^4$

Composite Calculation at Middle (Beam 53, 55, 57, 59, 61, 63, 65, 67)

$$\alpha_s := \frac{E_{sk}}{E_{ck}} = 6.563$$ Short term load

$$\alpha_l := \frac{E_{sk}}{E_{c.eff}} = 19.688$$ Long term load

$$\alpha := \begin{pmatrix} \alpha_s \\ \alpha_l \end{pmatrix}$$

$$A_{c.eff} := \frac{A_c}{\alpha} = \begin{pmatrix} 0.482 \\ 0.161 \end{pmatrix} m^2$$

$$A_{comp} := A_{c.eff} + A_s = \begin{pmatrix} 0.838 \\ 0.517 \end{pmatrix} m^2$$

$$e_c := h_s + t_{cm} + y_c = 3.104\,m$$

$$e_s := h_s + t_{cm} - y_s = 1.266\,m$$

$$e_{comp} := \frac{A_s \cdot e_s + A_{c.eff} \cdot e_c}{A_{comp}} = \begin{pmatrix} 2.322 \\ 1.837 \end{pmatrix} m$$

$$a_s := e_{comp} - e_s = \begin{pmatrix} 1.057 \\ 0.571 \end{pmatrix} m$$

$$a_c := e_c - e_{comp} = \begin{pmatrix} 0.782 \\ 1.267 \end{pmatrix} m$$

$$I_{comp} := I_{s.xx} + A_s \cdot a_s^2 + \frac{I_{c.xx}}{\alpha} + \overrightarrow{\left(A_{c.eff} \cdot a_c^2\right)} = \begin{pmatrix} 1.193 \\ 0.846 \end{pmatrix} m^4$$

The moment of inertia for the composite section at the mid-span is:
1.193 m^4 for a short-term load
0.846 m^4 for a long-term load

Stress Distrubution due to shrinkage

$E_{sr} := 200 \cdot GPa$ Reinforcement

$\varepsilon_{cs} := 0.025 \cdot \%$ Final concrete shrinkage

$L := 14 \cdot m$ Length of the steel beam 53, 55, 57, 59, 61, 63

$L_{65} := 13 \cdot m$ Length of the steel beam 65

$L_{67} := 11 \cdot m$ Length of the steel beam 67

Force

$$N := \begin{pmatrix} \varepsilon_{cs} \cdot E_{ck} \cdot A_c \\ \varepsilon_{cs} \cdot E_{c.eff} \cdot A_c \end{pmatrix} = \begin{pmatrix} 25.295 \\ 8.432 \end{pmatrix} \cdot MN$$ Force due to shrinkage

Distances

$$y_{ceb.top} := a_c - y_c + h_{sl.eb} = \begin{pmatrix} 1.466 \\ 1.951 \end{pmatrix} m$$ Distance, CGcomp to top edge beam

$$y_{cs.top} := a_c - y_c = \begin{pmatrix} 0.666 \\ 1.151 \end{pmatrix} m$$ Distance, CGcomp to top slab center

$$y_{c.bot} := a_c - y_c - t_{cm} = \begin{pmatrix} 0.378 \\ 0.863 \end{pmatrix} m$$ Distance, CGcomp to bottom slab

$$y_{s.bot} := e_{comp} = \begin{pmatrix} 2.322 \\ 1.837 \end{pmatrix} m$$ Distance, CGcomp to bottom steel

Stresses (As a simply supported beam)

$$\sigma_1 := -\frac{N}{\overrightarrow{(\alpha \cdot A_{comp})}} - \frac{\overrightarrow{(N \cdot a_c \cdot y_{ceb.top})}}{\overrightarrow{(I_{comp} \cdot \alpha)}} + \frac{N}{A_c} = \begin{pmatrix} -0.301 \\ 0.586 \end{pmatrix} \cdot MPa$$ Top of edge beam

$$\sigma_2 := -\frac{N}{\overrightarrow{(\alpha \cdot A_{comp})}} - \frac{\overrightarrow{(N \cdot a_c \cdot y_{cs.top})}}{\overrightarrow{(I_{comp} \cdot \alpha)}} + \frac{N}{A_c} = \begin{pmatrix} 1.72 \\ 1.1 \end{pmatrix} \cdot MPa$$ Top of slab center

$$\sigma_3 := -\frac{N}{\overrightarrow{(\alpha \cdot A_{comp})}} - \frac{\overrightarrow{(N \cdot a_c \cdot y_{c.bot})}}{\overrightarrow{(I_{comp} \cdot \alpha)}} + \frac{N}{A_c} = \begin{pmatrix} 2.447 \\ 1.284 \end{pmatrix} \cdot MPa$$ Bottom of slab

$$\sigma_4 := -\frac{N}{A_{comp}} - \frac{\overrightarrow{(N \cdot a_c \cdot y_{c.bot})}}{I_{comp}} = \begin{pmatrix} -36.439 \\ -27.214 \end{pmatrix} \cdot MPa$$ Top steel

$$\sigma_5 := -\frac{N}{A_{comp}} + \frac{\overrightarrow{(N \cdot a_c \cdot y_{s.bot})}}{I_{comp}} = \begin{pmatrix} 8.326 \\ 6.888 \end{pmatrix} \cdot MPa$$ Bottom steel

Shrinkage effect on beam

$$r_{cs} := \frac{E_{sk} \cdot h_s}{\sigma_5 - \sigma_4}$$

$$\frac{1}{r_{cs}} = \begin{pmatrix} 7.895 \times 10^{-5} \\ 6.014 \times 10^{-5} \end{pmatrix} \frac{1}{m}$$

Bending caused by shrinkage

Output values used in: <u>Moment at supports due to shrinkage</u>

$$\theta_{cs.mid} := \frac{L}{r_{cs}} = \begin{pmatrix} 1.105 \times 10^{-3} \\ 8.42 \times 10^{-4} \end{pmatrix}$$

Slope deflection from bending (beam 53, 55, 57, 59, 61, 63, 65, 67)

$$\theta_{cs.mid.65} := \frac{L_{65}}{r_{cs}} = \begin{pmatrix} 1.026 \times 10^{-3} \\ 7.819 \times 10^{-4} \end{pmatrix}$$

Slope deflection from bending (beam 65)

$$\theta_{cs.mid.67} := \frac{L_{67}}{r_{cs}} = \begin{pmatrix} 8.685 \times 10^{-4} \\ 6.616 \times 10^{-4} \end{pmatrix}$$

Slope deflection from bending (beam 67)

$$L_{mid} := L = 14\,m$$

$$L_{mid.65} := L_{65} = 13\,m$$

$$L_{mid.67} := L_{67} = 11\,m$$

$$I_{comp.mid} := I_{comp} = \begin{pmatrix} 1.193 \\ 0.846 \end{pmatrix} m^4$$

Moment of inertia and stress due to shrinkage for support section

Due to assymetri in the top flanges (smaller at the ends) of the steel over the supports a separate calculation (see **Moment of inertia for support end**) was done to see if this differnce could be neglected.

Concrete Properties

$E_{ck} := 32 \cdot GPa$

$t_{cm} := 288 \cdot mm$

$h_{sl.eb} := 0.8 \cdot m$

$\varphi_{eff} := 2$ BBK 94, 2.4.7

$E_{c.eff} := \frac{E_{ck}}{(1 + \varphi_{eff})} = 10.667 \cdot GPa$ Effect of creep, (long term)

Input from Lusas (Concrete)

$y_c := 0.116153 \cdot m$

$A_c := 3.16191 \cdot m^2$

$I_{c.xx} := 0.278442 \cdot m^4$

Steel Properties at Supports (Beam 52, 56, 60, 64)

$E_{sk} := 210 \cdot GPa$

$h_s := 2700 \cdot mm$

Input from Lusas (Support)

$y_s := 1.5687 \cdot m$

$A_s := 0.51543 \cdot m^2$

$I_{s.xx} := 0.710474 \cdot m^4$

Composite Calculation at Support (Beam 52, 56, 60, 64)

$$\alpha_s := \frac{E_{sk}}{E_{ck}} = 6.563$$ Short-term load

$$\alpha_l := \frac{E_{sk}}{E_{c.eff}} = 19.688$$ Long-term load

$$\alpha := \begin{pmatrix} \alpha_s \\ \alpha_l \end{pmatrix}$$

$$A_{c.eff} := \frac{A_c}{\alpha} = \begin{pmatrix} 0.482 \\ 0.161 \end{pmatrix} m^2$$

$$A_{comp} := A_{c.eff} + A_s = \begin{pmatrix} 0.997 \\ 0.676 \end{pmatrix} m^2$$

$$e_c := h_s + t_{cm} + y_c = 3.104\,m$$

$$e_s := h_s + t_{cm} - y_s = 1.419\,m$$

$$e_{comp} := \frac{A_s \cdot e_s + A_{c.eff} \cdot e_c}{A_{comp}} = \begin{pmatrix} 2.233 \\ 1.82 \end{pmatrix} m$$

$$a_s := e_{comp} - e_s = \begin{pmatrix} 0.814 \\ 0.4 \end{pmatrix} m$$

$$a_c := e_c - e_{comp} = \begin{pmatrix} 0.871 \\ 1.285 \end{pmatrix} m$$

$$I_{comp} := I_{s.xx} + A_s \cdot a_s^2 + \frac{I_{c.xx}}{\alpha} + \overrightarrow{\left(A_{c.eff} \cdot a_c^2\right)} = \begin{pmatrix} 1.46 \\ 1.072 \end{pmatrix} m^4$$

The Moment of inertia for the composite section at the support is:
1.46 m^4 for a short-term load
1.072 m^4 for a long-term load

Stress Distrubution due to shrinkage

$E_{sr} := 200 \cdot GPa$ Reinforcement

$\varepsilon_{cs} := 0.025 \cdot \%$ Final concrete shrinkage

$L := 14 \cdot m$ Length of the steel sections

Force

$$N := \begin{pmatrix} \varepsilon_{cs} \cdot E_{ck} \cdot A_c \\ \varepsilon_{cs} \cdot E_{c.eff} \cdot A_c \end{pmatrix} = \begin{pmatrix} 25.295 \\ 8.432 \end{pmatrix} \cdot MN$$ Force due to shrinkage

Distances

$$y_{ceb.top} := a_c - y_c + 0.8 \cdot m = \begin{pmatrix} 1.555 \\ 1.968 \end{pmatrix} m$$ Distance, CGcomp to top edge beam

$$y_{cs.top} := a_c - y_c = \begin{pmatrix} 0.755 \\ 1.168 \end{pmatrix} m$$ Distance, CGcomp to top slab center

$$y_{c.bot} := a_c - y_c - t_{cm} = \begin{pmatrix} 0.467 \\ 0.88 \end{pmatrix} m$$ Distance, CGcomp to bottom slab

$$y_{s.bot} := e_{comp} = \begin{pmatrix} 2.233 \\ 1.82 \end{pmatrix} m$$ Distance, CGcomp to bottom steel

Stresses (As a simply supported beam)

$$\sigma_1 := -\frac{N}{\overrightarrow{(\alpha \cdot A_{comp})}} - \frac{\overrightarrow{(N \cdot a_c \cdot y_{ceb.top})}}{\overrightarrow{(I_{comp} \cdot \alpha)}} + \frac{N}{A_c} = \begin{pmatrix} 0.56 \\ 1.023 \end{pmatrix} \cdot MPa$$

Top of edge beam

$$\sigma_2 := -\frac{N}{\overrightarrow{(\alpha \cdot A_{comp})}} - \frac{\overrightarrow{(N \cdot a_c \cdot y_{cs.top})}}{\overrightarrow{(I_{comp} \cdot \alpha)}} + \frac{N}{A_c} = \begin{pmatrix} 2.4 \\ 1.434 \end{pmatrix} \cdot MPa$$

Top of slab center

$$\sigma_3 := -\frac{N}{\overrightarrow{(\alpha \cdot A_{comp})}} - \frac{\overrightarrow{(N \cdot a_c \cdot y_{c.bot})}}{\overrightarrow{(I_{comp} \cdot \alpha)}} + \frac{N}{A_c} = \begin{pmatrix} 3.062 \\ 1.581 \end{pmatrix} \cdot MPa$$

Bottom of slab

$$\sigma_4 := -\frac{N}{A_{comp}} - \frac{\overrightarrow{(N \cdot a_c \cdot y_{c.bot})}}{I_{comp}} = \begin{pmatrix} -32.407 \\ -21.366 \end{pmatrix} \cdot MPa$$

Top steel

$$\sigma_5 := -\frac{N}{A_{comp}} + \frac{\overrightarrow{(N \cdot a_c \cdot y_{s.bot})}}{I_{comp}} = \begin{pmatrix} 8.334 \\ 5.908 \end{pmatrix} \cdot MPa$$

Bottom steel

Shrinkage effect on beam

$$r_{cs} := \frac{E_{sk} \cdot h_s}{\sigma_5 - \sigma_4}$$

$$\frac{1}{r_{cs}} = \begin{pmatrix} 7.185 \times 10^{-5} \\ 4.81 \times 10^{-5} \end{pmatrix} \frac{1}{m}$$

Bending caused by shrinkage

Output values used in: <u>Moment at supports due to shrinkage</u>

$$E_c := \begin{pmatrix} E_{ck} \\ E_{c.eff} \end{pmatrix} = \begin{pmatrix} 32 \\ 10.667 \end{pmatrix} \cdot GPa$$

$$\theta_{cs.sup} := \frac{L}{r_{cs}} = \begin{pmatrix} 1.006 \times 10^{-3} \\ 6.735 \times 10^{-4} \end{pmatrix}$$

Slope deflection from bending

$$L_{sup} := L = 14\,m$$

$$I_{comp.sup} := I_{comp} = \begin{pmatrix} 1.46 \\ 1.072 \end{pmatrix} m^4$$

Moment of inertia for support end section

Concrete Properties

$E_{ck} := 32 \cdot GPa$

$t_{cm} := 288 \cdot mm$

$\varphi_{eff} := 2$ BBK 94, 2.4.7

$E_{c.eff} := \frac{E_{ck}}{(1 + \varphi_{eff})} = 10.667 \cdot GPa$ Effect of creep, (long term)

Input from Lusas (Concrete)

$y_c := 0.116153 \cdot m$

$A_c := 3.16191 \cdot m^2$

$I_{c.xx} := 0.278442 \cdot m^4$

Steel Properties at Supports end (Beam 52, 56, 60, 64)

$E_{sk} := 210 \cdot GPa$

$h_s := 2700 \cdot mm$

Input from Lusas (Support end)

$y_s := 1.6894 \cdot m$

$A_s := 0.47259 \cdot m^2$

$I_{s.xx} := 0.637548 \cdot m^4$

Composite Calculation at Support end (Beam 52, 56, 60, 64)

$\alpha_s := \frac{E_{sk}}{E_{ck}} = 6.563$ Short-term load

$\alpha_l := \frac{E_{sk}}{E_{c.eff}} = 19.688$ Long-term load

$\alpha := \begin{pmatrix} \alpha_s \\ \alpha_l \end{pmatrix}$

$A_{c.eff} := \frac{A_c}{\alpha} = \begin{pmatrix} 0.482 \\ 0.161 \end{pmatrix} m^2$

$A_{comp} := A_{c.eff} + A_s = \begin{pmatrix} 0.954 \\ 0.633 \end{pmatrix} m^2$

$e_c := h_s + t_{cm} + y_c = 3.104\,m$

$e_s := h_s + t_{cm} - y_s = 1.299\,m$

$e_{comp} := \frac{A_s \cdot e_s + A_{c.eff} \cdot e_c}{A_{comp}} = \begin{pmatrix} 2.21 \\ 1.757 \end{pmatrix} m$

$a_s := e_{comp} - e_s = \begin{pmatrix} 0.912 \\ 0.458 \end{pmatrix} m$

$a_c := e_c - e_{comp} = \begin{pmatrix} 0.894 \\ 1.348 \end{pmatrix} m$

$I_{comp} := I_{s.xx} + A_s \cdot a_s^2 + \frac{I_{c.xx}}{\alpha} + \overrightarrow{\left(A_{c.eff} \cdot a_c^2\right)} = \begin{pmatrix} 1.458 \\ 1.042 \end{pmatrix} m^4$

The Moment of inertia for the composite section at the supports end is:

1.458 m^4 for a short-term load

1.042 m^4 for a long-term load

There is a smal difference in the moment of inertia between the at the supports (1.46 /1.072) and the moment of inertia at the end of the support steel section (1.458/1.042). The moment of inertia at the supports is therefore assumed to represent the whole support section.

Moment at Supports due to Shrinkage

The slope deflections caused, by bending from shrinkage, will increase the moments at the supports (*see Figure D.8*). The moments and stresses at the supports are calculated for both the short- and long-term load.

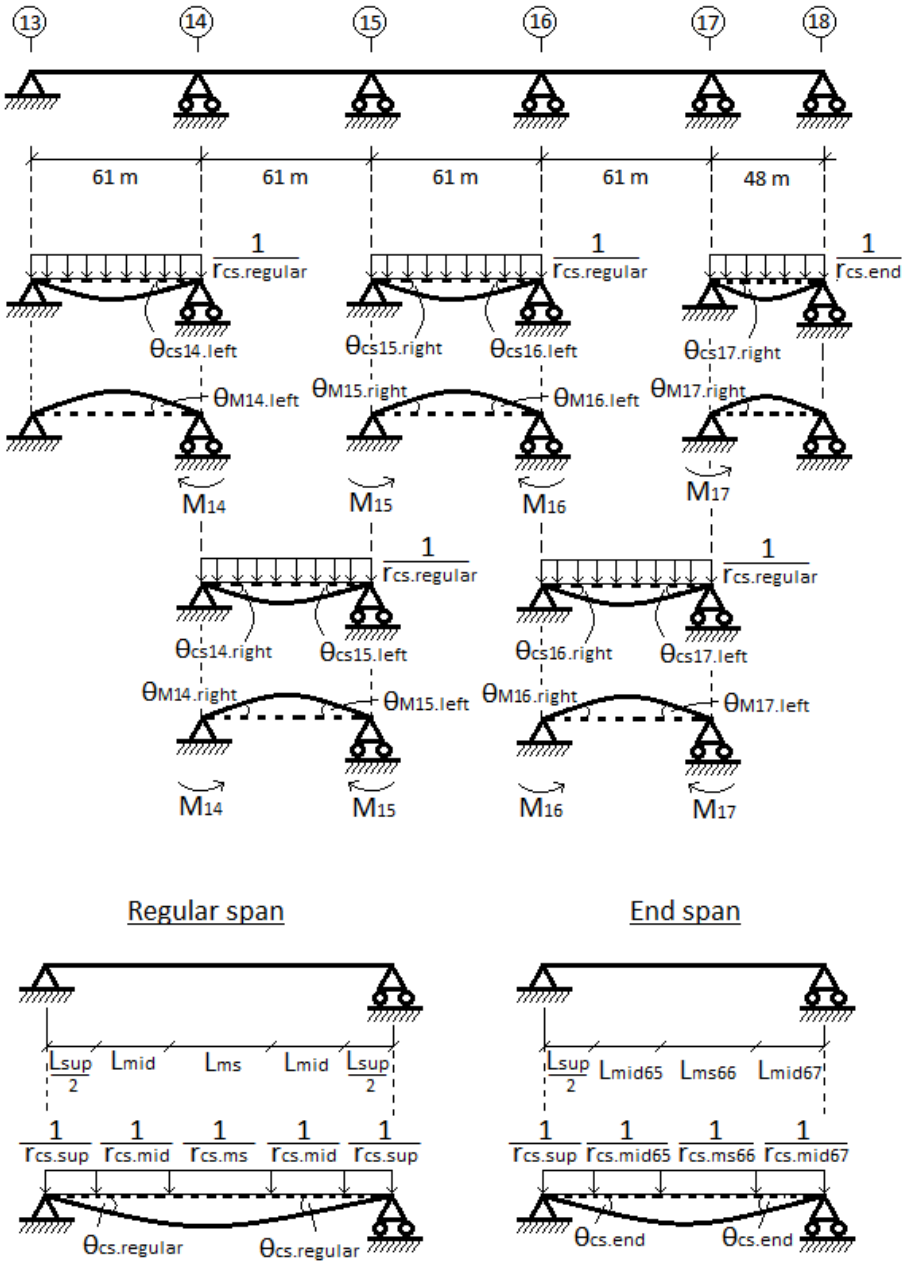

Figure D.8 Moments and slope deflections for the studied system (above). The different length and bending for the two different spans (below).

Moment at the supports due to shrinkage (short-term load)

Input from: **Moment of inertia and stress due to shrinkage for support section**

$E_c := 32 \cdot GPa$

$\theta_{cs.sup} := 1.006 \times 10^{-3}$ Slope deflection from bending

$L_{sup} := 14 \cdot m$ Length of the steel sections

$I_{comp.sup} := 1.46\ m^4$

Input from: **Moment of inertia and stress due to shrinkage for middle section**

$\theta_{cs.mid} := 1.105 \times 10^{-3}$ Slope deflection from bending (beam 53, 55, 57, 59, 61, 63, 65, 67)

$\theta_{cs.mid.65} := 1.026 \times 10^{-3}$ Slope deflection from bending (beam 65)

$\theta_{cs.mid.67} := 8.685 \times 10^{-4}$ Slope deflection from bending (beam 67)

$L_{mid} := 14 \cdot m$ Length of the steel beam 53, 55, 57, 59, 61, 63

$L_{mid.65} := 13 \cdot m$ Length of the steel beam 65

$L_{mid.67} := 11 \cdot m$ Length of the steel beam 67

$I_{comp.mid} := 1.193\ m^4$

Input from: **Moment of inertia and stress due to shrinkage for mid-span section**

$\theta_{cs.ms} := 1.471 \times 10^{-3}$ Slope deflection from bending (beem 54, 58, 62)

$\theta_{cs.ms.66} := 1.394 \times 10^{-3}$ Slope deflection from bending (beem 66)

$L_{ms} := 19 \cdot m$ Length of the steel beam 54, 58, 62

$L_{ms.66} := 18 \cdot m$ Length of the steel beam 66

$I_{comp.ms} := 1.275\ m^4$

Total slope deflection in spans caused by bending

$$\theta_{cs.regular} := \frac{\theta_{cs.sup} + 2 \cdot \theta_{cs.mid} + \theta_{cs.ms}}{2} = 2.344 \times 10^{-3}$$

Slope deflection coused by bending for all spans except the end span.

$$\theta_{cs.end} := \frac{\frac{\theta_{cs.sup}}{2} + \theta_{cs.mid.65} + \theta_{cs.ms.66} + \theta_{cs.mid.67}}{2} = 1.896 \times 10^{-3}$$

Corrections for the lengths in the end span

$\theta_{cs14.left} := \theta_{cs.regular}$ $\theta_{cs15.left} := \theta_{cs.regular}$

$\theta_{cs14.right} := \theta_{cs.regular}$ $\theta_{cs15.right} := \theta_{cs.regular}$

$\theta_{cs16.left} := \theta_{cs.regular}$ $\theta_{cs17.left} := \theta_{cs.regular}$

$\theta_{cs16.right} := \theta_{cs.regular}$ $\theta_{cs17.right} := \theta_{cs.end}$

Slope deflection at left and right side of the supports

Slope deflection at support from constraning moment at support

$$LdivIcompdivEc := \frac{1}{E_c}\cdot\left(\frac{L_{sup}}{I_{comp.sup}} + 2\cdot\frac{L_{mid}}{I_{comp.mid}} + \frac{L_{ms}}{I_{comp.ms}}\right) = 1.499\times 10^{-3}\cdot\frac{1}{MN\cdot m}$$

Part of the moment equaton often used

$$\theta_{M14.left} := \frac{M_{14}}{3}\cdot LdivIcompdivEc$$

$$\theta_{M14.right} := \frac{M_{14}}{3}\cdot LdivIcompdivEc + \frac{M_{15}}{6}\cdot LdivIcompdivEc$$

$$\theta_{M15.left} := \frac{M_{15}}{3}\cdot LdivIcompdivEc + \frac{M_{14}}{6}\cdot LdivIcompdivEc$$

$$\theta_{M15.right} := \frac{M_{15}}{3}\cdot LdivIcompdivEc + \frac{M_{16}}{6}\cdot LdivIcompdivEc$$

$$\theta_{M16.left} := \frac{M_{16}}{3}\cdot LdivIcompdivEc + \frac{M_{15}}{6}\cdot LdivIcompdivEc$$

$$\theta_{M16.right} := \frac{M_{16}}{3}\cdot LdivIcompdivEc + \frac{M_{17}}{6}\cdot LdivIcompdivEc$$

$$\theta_{M17.left} := \frac{M_{17}}{6}\cdot LdivIcompdivEc + \frac{M_{16}}{6}\cdot LdivIcompdivEc$$

$$\theta_{M17.right} := \frac{M_{17}}{3\cdot E_c}\cdot\left(\frac{\frac{L_{sup}}{2}}{I_{comp.sup}} + \frac{L_{mid.65}}{I_{comp.mid}} + \frac{L_{ms.66}}{I_{comp.ms}} + \frac{L_{mid.67}}{I_{comp.mid}}\right)$$

$\theta_{M.right} := \theta_{M.left}$ Due to symmetry

Continuity condition $\theta_{left} := \theta_{right}$ gives:

$\theta_{left} := \theta_{cs.left} - \theta_{M.left}$

$\theta_{right} := -\theta_{cs.right} + \theta_{M.right}$

$M_{14} := 0$ $M_{15} := 0$ $M_{16} := 0$ $M_{17} := 0$

Given

$\theta_{cs14.left} - \theta_{M14.left} = \theta_{M14.right} - \theta_{cs14.right}$

$\theta_{cs15.left} - \theta_{M15.left} = \theta_{M15.right} - \theta_{cs15.right}$

$\theta_{cs16.left} - \theta_{M16.left} = \theta_{M16.right} - \theta_{cs16.right}$

$\theta_{cs17.left} - \theta_{M17.left} = \theta_{M17.right} - \theta_{cs17.right}$

$$\begin{pmatrix} M_{14} \\ M_{15} \\ M_{16} \\ M_{17} \end{pmatrix} := \text{Find}(M_{14}, M_{15}, M_{16}, M_{17}) \rightarrow \begin{pmatrix} \frac{2.287 \times 10^{44} \cdot J^2 + 9.478 \times 10^{34} \cdot GPa \cdot J \cdot m^3}{2.558 \times 10^{28} \cdot GPa \cdot m^3 + 5.687 \times 10^{37} \cdot J} \\ \frac{1.524 \times 10^{44} \cdot J^2 + 1.009 \times 10^{35} \cdot GPa \cdot J \cdot m^3}{2.558 \times 10^{28} \cdot GPa \cdot m^3 + 5.687 \times 10^{37} \cdot J} \\ \frac{2.287 \times 10^{44} \cdot J^2 - 1.835 \times 10^{34} \cdot GPa \cdot J \cdot m^3}{2.558 \times 10^{28} \cdot GPa \cdot m^3 + 5.687 \times 10^{37} \cdot J} \\ \frac{1.812 \times 10^{22} \cdot GPa \cdot J \cdot m^3}{1.024 \times 10^{15} \cdot GPa \cdot m^3 + 2.277 \times 10^{24} \cdot J} \end{pmatrix}$$

$M_{14} = 3.923 \cdot MN \cdot m$

$M_{15} = 3.072 \cdot MN \cdot m$

$M_{16} = 2.551 \cdot MN \cdot m$

$M_{17} = 5.488 \cdot MN \cdot m$

Effect on the support section

Indata from: **Moment of inertia and stress due to shrinkage for support section**

$y_{ceb.top} := 1.555\ m$ Distance, CGcomp to top edge beam

$y_{cs.top} := 0.755 \cdot m$ Distance, CGcomp to top slab center

$y_{c.bot} := 0.467\ m$ Distance, CGcomp to bottom slab

Stresses caused by moment due to shrinkage in support 16

$M_{shr} := M_{16}$

$\sigma_1 := \frac{M_{shr} \cdot y_{ceb.top}}{I_{comp.sup}} = 2.717 \cdot MPa$

Concrete tensile strength

$f_{ctk} := 1.95 \cdot MPa$

$\sigma_2 := \frac{M_{shr} \cdot y_{cs.top}}{I_{comp.sup}} = 1.319 \cdot MPa$

$\sigma_3 := \frac{M_{shr} \cdot y_{c.bot}}{I_{comp.sup}} = 0.816 \cdot MPa$

The Stresses in the edge beam is larger than the strength of the concrete and will crack.

A cracked concrete model will be used to calculate the final stresses in the reinforcement.

Output value used in: **Moment of inertia and total stress for cracked concrete at support**

$M_{shr.short} := M_{shr} = 2.551 \cdot MN \cdot m$

Moments at the supports due to shrinkage (long-term load)

Input from: **Moment of inertia and stress due to shrinkage for support section**

$E_c := 10.667 \cdot GPa$

$\theta_{cs.sup} := 6.735 \times 10^{-4}$ Slope deflection from bending

$L_{sup} := 14 \cdot m$ Length of the steel sections

$I_{comp.sup} := 1.072\ m^4$

Input from: **Moment of inertia and stress due to shrinkage for middle section**

$\theta_{cs.mid} := 8.42 \times 10^{-4}$ Slope deflection from bending (beam 53, 55, 57, 59, 61, 63, 65, 67)

$\theta_{cs.mid.65} := 7.819 \times 10^{-4}$ Slope deflection from bending (beam 65)

$\theta_{cs.mid.67} := 6.616 \times 10^{-4}$ Slope deflection from bending (beam 67)

$L_{mid} := 14 \cdot m$ Length of the steel beam 53, 55, 57, 59, 61, 63

$L_{mid.65} := 13 \cdot m$ Length of the steel beam 65

$L_{mid.67} := 11 \cdot m$ Length of the steel beam 67

$I_{comp.mid} := 0.846\ m^4$

Input from: **Moment of inertia and stress due to shrinkage for mid-span section**

$\theta_{cs.ms} := 1.124 \times 10^{-3}$ Slope deflection from bending (beem 54, 58, 62)

$\theta_{cs.ms.66} := 1.065 \times 10^{-3}$ Slope deflection from bending (beem 66)

$L_{ms} := 19 \cdot m$ Length of the steel beam 54, 58, 62

$L_{ms.66} := 18 \cdot m$ Length of the steel beam 66

$I_{comp.ms} := 0.898\ m^4$

Total slope deflection in spans caused by bending

$$\theta_{cs.regular} := \frac{\theta_{cs.sup} + 2 \cdot \theta_{cs.mid} + \theta_{cs.ms}}{2} = 1.741 \times 10^{-3}$$

Slope deflection coused by bending for all spans except the end span.

$$\theta_{cs.end} := \frac{\frac{\theta_{cs.sup}}{2} + \theta_{cs.mid.65} + \theta_{cs.ms.66} + \theta_{cs.mid.67}}{2} = 1.423 \times 10^{-3}$$

Corrections for the lengths in the end span

$\theta_{cs14.left} := \theta_{cs.regular}$ $\theta_{cs15.left} := \theta_{cs.regular}$

$\theta_{cs14.right} := \theta_{cs.regular}$ $\theta_{cs15.right} := \theta_{cs.regular}$

$\theta_{cs16.left} := \theta_{cs.regular}$ $\theta_{cs17.left} := \theta_{cs.regular}$

$\theta_{cs16.right} := \theta_{cs.regular}$ $\theta_{cs17.right} := \theta_{cs.end}$

Slope deflection at left and right side of the supports

Slope deflection at support from constraning moment at support

$$LdivIcompdivEc := \frac{1}{E_c}\cdot\left(\frac{L_{sup}}{I_{comp.sup}} + 2\cdot\frac{L_{mid}}{I_{comp.mid}} + \frac{L_{ms}}{I_{comp.ms}}\right) = 6.311\times10^{-3}\cdot\frac{1}{MN\cdot m}$$

Part of the moment equaton often used

$$\theta_{M14.left} := \frac{M_{14}}{3}\cdot LdivIcompdivEc$$

$$\theta_{M14.right} := \frac{M_{14}}{3}\cdot LdivIcompdivEc + \frac{M_{15}}{6}\cdot LdivIcompdivEc$$

$$\theta_{M15.left} := \frac{M_{15}}{3}\cdot LdivIcompdivEc + \frac{M_{14}}{6}\cdot LdivIcompdivEc$$

$$\theta_{M15.right} := \frac{M_{15}}{3}\cdot LdivIcompdivEc + \frac{M_{16}}{6}\cdot LdivIcompdivEc$$

$$\theta_{M16.left} := \frac{M_{16}}{3}\cdot LdivIcompdivEc + \frac{M_{15}}{6}\cdot LdivIcompdivEc$$

$$\theta_{M16.right} := \frac{M_{16}}{3}\cdot LdivIcompdivEc + \frac{M_{17}}{6}\cdot LdivIcompdivEc$$

$$\theta_{M17.left} := \frac{M_{17}}{6}\cdot LdivIcompdivEc + \frac{M_{16}}{6}\cdot LdivIcompdivEc$$

$$\theta_{M17.right} := \frac{M_{17}}{3\cdot E_c}\cdot\left(\frac{\frac{L_{sup}}{2}}{I_{comp.sup}} + \frac{L_{mid.65}}{I_{comp.mid}} + \frac{L_{ms.66}}{I_{comp.ms}} + \frac{L_{mid.67}}{I_{comp.mid}}\right)$$

$\theta_{M.right} := \theta_{M.left}$ Due to symmetry

Continuity condition $\theta_{left} := \theta_{right}$ gives:

$\theta_{left} := \theta_{cs.left} - \theta_{M.left}$

$\theta_{right} := -\theta_{cs.right} + \theta_{M.right}$

$M_{14} := 0$ $M_{15} := 0$ $M_{16} := 0$ $M_{17} := 0$

Given

$\theta_{cs14.left} - \theta_{M14.left} = \theta_{M14.right} - \theta_{cs14.right}$

$\theta_{cs15.left} - \theta_{M15.left} = \theta_{M15.right} - \theta_{cs15.right}$

$\theta_{cs16.left} - \theta_{M16.left} = \theta_{M16.right} - \theta_{cs16.right}$

$\theta_{cs17.left} - \theta_{M17.left} = \theta_{M17.right} - \theta_{cs17.right}$

$$\begin{pmatrix} M_{14} \\ M_{15} \\ M_{16} \\ M_{17} \end{pmatrix} := \text{Find}(M_{14}, M_{15}, M_{16}, M_{17}) \rightarrow \begin{pmatrix} \frac{7.935 \times 10^{92} \cdot J^2 + 3.277 \times 10^{83} \cdot GPa \cdot J \cdot m^3}{5.017 \times 10^{77} \cdot GPa \cdot m^3 + 1.119 \times 10^{87} \cdot J} \\ \frac{5.29 \times 10^{92} \cdot J^2 + 3.497 \times 10^{83} \cdot GPa \cdot J \cdot m^3}{5.017 \times 10^{77} \cdot GPa \cdot m^3 + 1.119 \times 10^{87} \cdot J} \\ \frac{7.935 \times 10^{92} \cdot J^2 - 6.6 \times 10^{82} \cdot GPa \cdot J \cdot m^3}{5.017 \times 10^{77} \cdot GPa \cdot m^3 + 1.119 \times 10^{87} \cdot J} \\ \frac{1.575 \times 10^{84} \cdot GPa \cdot J \cdot m^3}{5.017 \times 10^{77} \cdot GPa \cdot m^3 + 1.119 \times 10^{87} \cdot J} \end{pmatrix}$$

$M_{14} = 0.692 \cdot MN \cdot m$

$M_{15} = 0.542 \cdot MN \cdot m$

$M_{16} = 0.449 \cdot MN \cdot m$

$M_{17} = 0.972 \cdot MN \cdot m$

Effect on the support section

Input from: **Moment of inertia and stress due to shrinkage for support section**

$y_{ceb.top} := 1.968\ m$ Distance, CGcomp to top edge beam

$y_{cs.top} := 1.168 \cdot m$ Distance, CGcomp to top slab center

$y_{c.bot} := 0.88\ m$ Distance, CGcomp to bottom slab

Stresses caused by moment due to shrinkage in support 16

$M_{shr} := M_{16}$

$$\sigma_1 := \frac{M_{shr} \cdot y_{ceb.top}}{I_{comp.sup}} = 0.824 \cdot MPa$$

$$\sigma_2 := \frac{M_{shr} \cdot y_{cs.top}}{I_{comp.sup}} = 0.489 \cdot MPa$$

$$\sigma_3 := \frac{M_{shr} \cdot y_{c.bot}}{I_{comp.sup}} = 0.369 \cdot MPa$$

Output value used in: **Moment of inertia and total stress for cracked concrete at support**

$M_{shr.long} := M_{shr} = 0.449 \cdot MN \cdot m$

Required Reinforcement

The required reinforcement is calculated both for 0.5 % and 1.0 % of the edge beam concrete area.

Minimum reinforcement

BRO 94:5
53.341
Longitudinal reinforcement should be added in the concrete slab so that the total amount of reinforcement is at least 0.50 % of the concrete cross-section area. This requirement also applies to compressed concrete.
In parts of the slab which are cracked due to load combination V:A (serviceability limit state), the longitudinal reinforcement together with additional reinforcement should be at least 1.0 % of the concrete cross-section area. The maximum allowed reinforcement diameter is 16 mm.

Imput from Lusas (Concrete)

$$A_c := 0.599087\text{m}^2$$

$$A_s := \begin{pmatrix} 0.5\% \cdot A_c \\ 1.0\% \cdot A_c \end{pmatrix} = \begin{pmatrix} 2.995 \times 10^3 \\ 5.991 \times 10^3 \end{pmatrix} \cdot \text{mm}^2$$

$$A_{16} := \left(\frac{16 \cdot \text{mm}}{2}\right)^2 \cdot \pi = 201.062\text{mm}^2$$

$$n_{16} := \frac{A_s}{A_{16}} = \begin{pmatrix} 14.898 \\ 29.796 \end{pmatrix}$$

Required reinforment area for 0.5% is 2995 mm^2, which represents 15ϕ16 in the edge beams
Required reinforment area for 1.0% is 5991 mm^2, which represents 30ϕ16 in the edge beams

Output values used in: Reinforcement moment of inertia

$$A_{r.eb} := A_s = \begin{pmatrix} 2.995 \times 10^{-3} \\ 5.991 \times 10^{-3} \end{pmatrix} \text{m}^2$$

Moment of Inertia and Total Stress for Cracked Section

The stress at the top of the edge beam tensile strength of the concrete. The whole concrete section is assumed to be cracked and stresses can only be absorbed by the reinforcement.

A new moment of inertia is calculated for the new slab section with only rebars (*see Figure D.9*).

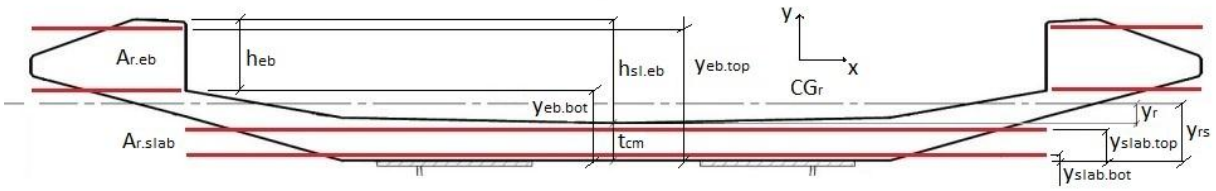

Figure D.9 Distances used in the reinforced moment of inertia calculation.

The moment of inertia for the cracked composite section (*see Figure D.10*) and the final stresses due to moment from shrinkage and loading are calculated.

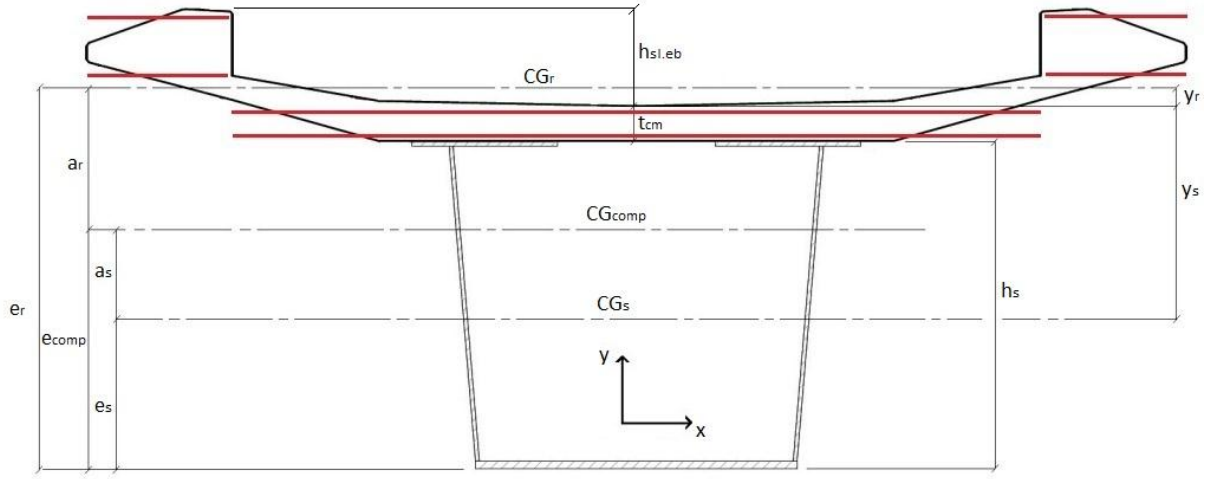

Figure D.10 Distances used in the moment of inertia calculation for the cracked composite section.

Reinforcement moment of inertia

Concrete measurements

$t_{cm} := 288 \cdot mm$

$h_{sl.eb} := 0.8m$

$h_{ebe} := 0.55 \cdot m$

Reinforcement properties

$E_r := 200 \cdot GPa$

$A_{r.slab} := 19640 \cdot mm^2$ Reinforcement area in slab

$A_{r.eb} := \begin{pmatrix} 2995 \cdot mm^2 \\ 5991 \cdot mm^2 \end{pmatrix}$ Reinforcement area in edge beam

Input from: Minimum reinforcement

$c_{slab} := 40 \cdot mm$ Concrete cover in slab

$c_{eb} := 45 \cdot mm$ Concrete cover in edge beam

$\phi := 16 \cdot mm$ Reinforcement diameter

Calculations of moment of inertia

$A_r := A_{r.slab} + 2 \cdot A_{r.eb} = \begin{pmatrix} 0.026 \\ 0.032 \end{pmatrix} m^2$ Total area

Distances fram slab bottom tp the reinforment layers

$y_{slab.bot} := c_{slab} + \frac{\phi}{2} = 0.048\,m$

$y_{slab.top} := t_{cm} - y_{slab.bot} = 0.24\,m$

$y_{eb.bot} := t_{cm} + h_{sl.eb} - h_{ebe} = 0.538\,m$

$y_{eb.top} := t_{cm} + h_{sl.eb} - c_{eb} - \frac{\phi}{2} = 1.035\,m$

$$y_{rs} := \frac{\left[\left(A_{r.eb}\cdot y_{eb.top} + A_{r.eb}\cdot y_{eb.bot}\right) + \frac{A_{r.slab}}{2}\cdot y_{slab.top}\right] + \frac{A_{r.slab}}{2}\cdot y_{slab.bot}}{A_r} = \begin{pmatrix} 0.294 \\ 0.387 \end{pmatrix} m$$

Distance from bottom slab to GC

$$y_r := y_{rs} - t_{cm} = \begin{pmatrix} 6.159 \\ 99.452 \end{pmatrix}\cdot mm$$

Distance from top slab to GC

Moment of inertia around x-axis

$$I_{rs} := \frac{\pi\cdot\phi^4}{64} = 3.217\times 10^{-9}\, m^4$$

Moment of inerta for a reinforcement bar

$$I_{r.eb.top} := I_{rs} + \overrightarrow{\left[A_{r.eb}\cdot\left(y_{eb.top} - y_{rs}\right)^2\right]} = \begin{pmatrix} 1.644\times 10^{-3} \\ 2.512\times 10^{-3} \end{pmatrix} m^4$$

Top edge beam reinf.

$$I_{r.eb.bot} := I_{rs} + \overrightarrow{\left[A_{r.eb}\cdot\left(y_{eb.bot} - y_{rs}\right)^2\right]} = \begin{pmatrix} 1.781\times 10^{-4} \\ 1.358\times 10^{-4} \end{pmatrix} m^4$$

Bottom edge beam reinf.

$$I_{r.slab.top} := I_{rs} + \frac{A_{r.slab}}{2}\cdot\left(y_{rs} - y_{slab.top}\right)^2 = \begin{pmatrix} 2.881\times 10^{-5} \\ 2.135\times 10^{-4} \end{pmatrix} m^4$$

Top slab reinf.

$$I_{r.slab.bot} := I_{rs} + \frac{A_{r.slab}}{2}\cdot\left(y_{rs} - y_{slab.bot}\right)^2 = \begin{pmatrix} 5.95\times 10^{-4} \\ 1.132\times 10^{-3} \end{pmatrix} m^4$$

Bottom slab reinf.

$$I_r := I_{r.eb.top} + I_{r.eb.bot} + I_{r.slab.top} + I_{r.slab.bot} = \begin{pmatrix} 2.446\times 10^{-3} \\ 3.993\times 10^{-3} \end{pmatrix} m^4$$

Total moment of inerta

Output values used in: **Moment of inertia and total stresses for cracked concrete section at support**

$$y_r = \begin{pmatrix} 6.159 \\ 99.452 \end{pmatrix} \cdot mm$$

$$A_r = \begin{pmatrix} 0.026 \\ 0.032 \end{pmatrix} m^2$$

$$I_r = \begin{pmatrix} 2.446 \times 10^{-3} \\ 3.993 \times 10^{-3} \end{pmatrix} m^4$$

Moment of inertia and total stresses for cracked concrete section at support

Concrete measurements

$t_{cm} := 288 \cdot mm$

$h_{sl.eb} := 0.8 \cdot m$

Reinforcement Properties

$E_r := 200 \cdot GPa$

Input from: Reinforcement moment of inertia

$y_r := \begin{pmatrix} 6.159 \\ 99.452 \end{pmatrix} \cdot mm$

$A_r := \begin{pmatrix} 0.026 \\ 0.032 \end{pmatrix} \cdot m^2$

$I_r := \begin{pmatrix} 2.446 \times 10^{-3} \\ 3.993 \times 10^{-3} \end{pmatrix} m^4$

Steel Properties at Supports

$E_{sk} := 210 \cdot GPa$

$h_s := 2700 \cdot mm$

Input from Lusas (Support)

$y_s := 1.5687 \cdot m$

$A_s := 0.51543 \cdot m^2$

$I_{s.xx} := 0.710474 \cdot m^4$

Composite Calculation at Support

$$\alpha := \frac{E_{sk}}{E_r} = 1.05$$

$$A_{r.eff} := \frac{A_r}{\alpha} = \begin{pmatrix} 0.025 \\ 0.03 \end{pmatrix} m^2$$

$$A_{comp} := A_{r.eff} + A_s = \begin{pmatrix} 0.54 \\ 0.546 \end{pmatrix} m^2$$

$$e_r := h_s + t_{cm} + y_r = \begin{pmatrix} 2.994 \\ 3.087 \end{pmatrix} m$$

$$e_s := h_s + t_{cm} - y_s = 1.419\,m$$

$$e_{comp} := \frac{A_s \cdot e_s + \overrightarrow{\left(A_{r.eff} \cdot e_r\right)}}{A_{comp}} = \begin{pmatrix} 1.491 \\ 1.512 \end{pmatrix} m$$

$$a_s := e_{comp} - e_s = \begin{pmatrix} 0.072 \\ 0.093 \end{pmatrix} m$$

$$a_r := e_r - e_{comp} = \begin{pmatrix} 1.503 \\ 1.575 \end{pmatrix} m$$

$$\begin{pmatrix} I_{comp0.5} \\ I_{comp1.0} \end{pmatrix} := I_{s.xx} + A_s \cdot a_s^{\,2} + \frac{I_r}{\alpha} + \overrightarrow{\left(A_{r.eff} \cdot a_r^{\,2}\right)} = \begin{pmatrix} 0.771 \\ 0.794 \end{pmatrix} m^4$$

Stress Distrubution

Moment and forces

$M_l := 30.5 \cdot MN \cdot m$ **From 2-D model**

$M_{shr.short} := 2.551\ MN \cdot m$ **Input from:** **Moments at the supports due to shrinkage (short-term load)**

$M_{shr.long} := 0.449\ MN \cdot m$ **Input from:** **Moments at the supports due to shrinkage (long-term load)**

$$M_{shr} := \begin{pmatrix} M_{shr.short} \\ M_{shr.long} \end{pmatrix}$$

$$M := M_l + M_{shr} = \begin{pmatrix} 33.051 \\ 30.949 \end{pmatrix} \cdot MN \cdot m$$

Distances

$c_{eb} := 45 \cdot mm$

$c_{slab} := 40 \cdot mm$

$\phi := 16 \cdot mm$

$$\begin{pmatrix} y_{eb.top0.5} \\ y_{eb.top1.0} \end{pmatrix} := a_r - y_r + h_{sl.eb} - c_{eb} - \frac{\phi}{2} = \begin{pmatrix} 2.244 \\ 2.223 \end{pmatrix} m$$

Distance, CGcomp to top edge beam reinforcement

$$\begin{pmatrix} y_{cs.top0.5} \\ y_{cs.top1.0} \end{pmatrix} := a_r - y_r - c_{slab} - \frac{\phi}{2} = \begin{pmatrix} 1.449 \\ 1.428 \end{pmatrix} m$$

Distance, CGcomp to top slab reinforcement

$$\begin{pmatrix} y_{s.top0.5} \\ y_{s.top1.0} \end{pmatrix} := a_r - y_r - t_{cm} = \begin{pmatrix} 1.209 \\ 1.188 \end{pmatrix} m$$

Distance, CGcomp to top steel

$$\begin{pmatrix} y_{s.bot0.5} \\ y_{s.bot1.0} \end{pmatrix} := e_{comp} = \begin{pmatrix} 1.491 \\ 1.512 \end{pmatrix} m$$

Distance, CGcomp to bottom steel

Stresses

0.5% reinforcement

$$\sigma_1 := \frac{\overrightarrow{\left(M \cdot y_{eb.top0.5}\right)}}{I_{comp0.5} \cdot \alpha} = \begin{pmatrix} 91.547 \\ 85.724 \end{pmatrix} \cdot MPa$$ Top reinforcement in edge beam

$$\sigma_2 := \frac{\overrightarrow{\left(M \cdot y_{cs.top0.5}\right)}}{I_{comp0.5} \cdot \alpha} = \begin{pmatrix} 59.107 \\ 55.347 \end{pmatrix} \cdot MPa$$ Top reinforcement in slab

$$\sigma_3 := \frac{\overrightarrow{\left(M \cdot y_{s.top0.5}\right)}}{I_{comp0.5}} = \begin{pmatrix} 51.779 \\ 48.486 \end{pmatrix} \cdot MPa$$ Top of steel section

$$\sigma_4 := \frac{\overrightarrow{\left(M \cdot y_{s.bot0.5}\right)}}{I_{comp0.5}} = \begin{pmatrix} 63.903 \\ 59.839 \end{pmatrix} \cdot MPa$$ Bottom of steel section

1.0% reinforcement

$$\sigma_{1.1} := \frac{\overrightarrow{\left(M \cdot y_{eb.top1.0}\right)}}{I_{comp1.0} \cdot \alpha} = \begin{pmatrix} 88.072 \\ 82.471 \end{pmatrix} \cdot MPa$$ Top reinforcement in edge beam

$$\sigma_{2.1} := \frac{\overrightarrow{\left(M \cdot y_{cs.top1.0}\right)}}{I_{comp1.0} \cdot \alpha} = \begin{pmatrix} 56.569 \\ 52.972 \end{pmatrix} \cdot MPa$$ Top reinforcement in slab

$$\sigma_{3.1} := \frac{\overrightarrow{\left(M \cdot y_{s.top1.0}\right)}}{I_{comp1.0}} = \begin{pmatrix} 49.412 \\ 46.27 \end{pmatrix} \cdot MPa$$ Top of steel section

$$\sigma_{4.1} := \frac{\overrightarrow{\left(M \cdot y_{s.bot1.0}\right)}}{I_{comp1.0}} = \begin{pmatrix} 62.929 \\ 58.926 \end{pmatrix} \cdot MPa$$ Bottom of steel section

Output values used in: <u>Crack width, edge beam</u>

$$\sigma_s := \begin{pmatrix} \max\left(\sigma_1\right) \\ \max\left(\sigma_{1.1}\right) \end{pmatrix} = \begin{pmatrix} 91.547 \\ 88.072 \end{pmatrix} \cdot MPa$$

Crack Width

The stresses from the cracked section are used to calculate the crack width for the edge beam (*see Figure D.11*). The calculation is done for both 0.5 % and 1.0 % reinforcement in the edge beams.

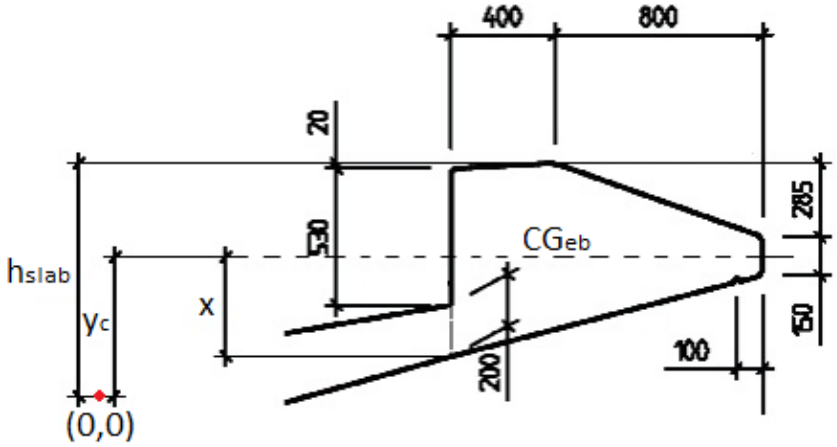

Figure D.11 Distances and dimensions of the edge beam, used in the crack width calculation (see Appendix A).

Crack width, edge beam

General Information

Environmental class: A2
Lifetime class: L2

Concrete cover: 45 mm

Maximum crack width $w_k := 0.30 \cdot mm$ BRO 94, sup. 4, table 41-6

Concrete

Concrete class: K40

$f_{cck} := 28.5 \cdot MPa$

$f_{ctk} := 1.95 \cdot MPa$

$E_{ck} := 32.0 \cdot GPa$

Reinforcement

Reinforcement B500B

$f_{yk} := 500 \cdot MPa$

$E_{sk} := 200.0 \cdot GPa$

Steel

$E_{sk.steel} := 210 \cdot GPa$

Minimum Reinforcement

BRO 94:5
53.341
Longitudinal reinforcement should be added in the concrete slab so that the total amount of reinforcement is at least 0.50 % of the concrete cross-section area. This requirement also applies to compressed concrete.
In parts of the slab which are cracked due to load combination V:A (serviceability limit state), the longitudinal reinforcement together with additional reinforcement should be at least 1.0 % of the concrete cross-section area. The maximum allowed reinforcement diameter is 16 mm.

Imput from Lusas (Concrete)

$y_c := 0.456116 \cdot m$

$A_c := 0.599087 \cdot m^2$

$h_{slab} := 0.8 \cdot m$

$$A_s := \begin{pmatrix} 0.5\% \cdot A_c \\ 1.0\% \cdot A_c \end{pmatrix} = \begin{pmatrix} 2.995 \times 10^3 \\ 5.991 \times 10^3 \end{pmatrix} \cdot mm^2$$

Reinforcement area

Crack Width Controll

$\sigma_s := \begin{pmatrix} 91.547 \\ 88.072 \end{pmatrix} MPa$

Stress due to load and shrinkage

Input from: **Moment of inertia and total stresses for cracked concrete section at support**

Crack Criteria

$\zeta := 1.0$

BBK 94, 4.5.3

If an incorrect assessment of the density or bending deformation does not involve personal injury, serious damage or substantial financial loss for other reasons the coefficient ζ can be set equal to 1.0

$h := 0.75 \quad (m)$ Hight of the cross section

$k := 0.6 + \frac{0.4}{\sqrt[4]{h}} = 1.03$ Figure 4.5.3

$\varphi_{ef} := 2.0$ 2.4.7

$E_{ef} := \frac{E_{ck}}{1 + \varphi_{ef}}$ 4.3

$\alpha := \frac{E_{sk}}{E_{ef}} = 18.75$

$k \cdot \sigma_n + \sigma_m \le k \cdot \frac{f_{ct}}{\zeta}$ (4.5.3a) Pulling normal force

$\sigma_{cr} := k \cdot \frac{f_{ctk}}{\zeta} = 2.008 \cdot MPa$

$\sigma_{sr} := \alpha \cdot \sigma_{cr} = 37.653 \cdot MPa$

4.5.5

is the value of σ_s at the load causing cracking, i.e. immediately after the formation of the crack.

Reinforcement Stress Reducing Factor v

$\kappa_1 := 0.8$ 4.5.5, Ribbed bars

$\beta := 0.5$ 4.5.5, Long-term loading

$$v := \max\left(1 - \frac{\beta}{2.5 \cdot \kappa_1} \cdot \frac{\sigma_{sr}}{\sigma_s}, 0.4\right) = 0.897 \qquad (4.5.5c)$$

Effective Hight and Area

$h := 750 \cdot mm$

$\phi := 16 \cdot mm$ $c := 45 \cdot mm$

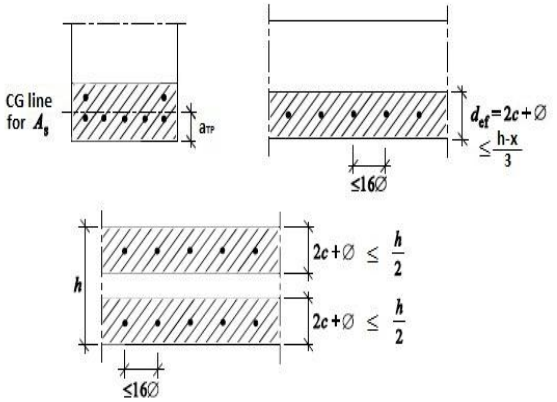

Figure 4.5.5

Determination of the effective concrete area A_{ef} for beam in bending (top left), slab in bending (top right) and member in tension (bottom)

The whole edge beam is in tension

$x := h - (h_{slab} - y_c) = 0.406\ m$

$\frac{h}{2} = 375 \cdot mm$

$d_{ef} := 2 \cdot \min\left(2 \cdot c + \phi, \frac{h}{2}\right) = 212 \cdot mm$ Whole section is in tension, bottom figure is used

$b_{ef} := \frac{A_c}{h} = 0.799\ m$ Effective width due to non rectangular shape

$A_{ef} := d_{ef} \cdot b_{ef} = 0.169\ m^2$

Crack Spacing

$$\kappa_2 := 0.25 - \frac{d_{ef}}{8\cdot(h - x)} = 0.173 \qquad (4.5.5)$$

$$\rho_r := \frac{A_s}{A_{ef}} = \begin{pmatrix} 0.018 \\ 0.035 \end{pmatrix}$$

$$s_{rm} := 50\cdot mm + \kappa_1\cdot\kappa_2\cdot\frac{\phi}{\rho_r} = \begin{pmatrix} 175.143 \\ 112.572 \end{pmatrix}\cdot mm \qquad (4.5.5d)$$

Crack Width

$$w_m := \overrightarrow{\left(v\cdot\frac{\sigma_s}{E_{sk}}\cdot s_{rm}\right)} = \begin{pmatrix} 0.072 \\ 0.044 \end{pmatrix}\cdot mm \qquad (4.5.5b)$$

$$w_k := 1.7\cdot w_m = \begin{pmatrix} 0.122 \\ 0.076 \end{pmatrix}\cdot mm \qquad (4.5.5a)$$

The maximum crack width in the edge beam is: 0.12 mm for 0.5% reinforcement
0.08 mm for 1.0% reinforcement

Based on the above relationship between the crack width and the used amount of reinforcement:

- Doubling the reinforcement ratio decreases the crack width by 1/3 of its value.
- Since the 0.5 % reinforcement ratio used in the edge beams results in 0.5 mm crack width.
- Therefore 1.1% reinforcement ratio in the edge beams will result in 0.3 mm crack width, satisfying the maximum code limits.

Appendix E Original Calculations

This is the original calculation (in Swedish) for the longitudinal reinforcement (Tyréns AB, 2004) regarding the amount of reinforcement used in the slab and edge beams. It also includes the expected crack width in the slab.

D.1.3 Armering i längsled

Dimensionering av armeringen i farbaneplattans längsled.

Armeringen dimensioneras utifrån snittkrafter som fås från Strukturas systemberäkning av samverkanskonstruktionen.

Allmänna förutsättningar

Miljöklass: B3/A2
Livslängdklass: L2

Täckande betongskikt: 40 mm

$\zeta := 1.0$ $w_k := 0.30$

Betong

Hållfasthetsklass K40

$\gamma_n := 1.2$

$f_{cck} := 28.5MPa$ $f_{cc} := \frac{f_{cck}}{1.5 \cdot \gamma_n}$ $f_{cc} = 15.833\,MPa$

$f_{ctk} := 1.95MPa$ $f_{ct} := \frac{f_{ctk}}{1.5 \cdot \gamma_n}$ $f_{ct} = 1.083\,MPa$

$E_{ck} := 32.0GPa$ $E_c := \frac{E_{ck}}{1.2 \cdot \gamma_n}$ $E_c = 22.222\,GPa$

Armering

Armeringstyp B500B.

$f_{yk} := 500MPa$ $f_{st} := \frac{f_{yk}}{1.15 \cdot \gamma_n}$ $f_{st} = 362.319\,MPa$

$E_{sk} := 200.0GPa$ $E_s := \frac{E_{sk}}{1.05 \cdot \gamma_n}$ $E_s = 158.73\,GPa$

Minimiarmering

Enligt 53.341 i BRO 94 skall de delar av farbaneplattan som är sprucken i bruksgränstillstånd ha en armeringsmängd av minst 1%.

Kantbalkarna betraktas separat. Kantbalken har en tvärsnittsarea på 0.593 m^2.

Farbaneplatta

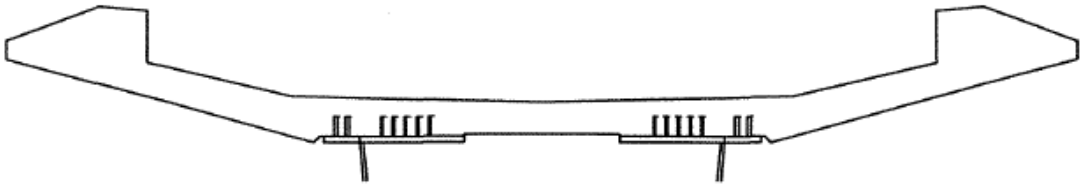

$A_{btg.tot} := 3.228m^2$ $A_{btg.kb} := 0.593m^2$

$A_{btg} := A_{btg.tot} - 2 \cdot A_{btg.kb}$ $A_{btg} = 2.042\,m^2$

$b_{fb} := 6.660m$

$A_{s.min} := 1.0\% \cdot A_{btg}$ $A_{s.min} = 20420\,mm^2$

$n_{16} := \frac{A_{s.min}}{201mm^2}$ $n_{16} = 101.6$

$s_{16} := 2 \cdot \frac{b_{fb}}{n_{16}}$ $s_{16} = 0.131\,m$

Erforderlig armeringsmängd är 20420 mm^2, vilket motsvarar ϕ16s130 i både över- och underkant.

Kantbalk

Kantbalken medverkar inte statiskt i "farbaneplattan" varför 1.0%-kravet enligt 53.341 i BRO 94 inte anses gälla kantbalken.

$A_{btg} := A_{btg.kb}$ $\quad A_{s.kb} := 0.5\% \cdot A_{btg}$ $\quad A_{s.kb} = 2965\,mm^2$

$$n_{16} := \frac{A_{s.kb}}{201\,mm^2} \qquad n_{16} = 14.8$$

Erforderlig armeringsmängd är 2965 mm^2, vilket motsvarar 15ϕ16 i vardera kantbalk.

Sprickviddskontroll

Spänningarna för kontroll av betong och armering beräknas utifrån normalkraften i "armeringselementet" beräknat i Strukturas systemberäkning.

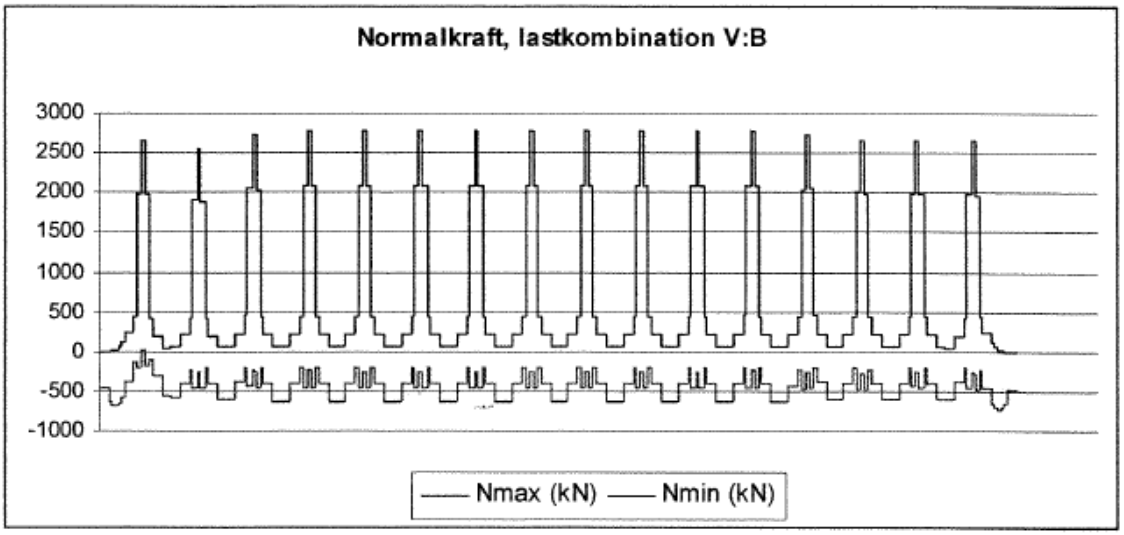

Normalkraften i armeringselementet varierar i brons längsled.

$N_{d.max} := 2786.7kN$ $N_{d.min} := -714.6kN$

Hela dragkraften anses upptas av armeringen i farbaneplattan.

$A_s := A_{s.min}$ (1% armeringsinnehåll) $A_s = 20420\,mm^2$

$\sigma_s := \frac{N_{d.max}}{A_s}$ $\sigma_s = 136.5\,MPa$

$\zeta = 1$ $k := 1.0$ $\varphi_{ef} := 2.0$

$E_{ef} := \frac{E_{ck}}{1 + \varphi_{ef}}$ $\alpha := \frac{E_{sk}}{E_{ef}}$ $\alpha = 18.75$

$\sigma_{cr} := k \cdot \frac{f_{ctk}}{\zeta}$ $\sigma_{cr} = 1.95\,MPa$

$\sigma_{sr} := \alpha \cdot \sigma_{cr}$ $\sigma_{sr} = 36.6\,MPa$

$\kappa_1 := 0.8$ $\beta := 0.5$

$$\nu := 1 - \frac{\beta}{2.5 \cdot \kappa_1} \cdot \frac{\sigma_{sr}}{\sigma_s} \qquad \nu := \max(\nu, 0.4) \qquad \nu = 0.933$$

Enligt 53.32 i BRO 94 godtas att medelsprickavståndet sätts till avståndet mellan svetsbultarna i längsled.

I stödsnittet där de största dragkrafterna uppstår är avståndet mellan svetsbultarna 150 mm, se Strukturas ritning 1-596068-108.

$s_{rm} := 150\text{mm}$

$$w_m := \nu \cdot \frac{\sigma_s}{E_{sk}} \cdot s_{rm} \qquad w_m = 0.095\,\text{mm}$$

$w_k := w_m \cdot 1.7$ $w_k = 0.162\,\text{mm}$

Aktuell sprickvidd är betydligt mindre än kravet på 0.3 mm.

Appendix F FEM Results

The Vertical shear forces (Fz) and displacement (DZ) results extracted from the 2-D model for the short and long term loading stiffness are presented (see *Figure F.1*, *Figure F.2* and *Figure F.3*).

The convergence analysis results of the 2-D model for the bending moment (My) and the vertical displacement (DZ) are presented (see *Figure F.4* and *Figure F.5*).

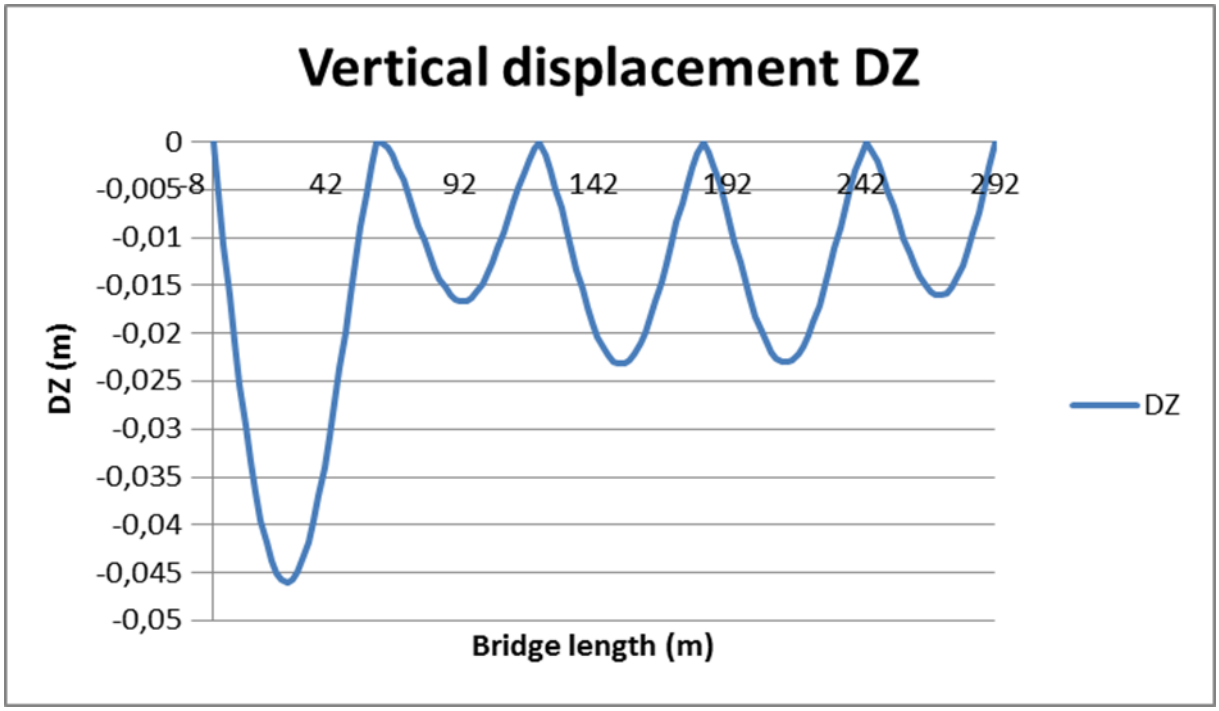

Figure F.1 Vertical displacement (DZ) along the bridge, due to ballast load with the appropriate load factor, calculated for the long-term loading stiffness.

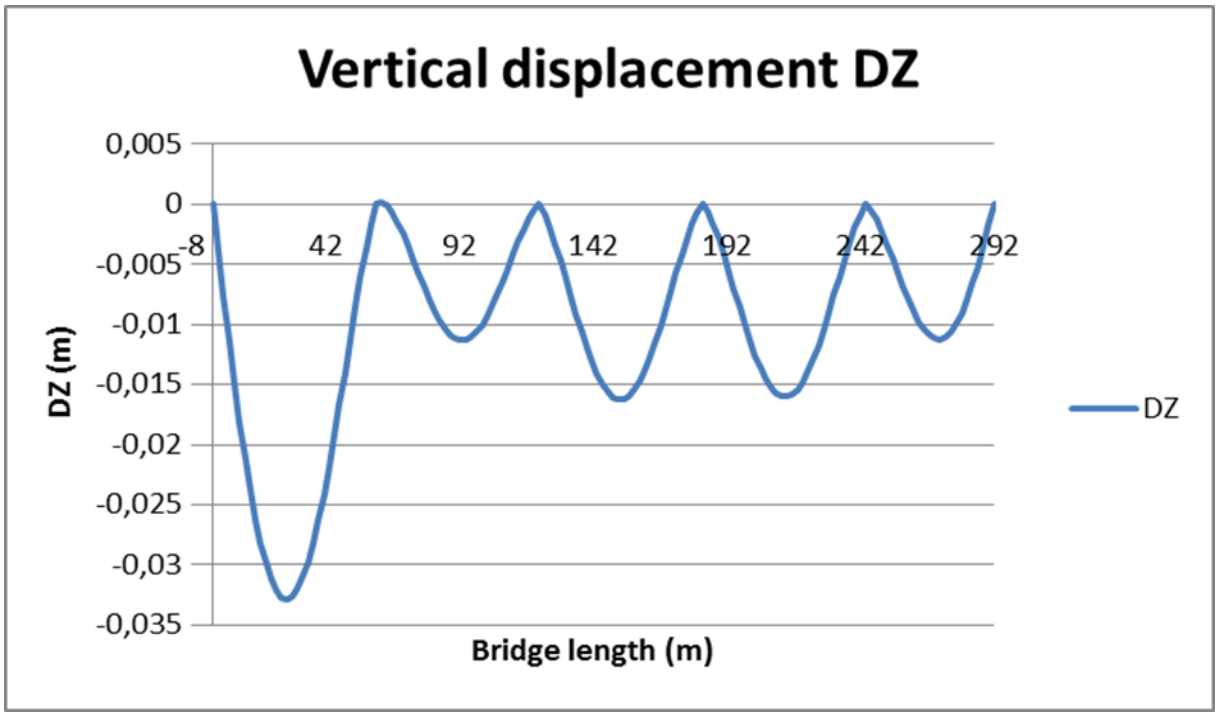

Figure F.2 Vertical displacement (DZ) along the bridge, due to ballast load with the appropriate load factor, calculated for the short-term loading stiffness.

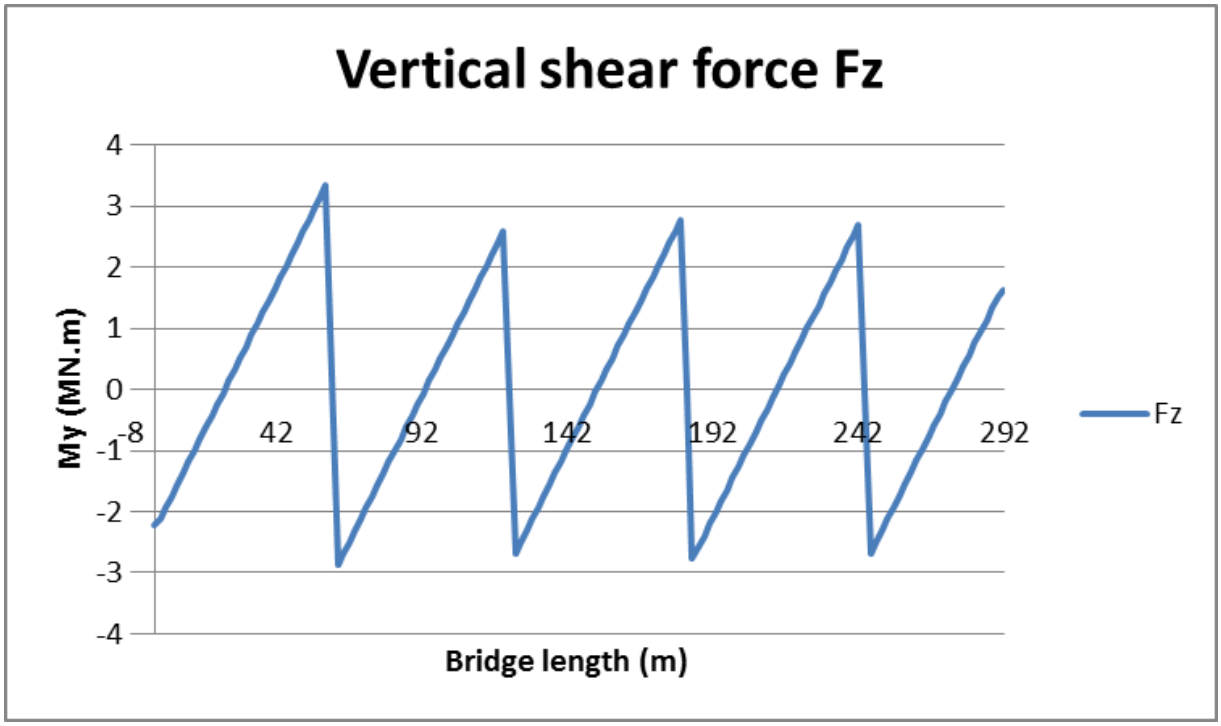

Figure F.3 Shear forces distribution (Fz) along the bridge due to ballast load with the appropriate load factor.

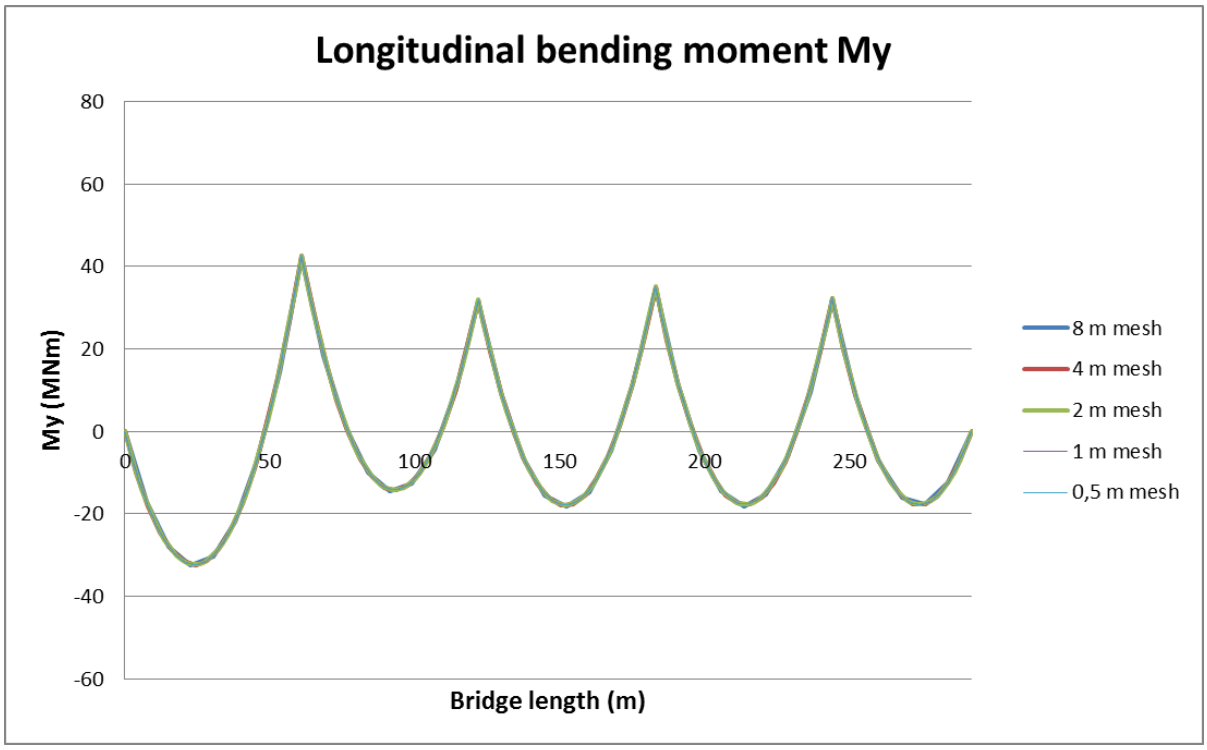

Figure F.4 Bending moment along the bridge length drawn for mesh sizes 8, 4, 2, 1, and 0.5m for the convergence of mesh size.

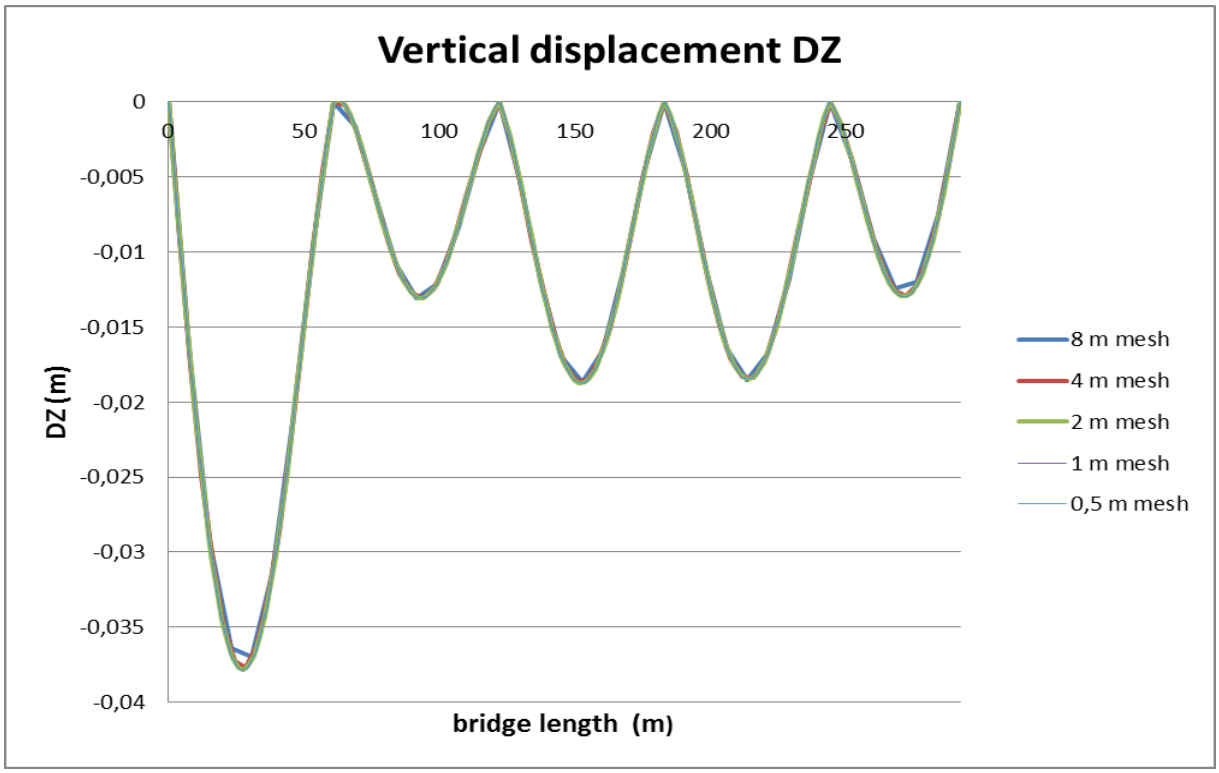

Figure F.5 Vertical displacement along the bridge length drawn for mesh sizes 8, 4, 2, 1, and 0.5m for the convergence of mesh size.

TRITA-BKN. Master Thesis 352,
Structural Design and Bridges 2012
ISSN 1103-4297
ISRN KTH/BKN/EX-352-SE

www.kth.se